LMSC-D558143
JUNE 1977

FINAL REPORT

SPRAYLON FLUOROCARBON ENCAPSULATION FOR SILICON SOLAR CELL ARRAYS

FOR THE
JET PROPULSION LABORATORY,
CALIFORNIA INSTITUTE OF TECHNOLOGY

CONTRACT NO. 954410

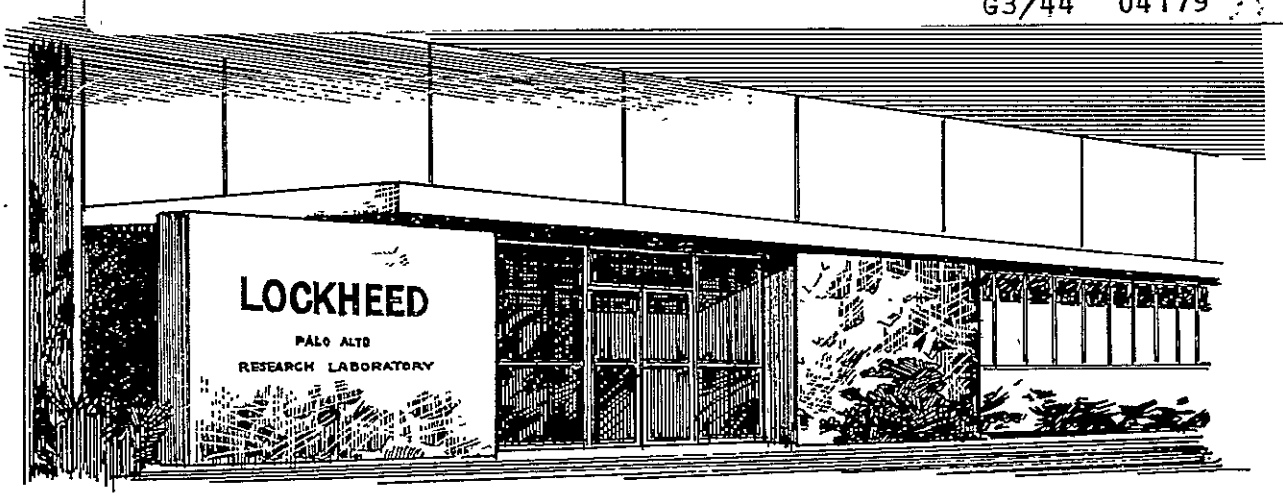

LOCKHEED

PALO ALTO RESEARCH LABORATORY

LOCKHEED MISSILES & SPACE COMPANY, INC. • A SUBSIDIARY OF LOCKHEED AIRCRAFT CORPORATION
PALO ALTO, CALIFORNIA

FINAL REPORT

SPRAYLON FLUOROCARBON ENCAPSULATION FOR SILICON SOLAR CELL ARRAYS

JUNE 1977 LMSC-D558143

E. N. Costogue, Program Manager
Solar Energy Group, JPL

Contract No. 954410

This work was performed for the Jet Propulsion Laboratory, California Institute of Technology, Sponsored by the National Aeronautics and Space Administration under Contract NAS 7-100.

Lockheed Palo Alto Research Laboratory
LOCKHEED MISSILES & SPACE COMPANY, INC.
A Subsidiary of Lockheed Aircraft Corporation
Palo Alto, California 94304

ACKNOWLEDGMENTS

Significant contributions have been made to this study by the members of the Jet Propulsion Laboratory, particularly from Mr. F. L. Bouquet, Member of the Structures and Materials Section, Applied Mechanics Division, who was responsible for carrying out all the mechanical tests, and Mr. E. N. Costogue, JPL Technical Manager of the LMSC effort.

Mr. S. J. Marsik, NASA/Lewis Research Center, also assisted LMSC personnel during the environmental tests performed at NASA/Lewis.

ABSTRACT

A development program was performed for evaluating, modifying, and optimizing the Lockheed formulated liquid transparent film-forming fluorocarbon (Spraylon) protective coating for silicon solar cells and modules. The program objectives were designed to meet the requirements of the low-cost automated solar cell array fabrication process being developed by JPL. As part of the study a computer program was used to establish the limits of the safe working stress in the coated silicon solar cell array system under severe thermal shock.

PRECEDING PAGE BLANK NOT FILMED

CONTENTS

PRECEDING PAGE BLANK NOT FILMED

ILLUSTRATIONS

TABLES

Section 1
INTRODUCTION

Recent design trends in spacecraft solar arrays have been directed toward achieving longer lifetime and higher reliability at lower costs and weight. With these goals in mind, every attempt is now being made to incorporate simplicity, modular construction, and ease of manufacture and repair into array design.

Major weight savings have been achieved in recent years by replacing the rigid array concept with a lightweight flexible printed circuit substrate such as Kapton. However, common to both systems is the fused silica cover glass which is applied to the individual cells comprising the array. There are many instances in which the function of these costly and heavy covers could be accomplished by much thinner and lighter covers, but the increased manufacturing and handling costs are unfortunately prohibitive.

A primary consideration in developing an optimum and economical replacement system for the silica covers is obviously the requirement for high transmittance in the solar spectral region with the added constraint that the optical properties be resistant to degradation from the space environment. Allied to this are the obvious requirements of good adhesion, flexibility, resistance to thermal cycling, humidity, and anticipated prelaunch environments.

This report discusses the results obtained in the initial phase of a program to develop a replacement for the fused silica cover glasses. The LMSC developed Spraylon system process parameters and environmental stability characteristics are presented.

The primary purposes of solar-cell covers are to provide protection from penetrating radiation and to lower the operating temperature, and thus improve the performance of the cells, via infrared emittance. Conventional solar arrays employ cover glass systems composed of 6- to 12-mil fused silica adhesive bonded to the cells. To

protect the transparent adhesive from damage induced by solar ultraviolet radiation, it is generally necessary to coat the cover glass with a multilayer film which does not transmit UV radiation. In addition, the front surface of the cover glass is provided with a low refractive index coating, such as MgF_2 ($n \simeq 1.38$), to provide lower front surface reflectance losses than the nominal 4 percent suffered by fused silica. Testing by this laboratory indicates that the various components associated with the cover glass (the clear silicone adhesive, the anti-reflective coating with the blue UV filter), whether tested separately or in combinations, degrade in solar transmittance as a result of exposure to the simulated space environment. This decrease in transmittance appears greatest in the spectral region between 6000 and 3500 Å for test samples of the fused silica covers containing a combination of all the above-mentioned components. Although this array performance loss is obviously not critical, it stands as an additional burden that must be borne by the conventionally covered solar cell system.

Although conventionally protected solar arrays have been quite successful in providing reliable power for numerous spacecraft missions, many limitations and compromises exist. For many missions, the use of 2- to 6-mil covers would be adequate to serve for both thermal control and radiation protection. Although this use would provide significant weight savings, especially for large arrays, it is not commercially feasible since thin fused silica is not currently available on a production basis at a reasonable cost. Solar arrays with conventional cover systems are thus forced to use the heavier cover glasses because of economic factors. An additional negative economic factor is the tendency of conventional solar-cell cover handling and application procedures to add a sizable amount to solar-array fabrication costs and, furthermore, replacement of damaged or imperfectly bonded cover glass is difficult and expensive.

In 1968 (Ref. 1) LMSC developed a unique and very effective solar cell cover system to directly replace the costly and cumbersome fused silica cover glasses. These covers consisted of clear FEP (fluorinated ethylene propylene) films heat sealed directly onto the bare solar cells, at moderate pressures and at temperatures in the range of 235° to 300°C. Test results have been obtained at LMSC using 5-mil FEP films applied directly by heat-sealing techniques to solar cells. In general,

the operating characteristics (I-V curves) of the bare and 5-mil FEP coated cells have been shown to be essentially equivalent. The emittance of such coated cells ($\epsilon = 0.85$) is slightly greater than adhesive-bonded 6-mil fused quartz, SiO_2 ($\epsilon = 0.83$). While no significant changes in optical properties had been observed due to 1500 equivalent sun hours of ultraviolet, 10^{16} protons/cm^2 (2 keV), or high-energy electrons (1 MeV), later work by investigators at TRW (Ref. 2) showed that for long term UV radiation some loss in transmittance did occur, while in combined environments (UV plus charged particles) large radiation doses caused embrittlement of the FEP Teflon.

An improved system has been envisioned, as a coating that could be applied by standard paint techniques (spraying, brushing, rolling, or dipping), and simultaneously provide the required optical, physical, and environmental properties. Dupont's powder coating (Ref. 3) could be used to deposit films of FEP, but the processing temperature in excess of 330°C, poses the same processing problems associated with the FEP film. To alleviate many of the problems incurred in the heat-sealing process, this laboratory conceived a variation on the clear fluorocarbon film application technique. This approach, designated Spraylon, is based on the ability to apply a transparent fluorocarbon plastic coating from solution by conventional paint techniques followed by processing at moderate temperatures compatible with soldered interconnects.

As with the heat-sealed FEP approach, the Spraylon system offers many functional and economic advantages over conventional solar cell cover glass technology:

- Spraylon eliminates the need for a transparent adhesive used to bond the cover glass to the cell. This adhesive layer itself adds weight, fabrication complexity, and the need for a UV protective multilayer.
- Spraylon eliminates the need for the antireflective coating since fluorocarbon films have a lower index of refraction than fused silica.
- Spraylon reduces material costs. The "painted-on" fluorinated polymer material is comparable in price to the extruded FEP films, and much cheaper than the fused silica for equivalent thicknesses.

The Spraylon system also offers additional advantages over heat-sealed FEP films as a cover for solar cells:

- Spraylon can be applied as cover material in any film thickness ranging from 0.25 to over 20 mils.
- Spraylon offers a wider range of temperature control, radiation protection, and array weight.
- Spraylon offers a low processing temperature range of 150 to 180 °C so no special bonding methods are needed to protect the conventional electronic solder bonds.
- Spraylon allows easier and cheaper repairs to be carried out on the finished array.
- Spraylon can be applied as a specular or diffuse surface.

Although encapsulation of optical and electrical systems and components is a common practice, the concept as applied to low cost, highly reliable, and high optical performance solar arrays poses many unique requirements. To achieve this desired system, LMSC has conducted the initial phase of a development program to evaluate low-cost methods of applying the liquid transparent film forming fluorocarbon (Spraylon) coating to silicon solar cell modules, employing methods consistent with projected automated production techniques for fabrication of low-cost arrays.

Section 2
PROGRAM OBJECTIVE

The overall program objective is to:

- Develop and qualify the Lockheed "Spraylon" system (a fluorocarbon encapsulant) for space solar cells and arrays
- Evaluate (low cost) automated methods for applying Spraylon to large flexible solar arrays

To achieve this objective, four tasks were identified and carried out according to the following task breakdown:

- Task 1 Composition Studies
  - Solvent system optimization
  - Intrinsic film properties
- Task 2 Deposition Technique Studies
  - Application procedures
- Task 3 Environmental Testing
  - Humidity
  - Ultraviolet, protons, and electrons
  - Thermal cycling
  - Mechanical
- Task 4 Process Optimization
  - Single cells and coupons

Section 3
TECHNICAL PROGRAM

Recognizing that the development, evaluation, and optimization of a low-cost method of applying Spraylon to silicon solar cell modules was necessary for the definition of an automated solar array fabrication process, a technical program was proposed and executed to provide the required data.

Four major task areas were identified as being the necessary areas to pursue. Since they were, by their very nature interrelated, the success of the program was dependent on feedback from each other. The four major task areas are:

- Composition studies
- Deposition techniques
- Environmental testing
- Optimization studies

Figure 3-1 shows the Spraylon processing sequence and indicates the interrelationship of the four main tasks and the importance of detailed feedback of information from task to task.

3.1 COMPOSITION STUDIES

The composition studies were devoted to evaluation and definition of the system formulation and establishment of the intrinsic properties of the deposited film. The parameters investigated were solution viscosity, solvent removal, and substrate/film adhesion properties.

3.1.1 Solvent System Optimization

The Spraylon system uses a two-solvent mixture whose concentration ratio is dependent on the required viscosity and, hence, mode of application. A detailed

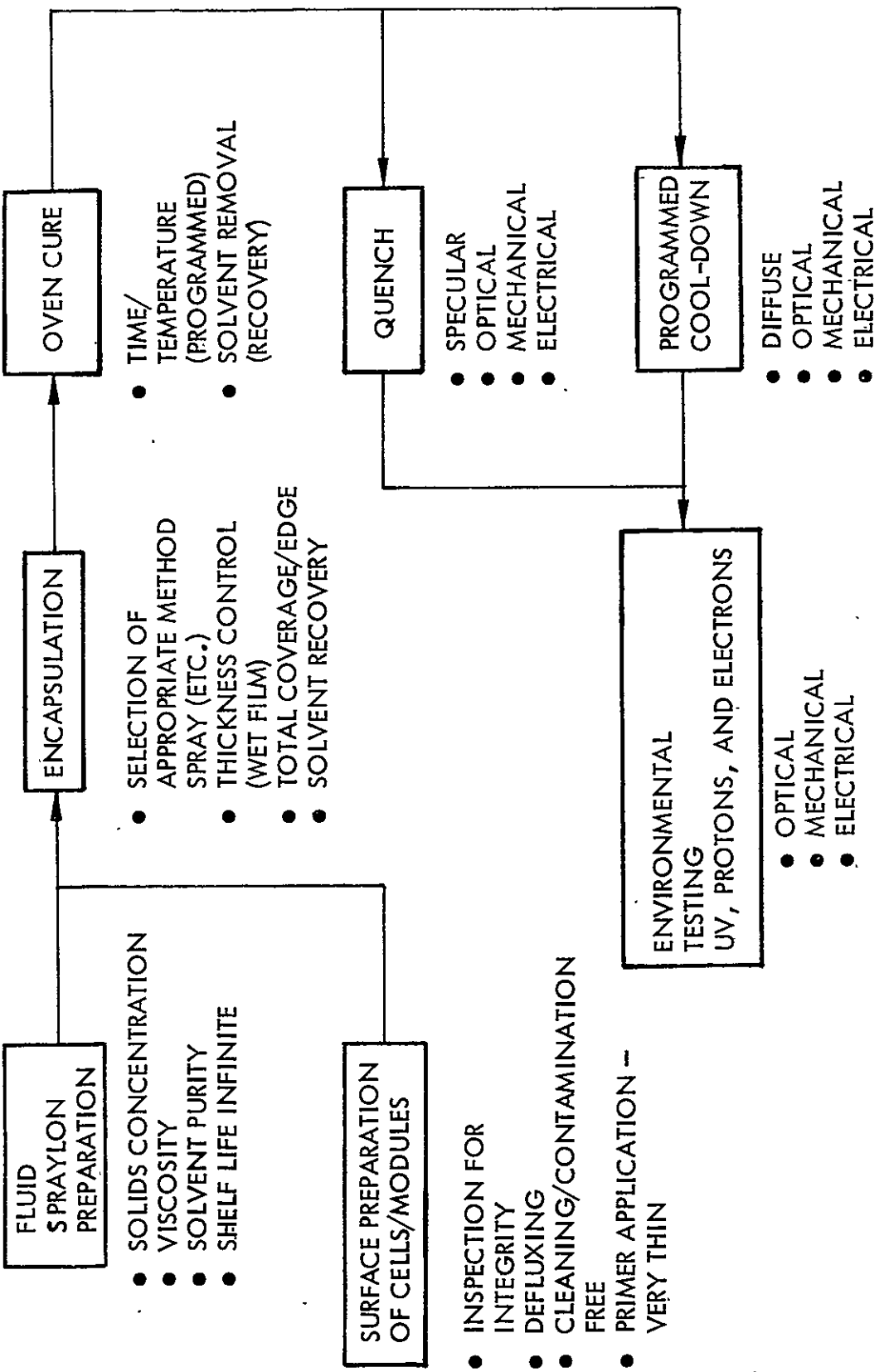

Fig. 3-1 Spraylon Processing Diagram for Solar Cells

ORIGINAL PAGE IS
OF POOR QUALITY

viscosity test matrix was set up for varying ratios of the two solvents, designated as Solvents A and F, and different solids concentrations. The matrix was designed to cover the total solids concentration/viscosity range appropriate to spray, brush, roll-on, and dip modes of application.

The solvent concentration ratios were 100 percent primary solvent A, 100 percent primary solvent F, 1:1 (A/F), 2:1 (2A/F), and 1:2 (A/2F), while the solid concentration range was from 5 to 30 percent by weight. The solvent blends were based on volume ratios.

Initial test results indicated that, for solids concentrations below 10 percent, the solution viscosity was too low to produce appropriate dry film thicknesses. For example, at 6 percent solids the solution viscosity was 152 cP, which is far too low for any of the four application modes under consideration. Based on this observation, all further studies were carried out at solids concentration of 10 to 30 percent.

The viscosity data obtained for the five solvent blends are presented in Table 3-1.

Table 3-1

VISCOSITY TEST MATRIX AT 23°C

Solids (wt %)	Solvent Systems (cP)*				
	A	2A/F	A/F	A/2F	F
30	99,700	88,200	82,000	77,100	67,700
20	10,010	8,550	7,840	7,030	5,940
15	2,268	2,015	1,938	1,830	1,673
12.5	1,120	918	832	734	602
10	528	419	373	338	295
9	—	—	—	262	—
7.75	—	—	—	191	—
7	—	—	—	151	—
6	—	—	—	114	—

*Solvent blends based on volume ratios.

Figure 3-2 summarizes the relationship among viscosity, solvent composition, and solids content, while Fig. 3-3 illustrates the change in viscosity as a function of percent solids for the various solvent blends. These data indicate the nonlinearity between the two parameters spanning almost three orders of magnitude in viscosity, for solids concentration between 10 to 30 percent. This range of available viscosities provides considerable latitude in selection of the application mode. By contrast, however, the effect of temperature on Spraylon viscosity is relatively small, particularly at high solids concentration as shown graphically in Fig. 3-4.

3.1.2 Treatment Time and Temperature (Solvent Removal)

Complete removal of residual organic solvents is critical to the stability of the formed Spraylon film on exposure to electromagnetic radiation. Under the influence of UV radiation these materials degrade and cause discoloration of the film.

Parametric studies were performed of the relationship between the curing temperature and time and the intrinsic optical properties of the film. Films of various thickness were cast on glass and polished aluminum substrates, and the time and temperature of curing varied. The changes in transmittance and reflectance of the coated substrates were measured before and after UV exposure.

Pertinent to successful operation of a spacecraft in orbit is the question of using low outgassing materials to minimize the possibility of contamination of critical surfaces. Outgassing and smoke tests (see Appendix A) were performed on a number of the free-standing Spraylon films and on Spraylon encapsulated single solar cells. The results of those tests as they were performed at JPL and LMSC are given in Tables 3-2 to 3-4. As can be seen, the Spraylon film exhibits negligible outgassing characteristics and presents no problems from the point of view of qualifying as a spacecraft material.

Based on the results of the outgassing tests and the film optical property measurements, an optimum processing sequence was established for single solar cell and small

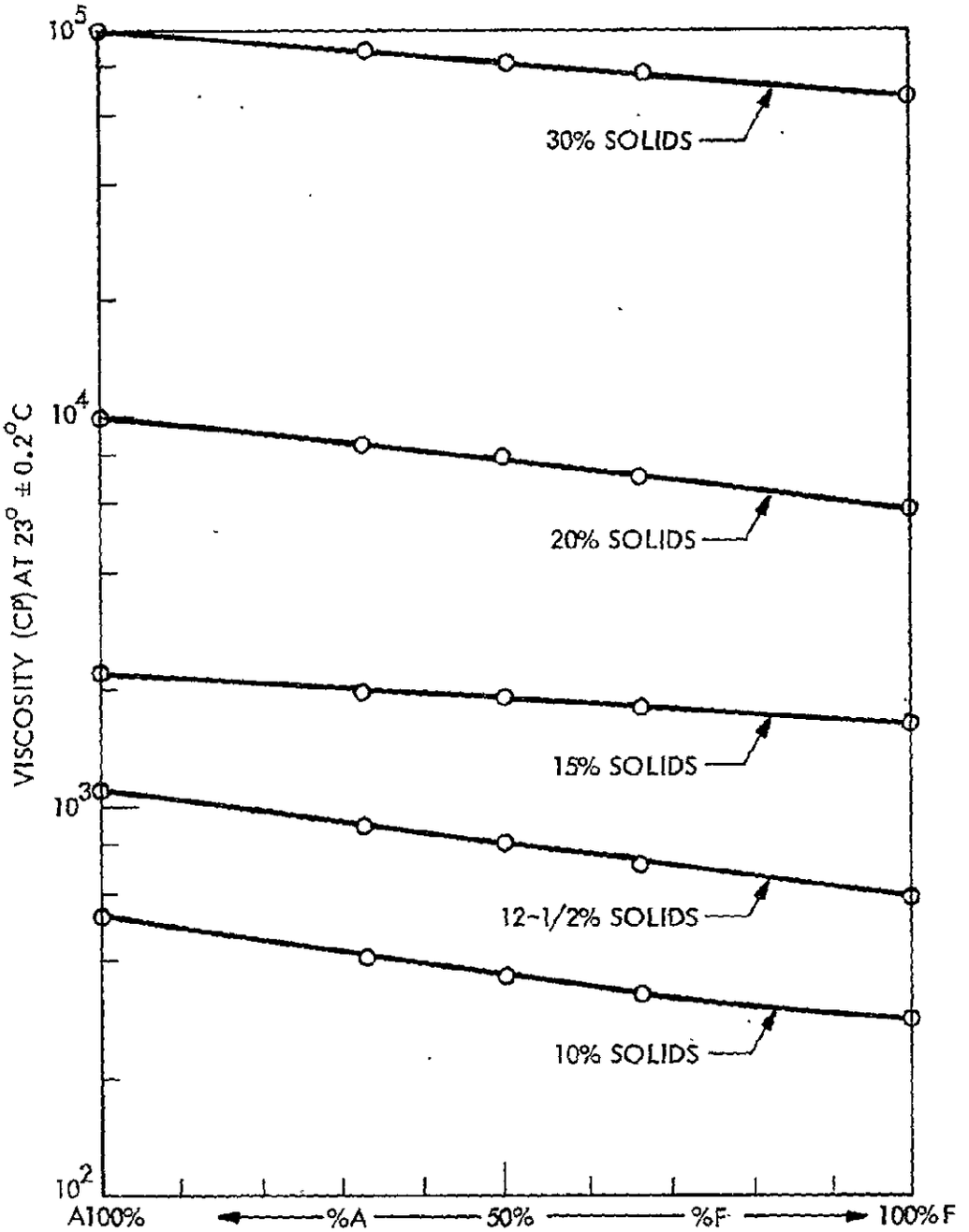

Fig. 3-2 Viscosity of Spraylon Versus Solvent Composition

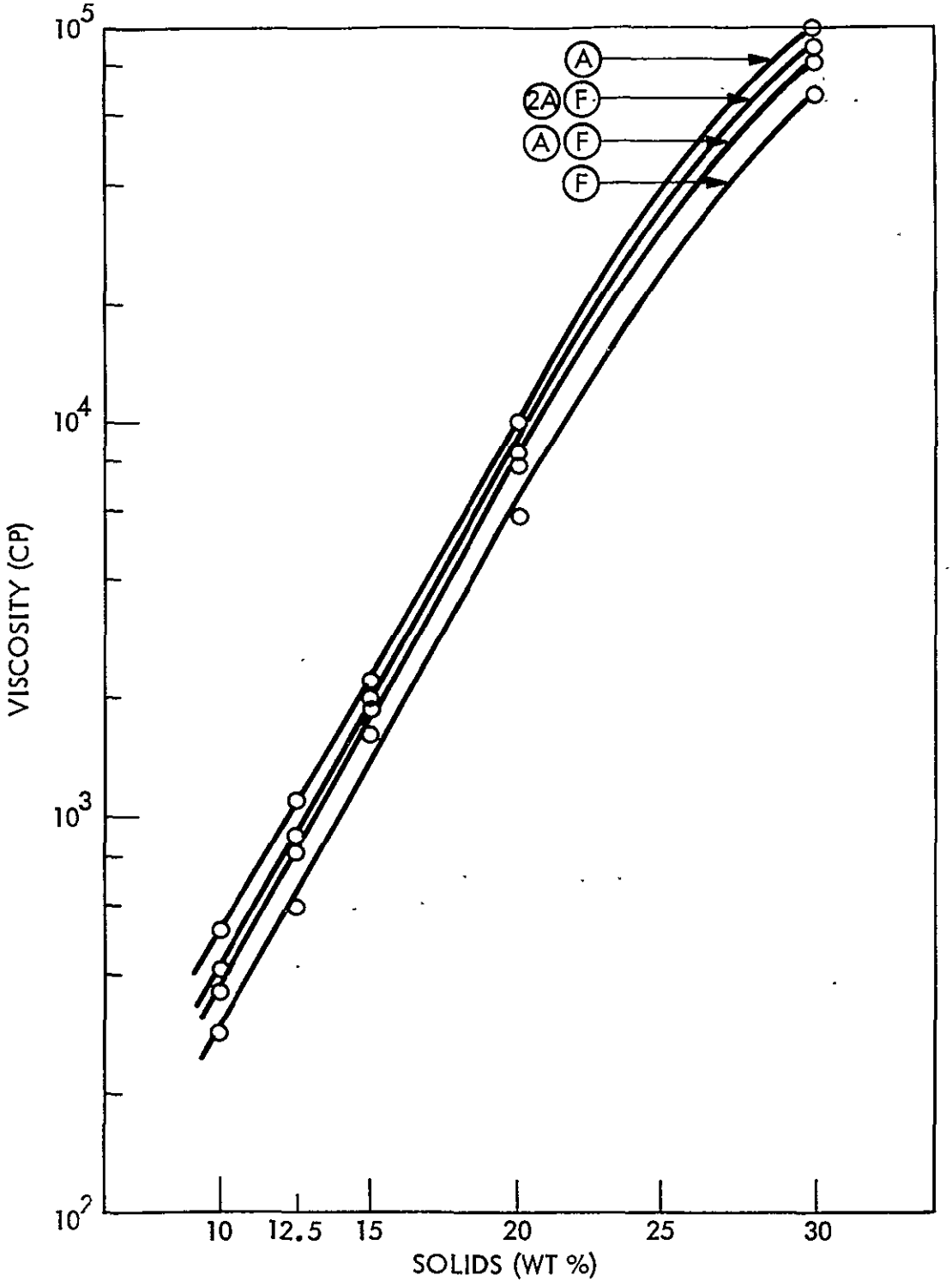

Fig. 3-3 Viscosity of Spraylon Versus Solids Concentration at Various Solvent Compositions (23°C)

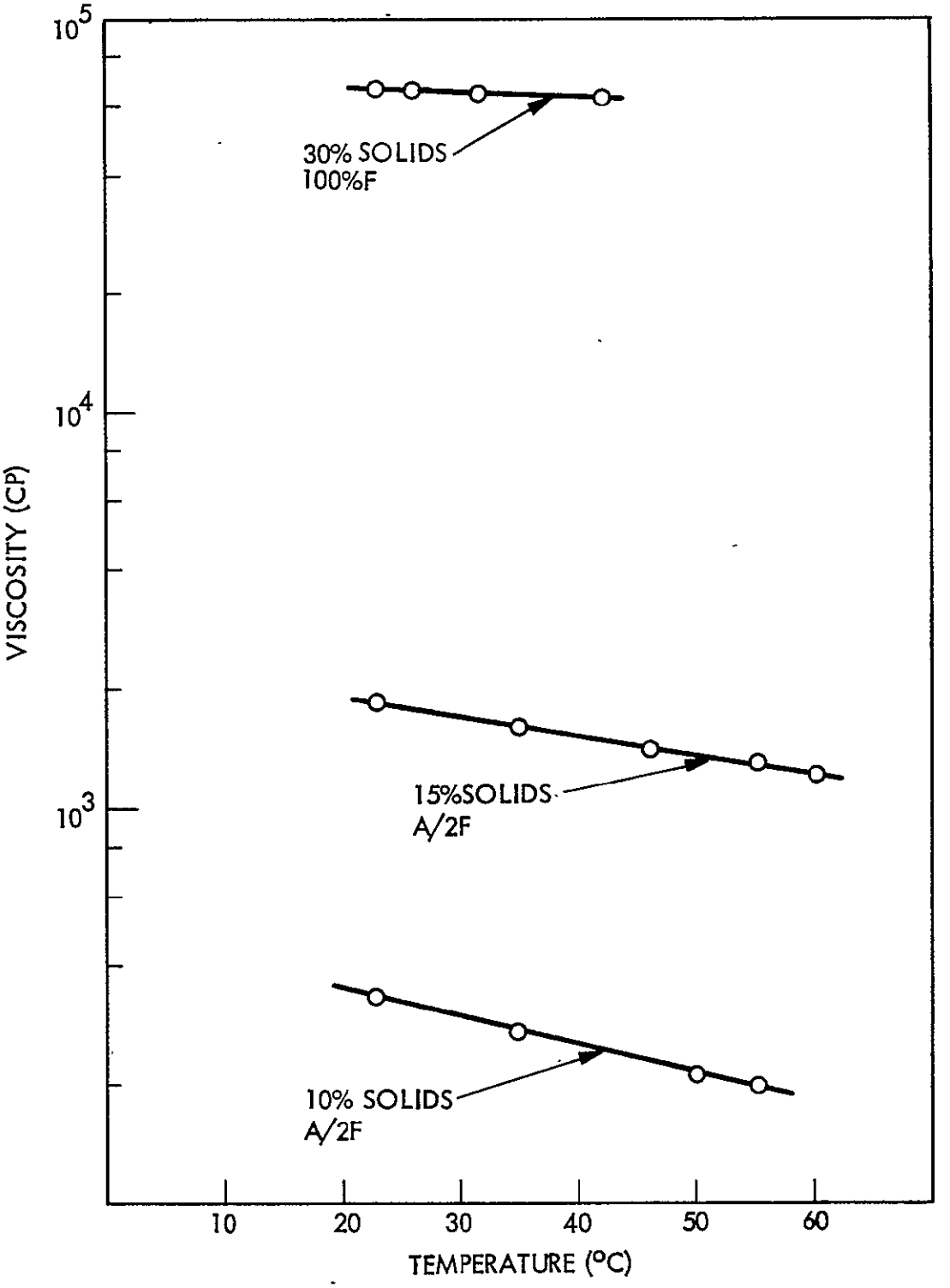

Fig. 3-4 Viscosity of Spraylon Versus Temperature

Table 3-2

RESULTS OF MACRO-VCM (OUTGASSING)MEASUREMENTS

Specimen Number	Coating Weight (g)	VCM (%), Tested at 125°C for 24 hr at 10^{-6} Torr
1	0.0550	Less than 0.01% – limit of detection*
2	0.0763	Same
3	0.0681	Same
4	0.0546	Same
5	0.0682	Same
6	0.0486	Less than 0.01% – limit of detection*
7	0.0511	Same
8	0.0449	Same
9	0.0280	Same
10	0.0420	Same
11	0.0538	Less than 0.01% – limit of detection*
12	0.0393	Same
13	0.0464	Same
14	0.0500	Same
15	0.0438	Same

*Test results show that the outgassing VCM is less than 0.01%, the lower limit of detectability of the test apparatus.

Table 3-3

MACRO-VCM OUTGASSING MEASUREMENTS ON FREE-STANDING SPRAYLON FILMS

Sample Number	Size (cm)	Weight Loss (%)		VCM (%) at 125 °C for 24 hr At 10^{-6} Torr	
1	2 × 2	0.10		0.01	
2	2 × 2	0.10		0.00	
3	2 × 2	0.10	Average Weight Loss (%)	0.01	Average VCM (%)
4	2 × 2	0.09	= 0.094	0.00	= 0.004
5	2 × 2	0.08		0.00	
6	10 × 13	0.11	Average Weight Loss (%)	0.01	Average VCM (%)
7	10 × 13	0.11	= 0.11	0.01	= 0.01

Table 3-4

RESULTS OF LMSC "SMOKE" (TD/V) TESTS PERFORMED ON SPECIMENS OF SPRAYLON FREE-STANDING FILMS

Specimen Film Designation	Temperature of Heated Film (°F)	Ambient Vacuum (Torr)	Results of Heating for 3 hr in Vacuum
15-A	150	6.2×10^{-5}	No TD/V* products detected
	200	6.2×10^{-5}	
	250	6.2×10^{-5}	Same
	300	6.2×10^{-5}	Same
	350	6.4×10^{-5}	Same
	425	1.1×10^{-4}	Slight, 5% degradation of reflectance at 0.23 μm
15-2A/F	300	5.1×10^{-5}	No TD/V products detected
	350	5.2×10^{-5}	Same
15-A/F	300	6.0×10^{-5}	No TD/V products detected
	350	6.3×10^{-5}	Same
15-A/2F	300	6.2×10^{-5}	No TD/V products detected
	350	6.4×10^{-5}	Same
15-F	300	6.2×10^{-5}	No TD/V products detected
	350	6.3×10^{-5}	Same
	375	6.5×10^{-5}	Same
	400	7.4×10^{-5}	Same
	425	9.4×10^{-5}	Slight, 5% degradation of reflectance at 0.23 μm

*TD/V = thermal decomposition/volatilization, effluent condensed on cold collector mirror.

module encapsulation. The primed substrate, after application of the required amount of Spraylon (12 mil wet film $\simeq$ 1 mil of dry film), is placed in a vented oven and brought up to 350 °F in 10 min to facilitate solvent flash-off. Complete curing is achieved by maintaining the sample at 350 °F for an additional 15 min. The cured film is then subjected to one of two post-deposition treatments, either a programmed cool-down or a cold-water quench. The former treatment results in a diffuse film finish while the latter produces a clear, nonscattering film. In this program where the main objective was to develop Spraylon as a solar cell cover material, the cold water quench treatment was used.

3.1.3 Primer Selection

Good adhesion of the Spraylon film to the solar cell surface, including grids, substrates, and interconnects under the various environments which the solar array is likely to encounter in space, is an important property that must be attained. Considering these environmental conditions that the system must overcome successfully, a candidate primer substance must meet the following requirements:

- Ease and reproducibility of application of very thin films
- Optimum adhesive properties between the Spraylon film and the solar-cell surface
- Good optical transparency
- Good UV and thermal stability

Spraylon by virtue of the inherent chemical inertness of the fluorocarbon polymer does not readily form coatings which have adequate adhesion to most solar-cell array substrates. When spread in liquid form onto a substrate, the material has a marked tendency to retract from the original continuous film and leave areas uncovered, especially at edges and interfaces. This tendency not to wet the surface becomes more pronounced as the temperature of the coating is increased during the processing cycle. What started out in the processing as a uniformly and evenly coated solar cell before solvent flash-off would be observed to have incomplete coverage toward the edges after removal from the hot zone. It was also observed that the adhesion of the film to the surface where this effect was noted was characteristically poor.

To ensure adequate cell and module coverage by the Spraylon material, the wetting characteristics of the liquid on all cell and substrate constituents were investigated. The wetting properties on various anti-reflective coatings on the silicon solar cells, back-face surfaces, interconnects, and cell flexible circuit substrates were studied in conjunction with the employed range of formulations and processing schedules.

The primary criterion for evaluating the wetting characteristics (i.e., whether surface attractive forces exceeded the wet film's surface free energy) was based on physical observations. Qualitative comparisons were made to compare the ability of the various surfaces to permit the liquid Spraylon to be spread uniformly over the surface without the wet film subsequently contracting to form beads (or retracting from the edges), either immediately after application or after exposure to heating.

The results of these observations indicated that there was a serious problem of "lack of wetting" on practically all of the surfaces that comprise the solar cell array. Also, the effect of the various solvent formulations on the wetting characteristic of Spraylon was minimal. None of the compositions showed any appreciable advantage over any other in this regard. There was, however, a decreasing tendency of the liquids to retract during processing as the initial viscosities were increased. However, it was not practical to utilize this effect since the required viscosities were far too high and adhesion of the cured film was still poor. The results demonstrated beyond question the need for an adhesion promoter in the Spraylon system.

The effects of primers, applied at high dilutions onto the various appropriate substrates, were investigated with respect to wetting enhancement and film adhesion. The initial primer selection was based on the analysis of film adhesion, optical properties, and environmental stability.

The results of the adhesion tests performed by JPL were employed to verify the selection of the primer on the basis of adhesion (Appendix B).

Obviously, the main purpose of a primer is to ensure good adhesion of the final film to the substrate surface. But in the case of a very transparent film such as

Spraylon, the primer layer can also reduce transmittance initially and be a major source of ultraviolet degradation. To address this concern, therefore, optical measurements and simulated near-ultraviolet irradiation tests were performed on the more promising primer samples selected from initial screening tests. These UV exposures were conducted concurrently with the adhesion tests. The test results were fed back into the evaluation loop and served as the basis for the primer selection process.

For economy of effort and practicality, the substrates used for much of the laboratory bench and optical evaluation were microscope glass slides, bright etched aluminum panels, and Class II mechanical silicon solar cells. The primers used in the matrix of the initial screening effort are listed in Table 3-5. The compositions of Spraylon in this matrix were 20 and 15 percent compositions A, A/F, and F.* The primers used in the subsequent adhesion promoter selection studies are listed in Table 3-6, with the Spraylon composition constant at designation 15A.

In all cases, silane primer compounds were selected as the adhesion promoters because of the surface chemistry similarity of the antireflective coating used on the silicon solar cells and the surface of silica, to which the silanes have demonstrated superior adhesion properties as coupling agents.

It was expected that variations in adhesion resulting from the various silanes tested would be attributable to (1) the hydrolyzable portions (alkoxy groups or halogens), which either react with surface adsorbed moisture or added water and (2) the non-hydrolyzable but reactive groups that can exhibit the typical reactions of organic compounds. What was sought was an adhesion promoter whose reactive nonhydrolyzable groups would exhibit a chemical affinity for the fluorocarbon polymer after the silane had hydrolyzed and bonded to the substrate.

Surprisingly, it turned out that the amino functional, especially the combination primary and secondary diamino types of adhesion promoters proved the most effective.

*Solvent system A, solvent F, and equally combined A and F (A/F).

Table 3-5

PRIMERS EMPLOYED IN THE INITIAL ADHESION PROMOTER SCREENING

Material	Source	Composition
A-4094 (as received)	Dow Corning	*
Z6020 (0.5% in Methanol)	Dow Corning	N, beta (aminoethyl) gamma aminopropyl trimethoxy silane
Z6020 (0.05% in Methanol)	Dow Corning	Same
Z6020 (0.5% in Chloroform)	Dow Corning	Same
SS-4004 (as received)	General Electric	*
SS1201 (as received)	General Electric	*
A-174 (as received)	Union Carbide	gamma-methacryloxy propyl-trimethoxy silane
A154 (as received)	Union Carbide	Methyl trichloro silane
SS-4120 (as received)	General Electric	*
SS-4120 (0.5% in Methanol)	General Electric	*

*Structural formula not obtainable from vendor.

Table 3-6

PRIMERS EMPLOYED IN ADDITIONAL ADHESION PROMOTER SELECTIONS

Material	Source	Composition
A-154 (as received)	Union Carbide	Methyl-trichlorosilance
A-151 (as received)	Union Carbide	Vinyl-triethoxysilane
A-172 (as received)	Union Carbide	Vinyl-tris (β-methoxy ethoxy) silane
A-1100 (as received)	Union Carbide	gamma amino propyltriethoxy silane
A-1100 (various dilutions in methanol)*	Union Carbide	gamma amino propyltriethoxy silane
Z6020 (various dilutions in methanol)*	Dow Corning	N, beta (amino ethyl) gamma amino propyltrimethoxy silane
Q1-6011 (various dilutions in methanol)*	Dow Corning	gamma-amino propyltriethoxy silane
A1-6082 (various dilutions in methanol)*	Dow Corning	Vinyl tris (β-methoxy ethoxy) silane
Q1-6032	Dow Corning	N-β-(N-vinyl benzyl amino) ethyl-γ-amino propyl trimethoxy silane mono HCl
Q1-6011 (various dilutions in methanol)	Dow Corning	gamma-amino propyltriethoxy silane

*Also employed as approximately 5 percent by weight silane in methanol-distilled water (90:10)

However, the amino versions lived up to their tradition of having poorer thermal and UV stability when compared with the nonamino versions. Thus, selection of the N, beta (amino ethyl) gamma amino propyl trimethoxy silane (Z6020) as the compromise primer took into account the tradeoffs of superior adhesion and the penality of some optical degradation. It was the goal of this effort to minimize these latter drawbacks by keeping the primer layer to a minimal thickness; employing high dilution followed by controlled rinsing.

The effectiveness of this work is documented by the adhesion results (see Appendix B) and by the optical property results typified by the presentations given in the appropriate figures of pre- and post-UV exposure tests.

3.1.4 Intrinsic Film Properties

Those intrinsic film properties that were studied included optical and mechanical properties, permeability, and outgassing. The film optical properties, measured on polished aluminum substrates, glass slides, and solar cells, included transmittance (T_λ), absorptance (α_λ), reflectance (R_λ), and emittance (ϵ_{IR}). The mechanical properties that were measured at JPL, and reported in detail in Appendix B, included adhesion strength, tensile strength, flexure strength, abrasion resistance, and tear strength. In most cases, these properties were measured on samples prior to and after environmental exposure.

Optical Properties. Figures 3-5, 3-6, and 3-7 summarize the changes in emittance and transmittance as a function of Spraylon film thickness for both quenched and unquenched films. The data show that there is no significant change in emittance between a quenched or unquenched film and that for films thicker than 5 mils the emittance is constant.

Included for comparison is the emittance of 6- and 12-mil AR-coated fused-silica slipcovers; it can be seen that the same cell emittance is achieved by a 1-mil Spraylon coating. Figure 3-7 shows changes in transmittance of a 3-mil Spraylon film as a function of a quenched or unquenched treatment. A significant increase in overall

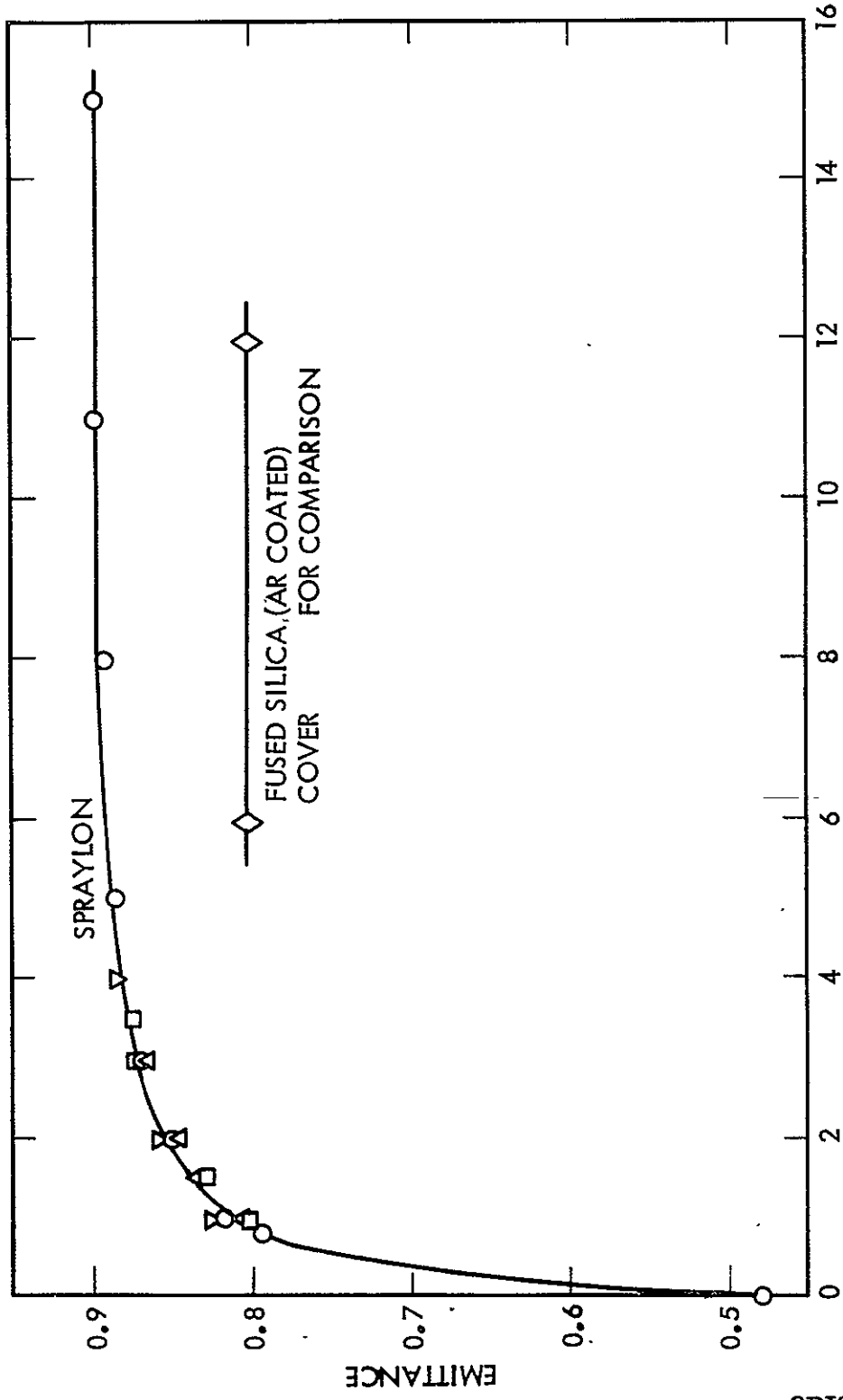

Fig. 3-5 Effect of Spraylon Thickness and Formulation on Emittance

ORIGINAL PAGE IS
OF POOR QUALITY

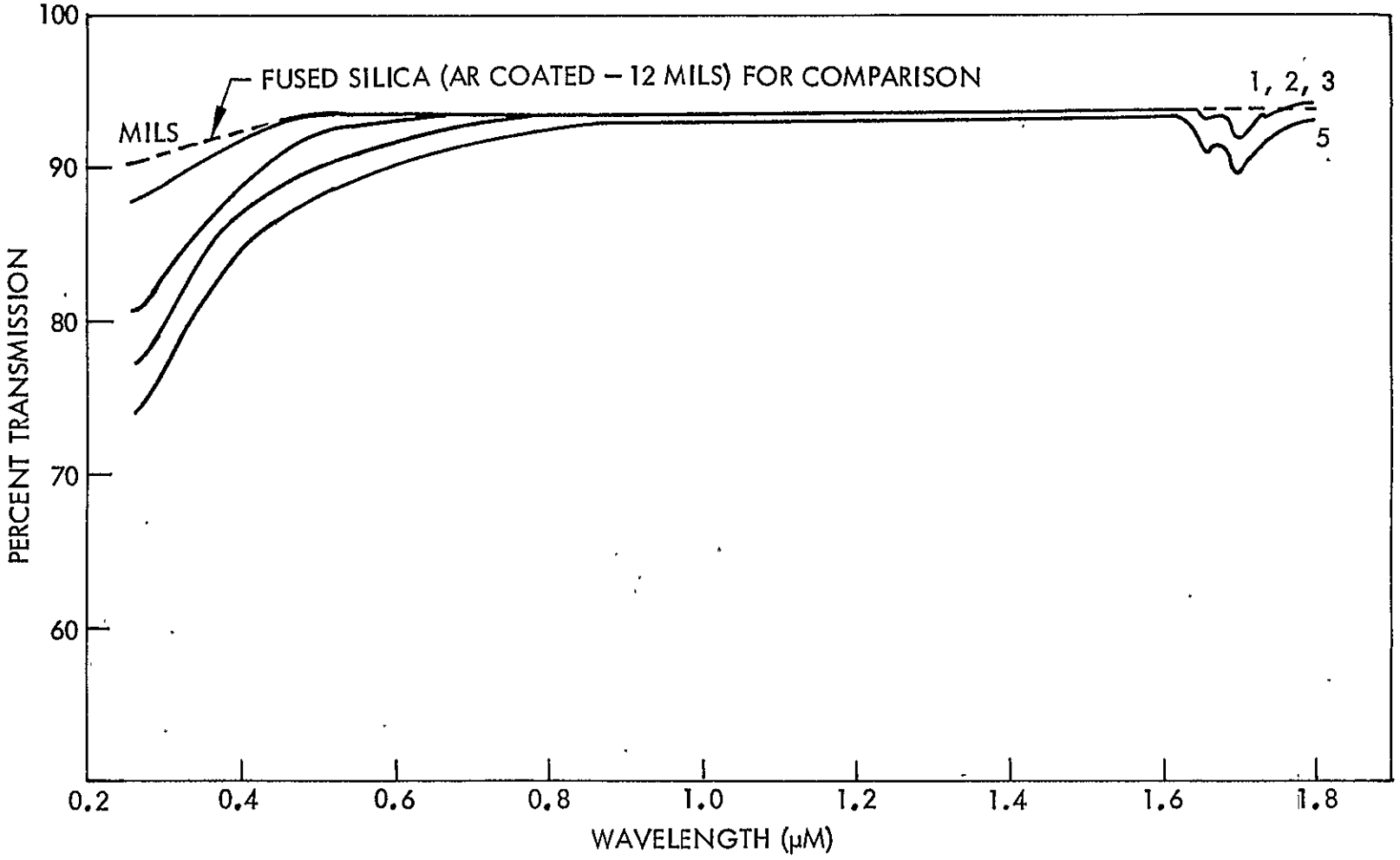

Fig. 3-6 Effect of Film Thickness on Spraylon Transmittance

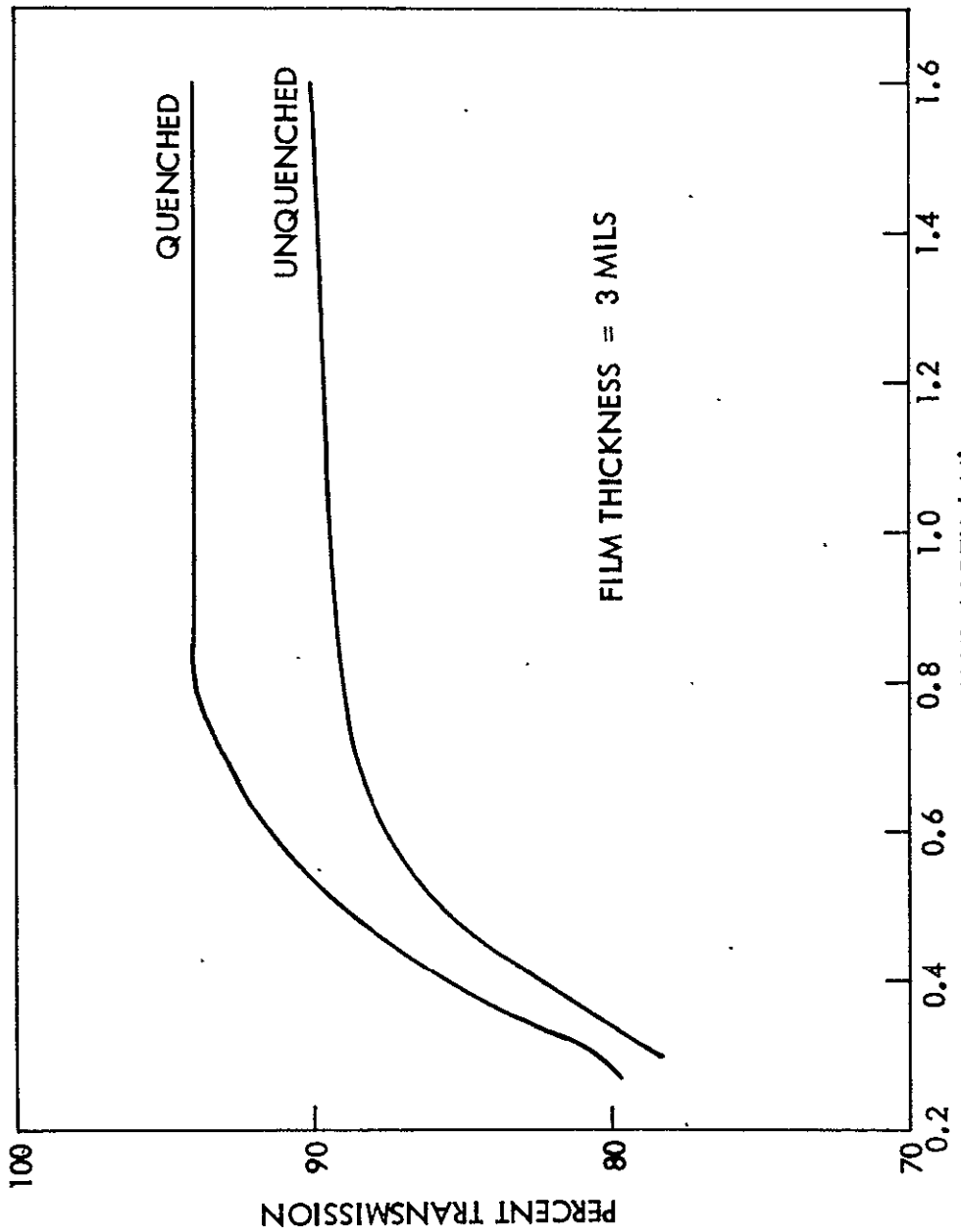

Fig. 3-7 Effect of Quenching on Spectral Transmittance of Spraylon Films

transmittance (from 0.27 to 1.6 μm) is observed for the specular quenched film attributable in large measure to a decrease in front surface scattering.

The dependence relationship between film thickness and film transmittance is given in Fig. 3-6, where it is shown that the effect of film thickness is somewhat insignificant except for the very short wavelength region below 0.35 μm. However, in the UV region the cell response is low and thus the consequences are less significant.

Mechanical Properties. Mechanical property measurements on free-standing Spraylon films as well as on single cells and two-cell modules (coupons) were performed by JPL in conjunction with this effort. The results of the mechanical property evaluations are presented in Appendix B.

Permeability. In evaluating the life expectancy of any spacecraft, consideration must be given to the material handling conditions during manufacture and storage as well as the actual prelaunch conditions encountered prior to flight. Moisture permeability is therefore, a critical characteristic of any exposed surface material and should be evaluated with regard to its impact on the practical use of the candidate material or system.

Since this study is concerned with evaluation of the Spraylon system as a possible encapsulant in a flexible solar array module, evaluation of the permeability in conjunction with that of the other polymer material used in such arrays is pertinent. Samples were prepared and moisture permeability tests performed in accordance with ASTM E96-63T Procedure A at 23°C. The following materials were evaluated as free-standing films:

- Kapton: 2.0 mils
- FEP Teflon: 5.0 mils
- Spraylon: 1.2 and 3.3 mils

The results expressed in terms of weight gain of the encapsulated dessicant as a function of exposure time are represented in Fig. 3-8. Of note is the fact that

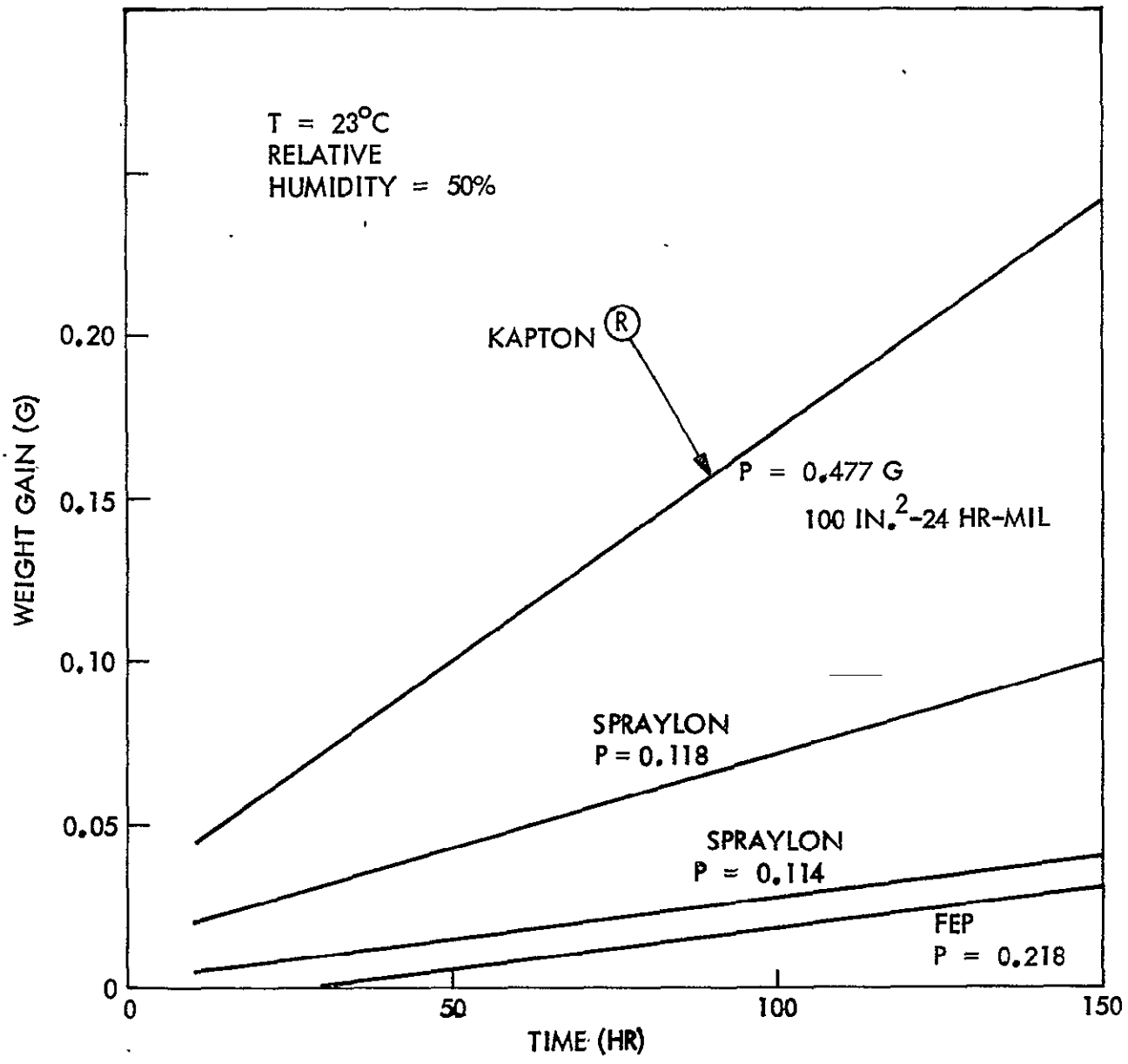

Fig. 3-8 Permeability of Spraylon, FEP, and Kapton to Water Vapor

the Spraylon exhibits lower moisture permeability than both the Kapton and FEP Teflon so that in a flexible array design the Spraylon will not be the most vulnerable component.

Outgassing. All organic materials that are candidates for spacecraft use are required to meet the outgassing specifications set up by NASA and measured by the standard Macro-VCM (Volatile Condensible Material) test. In this study free-standing films and Spraylon coated solar cells were tested using the VCM Test and the LMSC "Smoke Test" method.

- Macro-VCM Test. These tests were performed by JPL on a series of samples provided by LMSC. The samples tested consisted of 15 Spraylon Coated Class II Mechanical Solar Cells, five 2 by 2 cm free-standing films, plus two additional 4 by 5 in. films. The tests were performed in vacuum (10^{-6} torr) at 125 °C for 24 hr, and the weight loss and volatile condensible materials measured (see Appendix A for complete description of test methods). The test results are given in Tables 3-3 and 3-4 for the Spraylon-covered cell samples from which it can be seen all samples meet the NASA outgassing requirements for percent VCM. The free-standing films also meet the NASA requirements as evidenced by the results given in Table 3-3.
- Smoke Test. Free-standing films of the Spraylon were subjected to the LMSC Smoke Test, and the resultant condensible materials were evaluated as potential surface contaminants. This test involved heating the thermocouple instrumented sample in a vacuum and collecting the outgassing products on a cooled front surface aluminized glass mirror. The spectral reflectance characteristic of the mirror was measured prior to and after contamination, between 0.27 and 1.8 μm. (See Appendix A for a detailed description of the test method and apparatus.) The results obtained for the films formed from different solvent ratios are given in Table 3-4. A typical spectral reflectance trace of the collector mirror is plotted in Fig. 3-9, from which it can be seen that there is very little change in mirror reflectance due to condensible material and that the free-standing films can be considered to be "nonsmoking" (Table 3-4).

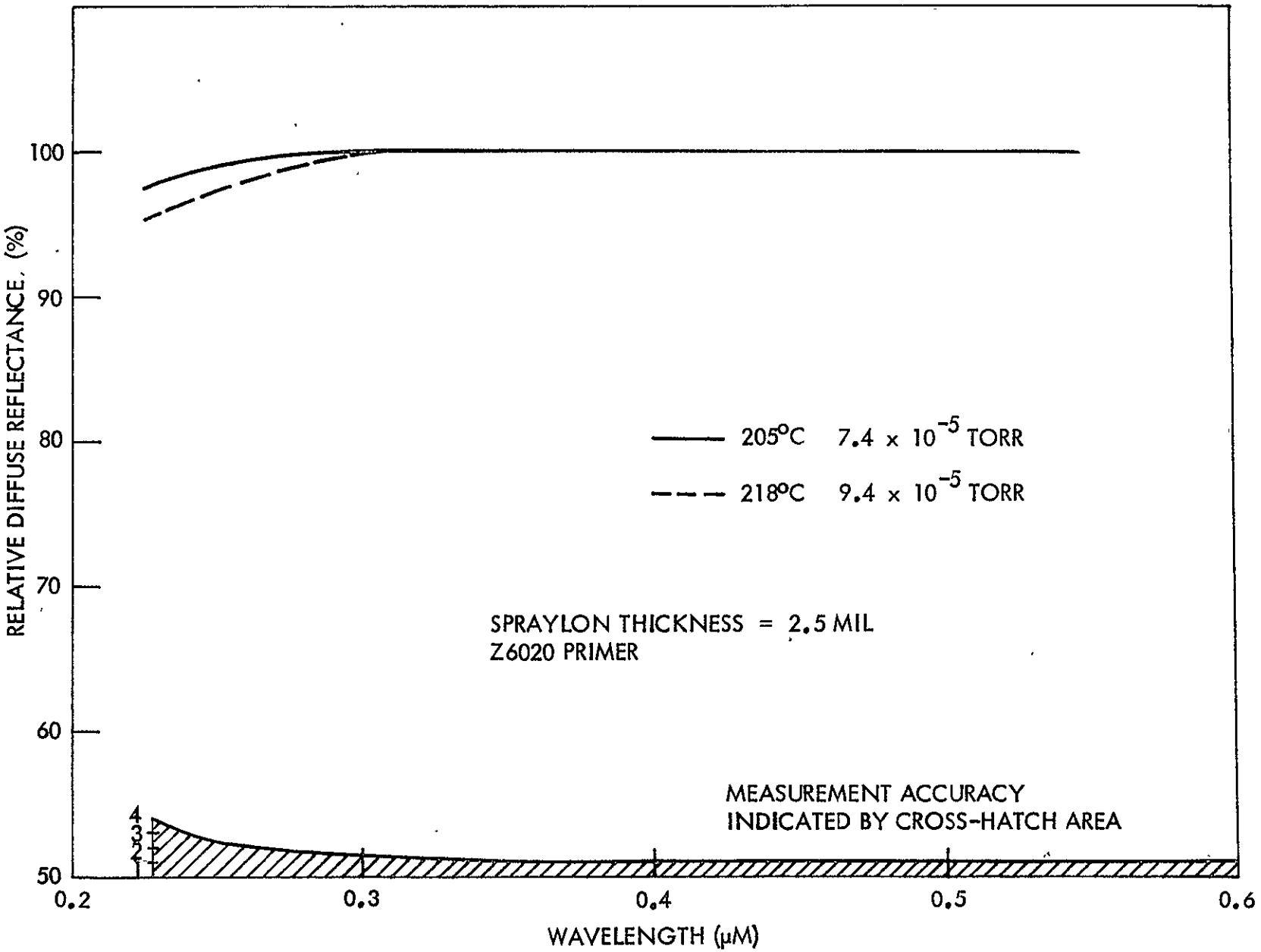

Fig. 3-9 Typical Plot of Relative Spectral Reflectance of Mirrors Exposed to Spraylon Films Heated in Vacuum

3.2 DEPOSITION TECHNIQUES

A major advantage in the use of Spraylon as a solar-cell array encapsulant, lies in the versatility of application that it affords as a polymer solution as opposed to a sheet or film form requiring adhesive or heat sealing. Having met the necessary requirement of environmental stability, it is important that the encapsulant be easily applied, readily cleaned, and amenable to on-site repair. Spraylon by its very nature meets all of these requirements and, in this study, the various modes of application were evaluated from the point of view of amenability to integration into an automated solar-array process.

The techniques evaluated in the laboratory for applying the Spraylon system to single cells and small modules included spray, dip, roll, and brush. The criteria used to judge the merits of each technique were adhesion, optical properties, and thickness control. With regards to optical characteristics and adhesion properties, they were found to be independent of the mode of application and readily optimized to any solvent/solids composition. Concerning film thickness control, some difficulty was experienced using a "suction-pot" type spray gun because of the high dilution level (below 10% solids) necessary for this method of application. The result was a very thick wet film (70 to 75 mils of Spraylon to obtain 2 mils of dry-film thickness) that was difficult to handle, in particular along the cell edges. No further work was done using a spray technique, and recommendation was that future work be done using either a "pressure-pot" gun or an electrostatic spray technique.

It was found that for film-thickness control in the laboratory, the best results were obtained by volumetrically monitoring the Spraylon solution. Using this controlled monitoring technique it was determined that:

- For quenched films (specular), a wet film thickness of 11.4 to 11.6 mils is required for a dry film thickness of 1 mil.
- For unquenched films (diffuse), a wet film thickness of 10.2 to 10.6 mils is required for a dry film thickness of 1 mil.

The correlation of wet to dry film thickness was found to be linearly dependent on solvent/solid composition. The differences in wet/dry film thicknesses for different cooling profiles is thought to be related to the degree of crystallinity of the coating, the more crystalline state also providing diffuse reflectance properties.

3.3 ENVIRONMENTAL TESTING

3.3.1 Thermal Cycling

Earlier work in this laboratory (Ref. 4) with the heat-sealed Teflon system clearly demonstrated the problems associated with thermal cycling of coated single cells and small modules. Because of the thermal mismatch between the Teflon and the silicon, catastrophic failure modes were exhibited by the cells such as cell fracture, cell cleavage, silicon divoting, Teflon cracking, and delamination. As a result of these failures with the heat-sealed system, LMSC developed the Spraylon system in the expectation that film forming from solution on the substrate surface would relieve some of the stress setup by the heat-sealing process and thereby reduce the impact of the difference in thermal expansion between the Spraylon and the silicon.

As can be seen from the following test results, only limited success was achieved initially, with the samples exhibiting the same failure modes as in the heat-sealed system. However, as a result of detailed analytical calculations and careful thermal expansion measurements of the individual components of the system, namely silicon, solder, and Spraylon films, ultimate success was attained for the total system as a cover for single cells or small modules.

The Program Plan called for thermal cycling of both coated single cells and two-cell coupons on a Kapton substrate, at temperatures ranging from +100° to -196°C. The test parameters and results are detailed below for each series of exposed samples:

- The first test included eight coated single cells and five coated coupons, which were subjected to 10 cycles at +100° to -190°C. Radiant heating and conductive cooling were employed in a vacuum chamber. In this test the samples were mounted on a copper block using double-backed Kapton tape and can be monitored visually during the entire test.

After only one complete cycle it was observed that some of the samples, on reheating to 100 °C, lost contact with the block. The test was terminated and the chamber opened, when inspection revealed that all but three single cells and one coupon had experienced catastrophic failure. The failure modes were cell fracture, divoting, Spraylon cracking, delamination, and breaking of soldered interconnects.

- The test was repeated with the same number of samples except that the cells were mounted on the copper block with screws and not Kapton tape. Also the thermal cycle was less severe in that the minimum temperature was -120 °C. After 10 cycles the chamber was opened and the samples inspected visually and under the microscope. Only three coupons and two single cells showed no failure, while the remaining samples exhibited the same failure characteristics as before.
- A third series of tests were run in which the cycling temperatures were even less severe (+80 °C to -40 °C). It was hoped that complete survival would be demonstrated under these conditions. Three coupons and four single cells were used in this test sequence. After 10 cycles the chamber was opened and the samples subjected to a detailed visual and microscopic investigation. No failure was detected in any of the samples. The chamber was then pumped down and the samples subjected to two cycles of +100° to -100 °C. Inspection again showed no failure of any of the samples. The samples, under vacuum, were then subjected to another two cycles at +100° to -120 °C and again, as before at this lower temperature, failures were observed in all but one coupon and one single cell.

As a result of these thermal cycling tests it was concluded that failure was initiated at temperatures between -100° and -120 °C for cells both rigidly mounted or freely suspended, with the severity of damage increasing with decreasing temperatures. Both visual and microscopic examination proved conclusively that the failure was due to the mismatch of the thermal expansion characteristics of the Spraylon and the silicon cells. In all of the tests performed, the time for each cycle was about 15 min so that severe thermal shocks were not imparted to the systems.

Further experimental efforts to ameliorate effects of the thermal mismatch were conducted by totally encapsulating the cell. Only single cells were evaluated and after 10 cycles at +100° to -170°C no failure modes were found in all the five cells tested. However, total encapsulation of each cell prior to assembly was not compatible with future JPL plans for an automated cell array manufacturing process so no further effort was expended on this investigation.

During the earlier thermal cycling tests it was observed that any lifting of the Spraylon film from the cell surface during the cycle caused immediate delamination over most of the cell surface. In particular, it was noted that most of the delamination was initiated at the cell edges. Eight single cells were coated, with special care being given to ensure overcoating of the edges, and subjected to 10 cycles between +100° to -180°C. Only one cell showed any of the previous failure modes while another two showed slight delamination close to the soldered tabs, which was attributed to residual solder flux causing poor initial adhesion.

It became apparent that the temperature excursions experienced by the coated cells, during the thermal cycling, result in a severe thermal expansion mismatch of the materials so that the resultant stresses on the silicon caused by the contracting Spraylon induce a pronounced bowing of the cell. The bowing, if excessive, results in catastrophic cleavage or divoting of the silicon.

Subsequent discussions with the solar-cell manufacturers indicated that they encounter a similar bowing in the opposite direction due to the contraction of the back solder coating if the coating is thicker than 0.5 mil.

To better understand the parameters associated with the thermal cycling damage, two studies were undertaken:

- A computer study to establish the limits of the safe working stress in the coated silicon solar-cell system under thermal shock
- Determination of the thermal expansion characteristics of the three major components of the system — silicon, solder, and free-standing Spraylon film

The nonlinear, thermoelastic analysis capability of the LMSC-developed advanced laminate computer program was used to analyze those geometric parameters important to successful design of a Spraylon encapsulated solar cell and hence a complete array. In the code, developed for a prior LMSC research program, the following relationships were treated analytically:

- Maximum tensile stress within the silicon at -196°C as a function of Spraylon thickness
- Maximum tensile stress on various silicon thicknesses for a 2-mil Spraylon film thickness
- Effect of variations in the thickness of one component of the system on the radius of curvature — i.e., amount of bowing

The analytical results are presented in Figs. 3-10 through 3-12, from which it can be seen that for a typical 12-mil thick solar cell with a maximum of 1 mil of solder, a Spraylon thickness of less than 4 mils should be used. Further thermal cycling tests within the laboratory confirmed these findings, with less than 1 percent of the cells exhibiting any failure mode with 12-mil solar cells covered with 3 to 4 mils of Spraylon.

Experimental determination of the thermal expansion characteristics of the three major system components was undertaken in an effort to calculate accurately the magnitude of the contribution that each makes to the total stresses set up within the system during thermal shock. The measurements were made on a silicon single crystal cut in the 1:1:1 plane, a free-standing 5 mil Spraylon film, and a sample of vendor solder of the type used in solar-cell manufacture (MIL SN-62 containing 62% tin, 36% lead, and 2% silver.

The data are given in Table 3-7, and are represented graphically in Fig. 3-13. Included for comparison are the results for an FEP Teflon 5-mil free-standing film measured under identical conditions as the Spraylon. A difference in the thermal expansion properties of the two film materials is apparent, and indicates that over the temperature range +150° to -185°C the Spraylon film shows a better thermal match to the silicon than does the FEP Teflon film.

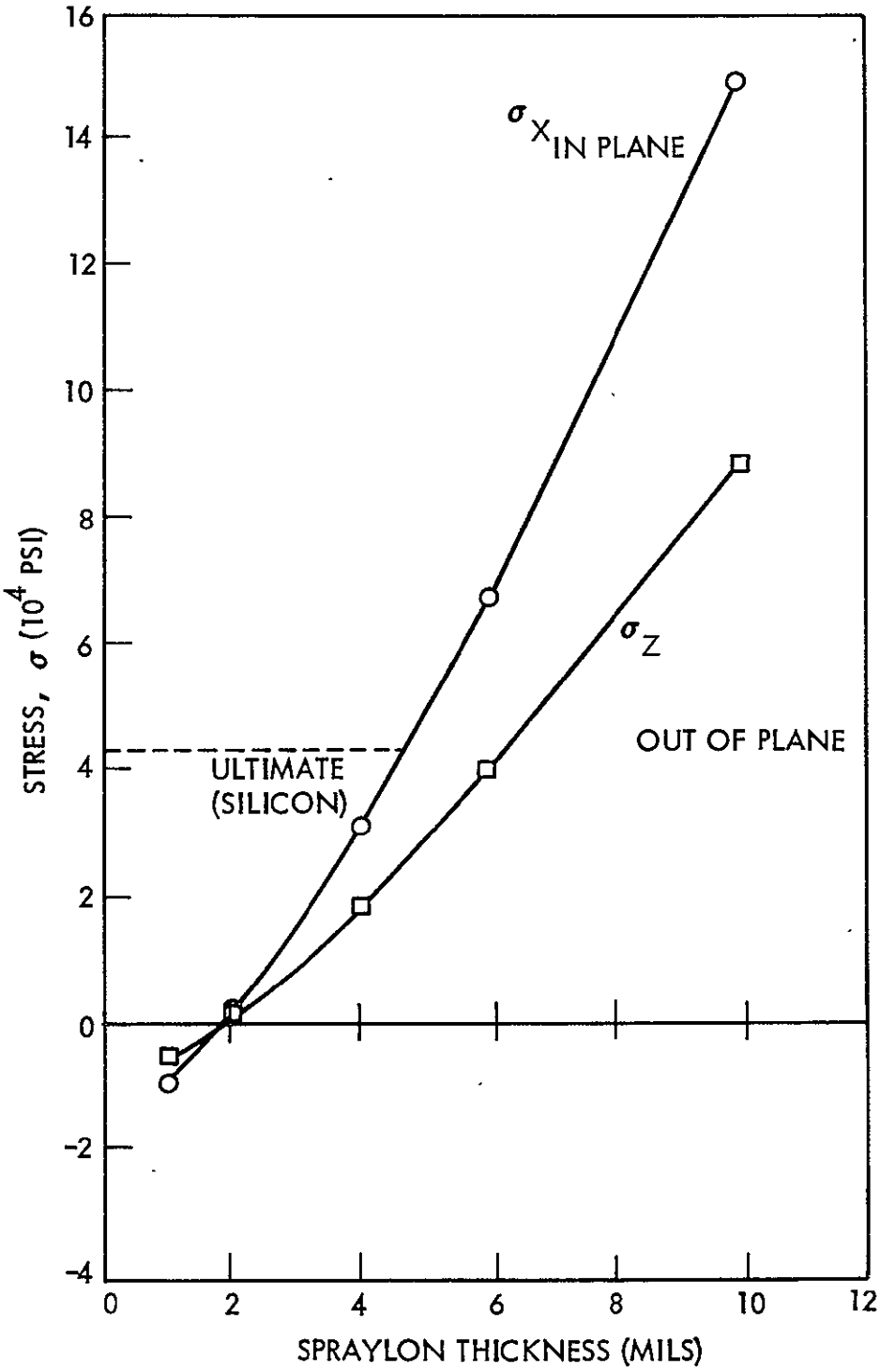

Fig. 3-10 Computer Program Analysis — Maximum Tensile Stress in Silicon Layer at -196 °C Versus Spraylon Thickness (Silicon Thickness = 0.012 in. and Solder Thickness = 0.001 in.)

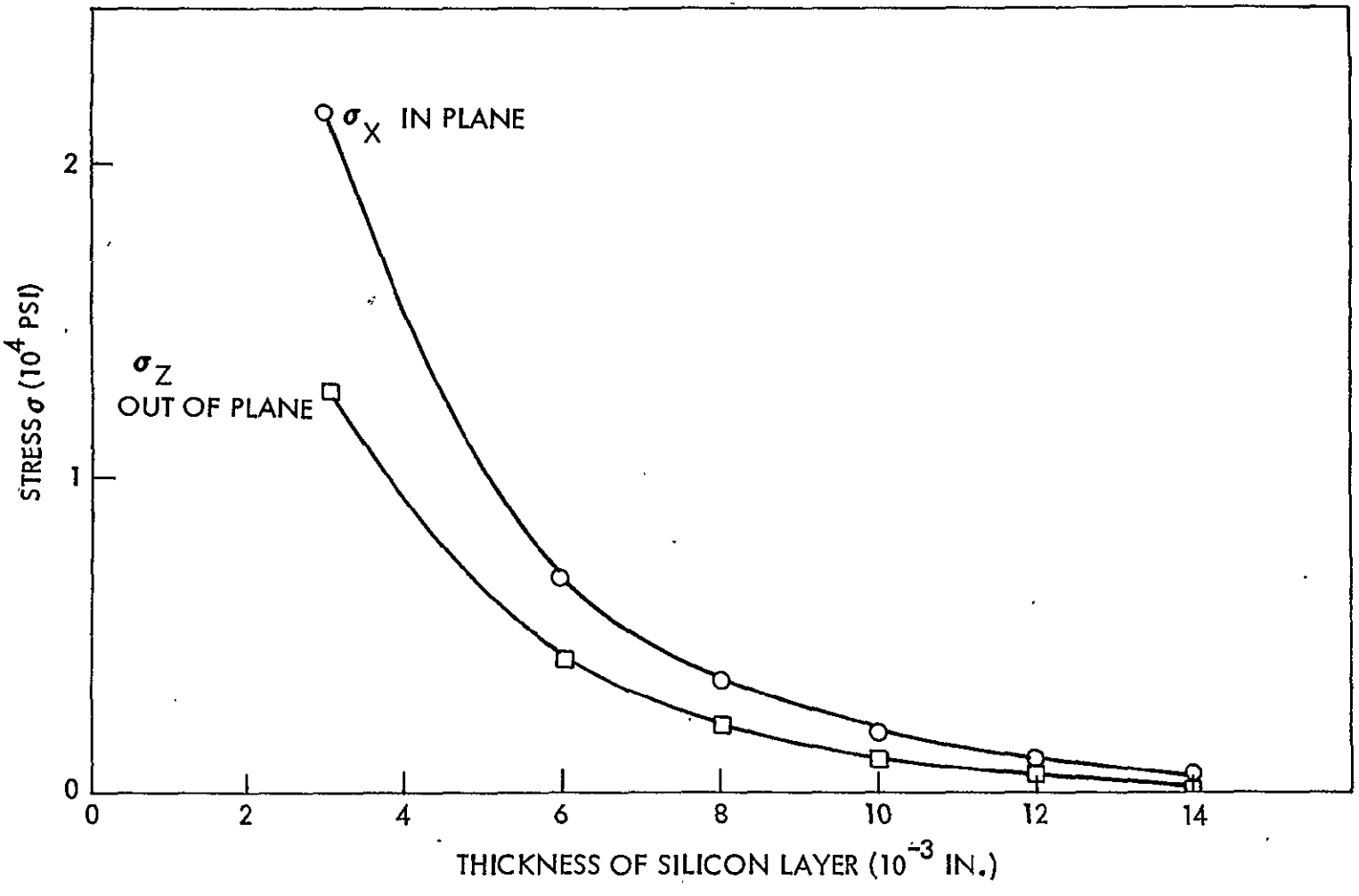

Fig. 3-11 Computer Program Analysis — Maximum Tensile Stress in Silicon Layer at — 196°C for Spraylon Thickness at 2 mils and Solder at 1 mil

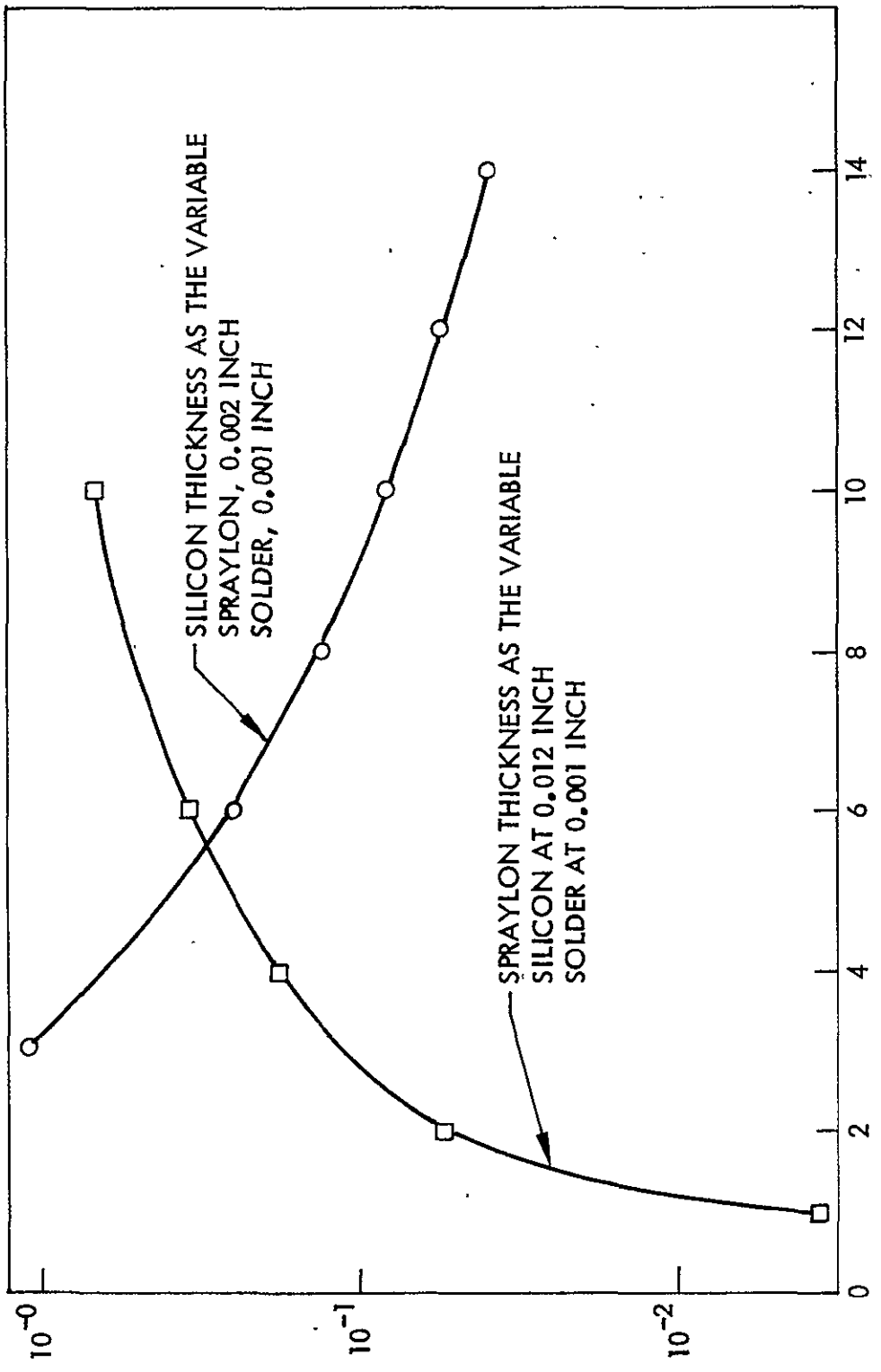

Fig. 3-12 Computer Program Analysis – Effect of Variations in Thickness of One Component on Radius of Curvature

ORIGINAL PAGE IS
OF POOR QUALITY

Table 3-7

THERMAL EXPANSION MEASUREMENTS
ON SOLDER, FEP TEFLON, SILICON, AND SPRAYLON

Temperature (°F)	Change of Length per Unit Length ($\Delta L/L$) $\times 10^3$			
	Spraylon 5-mil Film	Solder	Silicon	FEP Teflon 5-mil Sheet
200	13.88	1.76	0.316	10.65
175	10.87	1.42	0.250	8.70
150	8.08	1.07	0.189	6.48
125	5.28	0.75	0.135	4.59
100	2.70	0.45	0.079	2.77
75	0.66	0.11	0.023	0.56
67	0	0	0	0
50	-1.27	-0.20	-0.038	-1.22
25	-3.02	-0.53	-0.083	-2.78
0	-4.62	-0.84	-0.136	-4.52
-25	-6.08	-1.16	-0.187	-6.03
-50	-7.38	-1.48	-0.233	-7.74
-75	-8.32	-1.77	-0.275	-9.21
-100	-8.92	-2.09	-0.315	-10.53
-125	-9.84	-2.38	-0.350	-11.62
-150	-10.54	-2.69	-0.388	-12.63
-169	—	—	—	—
-175	-11.22	-2.86	-0.441	-13.41
-200	-11.83	-2.87	-0.462	-14.19
-225	-12.43	-2.87	-0.462	-14.80
-250	-13.00	-2.87	-0.459	-15.38
-275	-13.90	—	-0.460	-16.03
-300	-14.09	—	—	-16.61

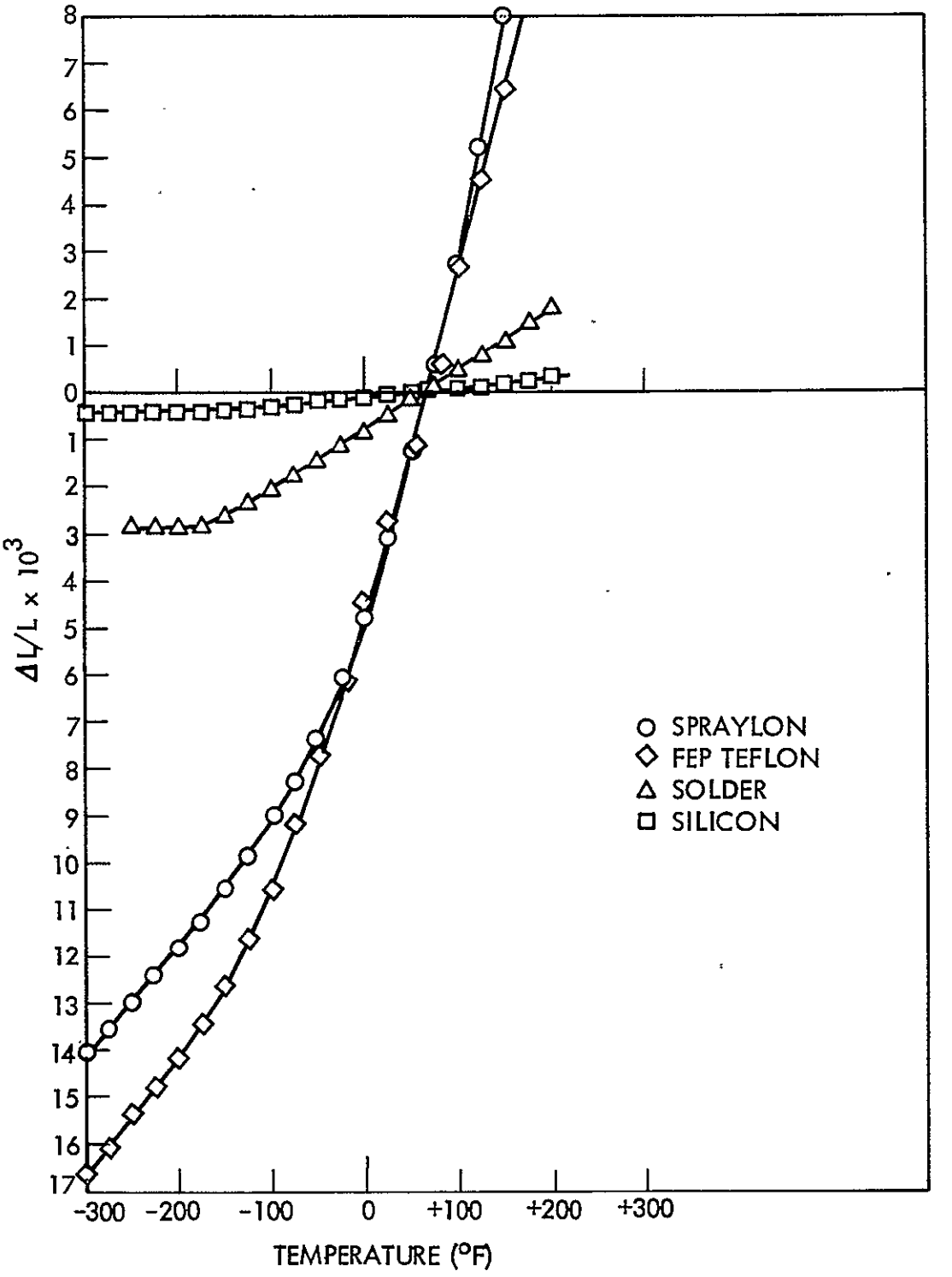

Fig. 3-13 Thermal Expansion Measurements

3.3.2 Humidity

Prior to launching, spacecraft materials are exposed to many potentially degradative environments. Among these is possible exposure to a high-humidity atmosphere, such as might be experienced during storage or on the launch pad. The behavior therefore of the Spraylon system in such an environment is necessary to the overall evaluation of the system as a candidate encapsulant.

In the laboratory, six coated cells and two coated coupons were exposed to an environment of 90 to 95% relative humidity and 40 °C for 180 days. The samples were monitored continually throughout the test visually and under the microscope and also their adhesion properties evaluated. After 180 days no delamination, blistering, or adhesion failure was noted, although a slight discoloration was observed on a few of the cell grids.

3.3.3 Radiation Effects Testing

Within the scope of the development effort, most of the work to optimize the Spraylon encapsulant was expended in the areas of physical properties. As previously described, these areas included intrinsic film properties such as optical and mechanical, permeability, and adhesion. Having made a preliminary optimization selection, it was necessary as part of the feedback process to evaluate the encapsulant system (both Spraylon and primer) on the basis of radiation stability. In these irradiation exposures, the sample temperature limits were restricted nominally to room-temperature to correspond to the program plan. All the preliminary screening tests gave good evidence that the Z6020 primed system offered the most in terms of the aforementioned tradeoffs in adhesion versus environmental stabilities.

The objective of radiation effects testing was to look at the combined Spraylon system with respect to its performance in the test environment, already knowing that the Spraylon film material itself had demonstrated adequate stability for the anticipated applications (Fig. 3-1).

Primer Stability in UV. Brief ex-situ UV exposure tests were performed to evaluate the stability of the Z6020 primer applied in a variety of concentrations, and of several additional candidate adhesion promoters which were included at the suggestion of the vendors. In this series of tests, the substrate consisted of bright aluminum panels 3-mil 2020 Alclad pre-etched with a commercial phosphoric-hydrofluoric acid brightener (Cee Bee B-66, Cee Bee Chemical Co., Inc., Downey, Calif.).

As a first approach, the primer material was applied and irradiated bare (without a Spraylon topcoat), as shown in Fig. 3-14 to determine the relative stability of the candidate primers under ultraviolet exposure in vacuum.

A series of primers that were applied by various techniques were overcoated with Spraylon and exposed. Some of the variations in application procedures included differences in primer/solvent concentration, and application of the primer followed by forced drying and also followed by solvent rinse. A comparison of Fig. 3-15 with Fig. 3-16 (where the primers were not rinsed off in processing) demonstrates the trend in susceptibility to UV degradation of the system with increasing Z6020 primer thickness. The same results were obtained with all the other primers tested. As expected, where the primer was rinsed-off to produce a very thin final layer under the Spraylon (Figs. 3-17 and 3-18), the overall degradation contribution of the primer is small, especially when the silicon solar cell's spectral response is considered.

Obviously, some of the primers exhibited a better UV stability than others. With all factors taken into consideration (adhesion promotion, thermal and UV stability), the compromise primer still proved to be Z6020.

Prior to making a final commitment, the three most promising primers — Q1-6011, Q1-6082, and Z6020 — were applied onto silicon solar cells. Heretofore, most of the UV exposure tests were performed on bright aluminum test coupons because of the increased detectability of small reflectance changes when using a spectrophotometer. Acknowledgment was made of the fact that the UV dose was actually higher because of a partial second pass through the film due to reflection, and also to the fact that the same

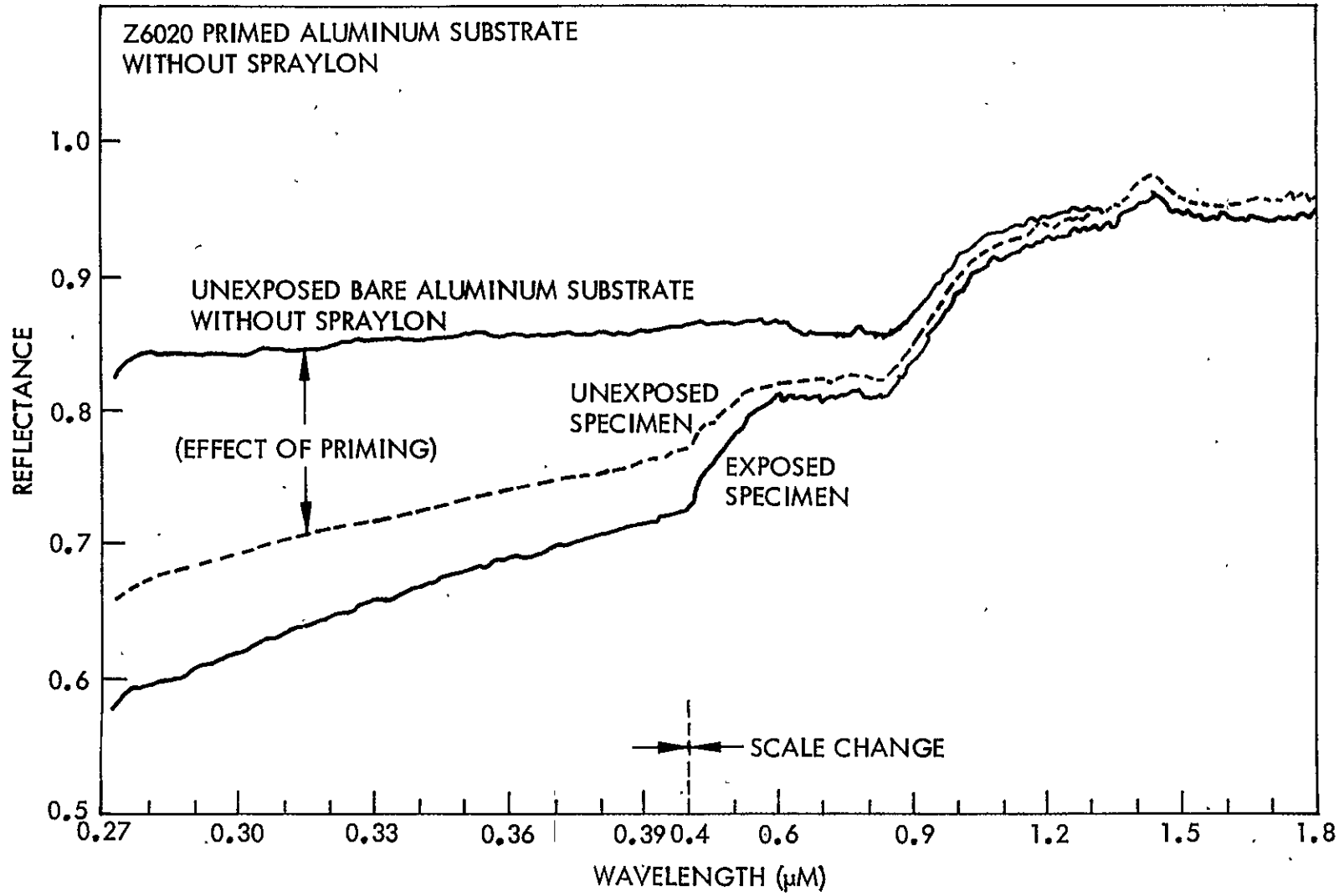

Fig. 3-14 Effect of 323 ESH UV Exposure on Reflectance

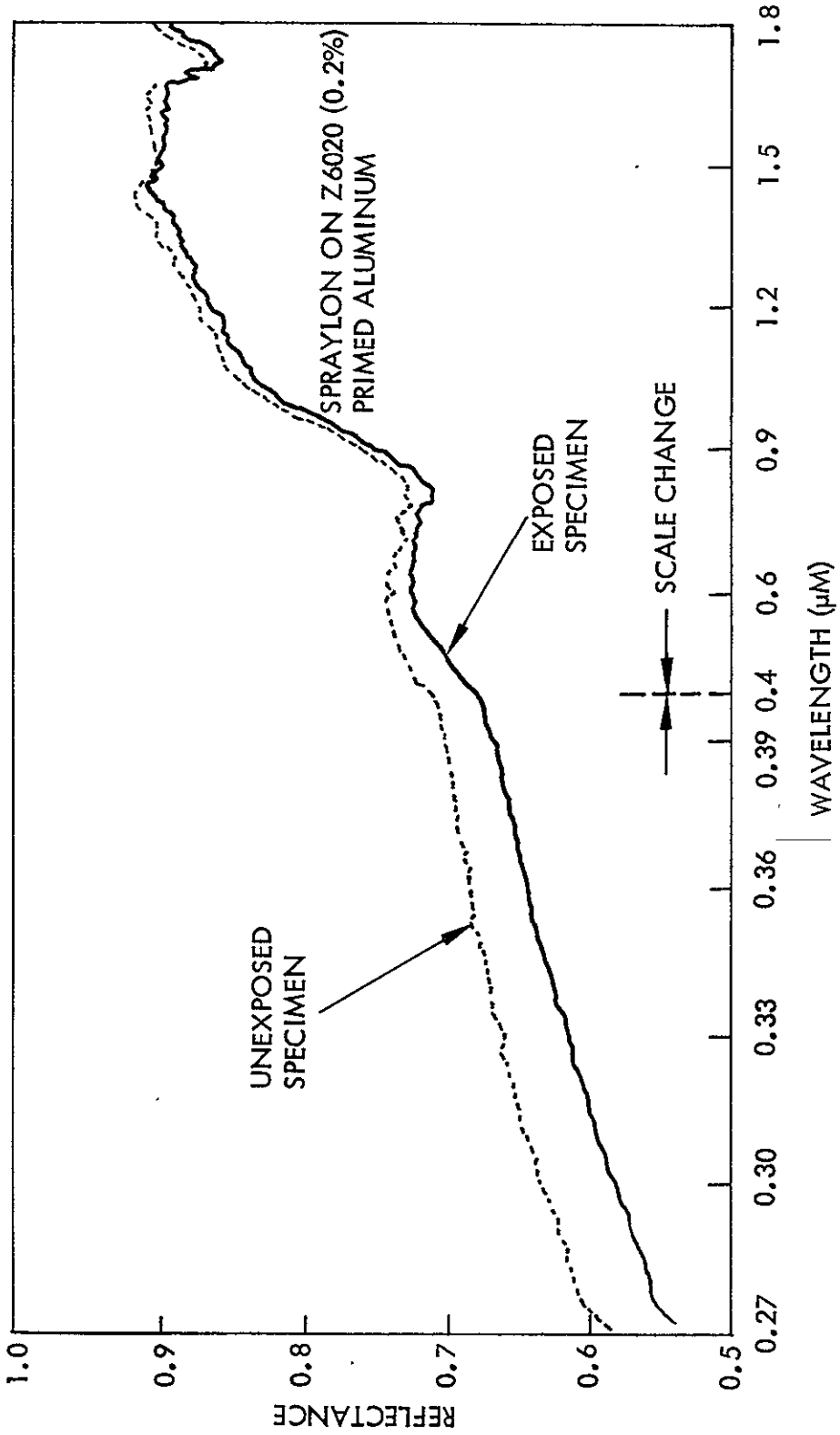

Fig. 3-15 Effect of 323 ESH UV Exposure on Reflectance

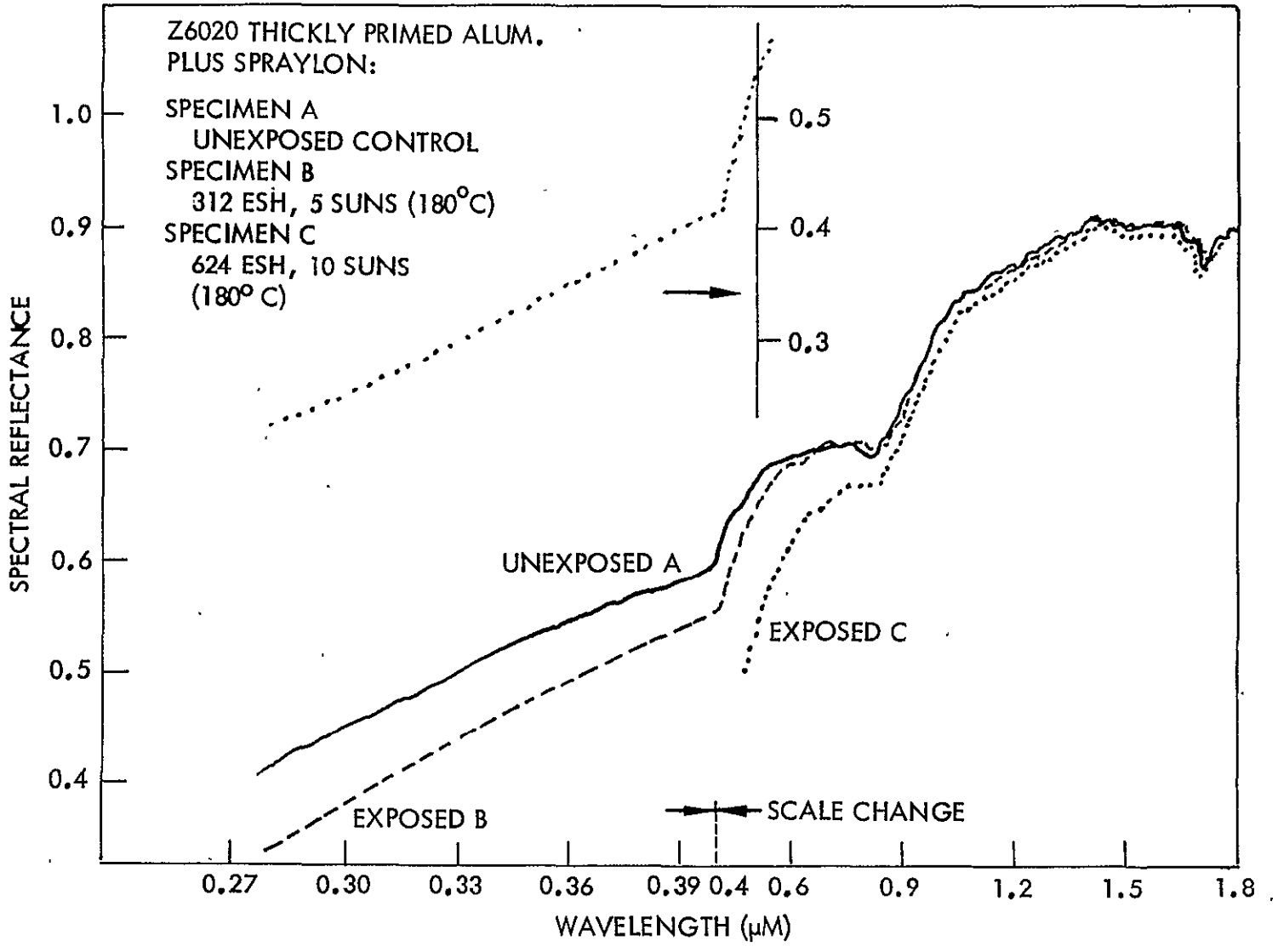

Fig. 3-16 Effect of UV Exposure Conditions on Reflectance

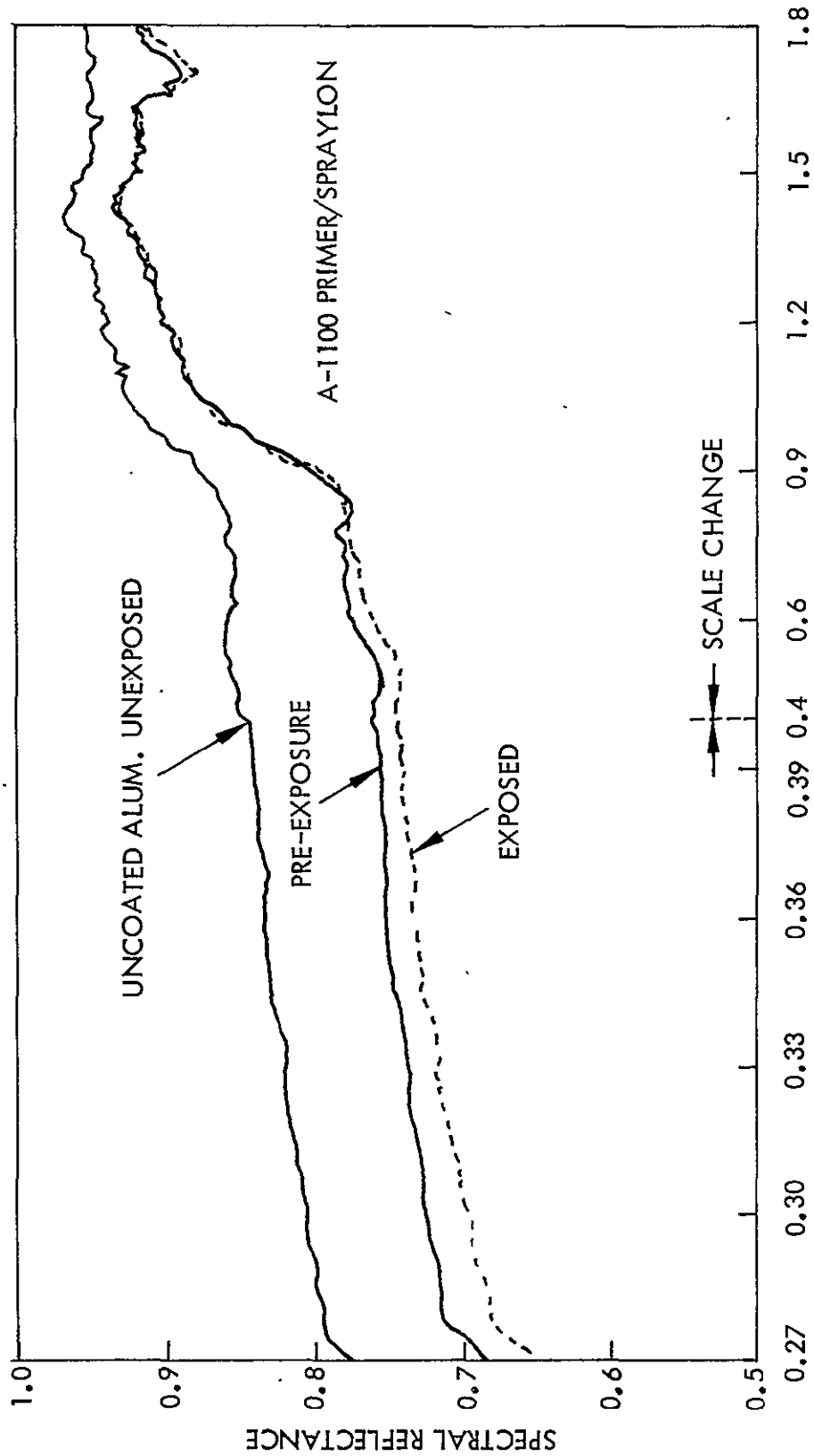

Fig. 3-17 Effect of 365 ESH UV Exposure on Reflectance

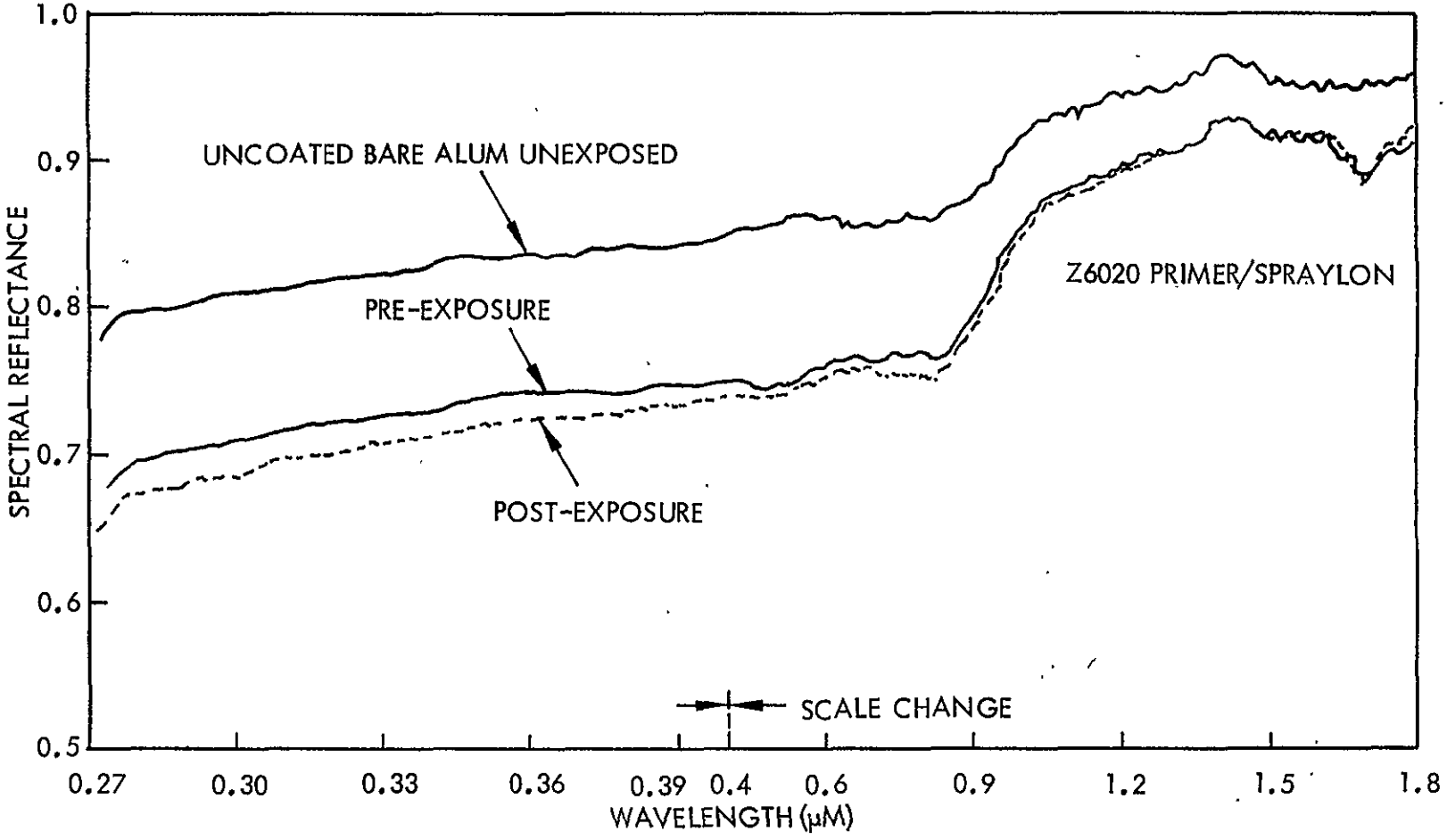

Fig. 3-18 Effect of 365 ESH UV Exposure on Reflectance

held for changes in reflectance compared to transmittance. Thus, small changes in reflectance could be magnified on the aluminum, while the same small change would result in a correspondingly small change in cell response.

The results of a test to compare the validity of the two measurement techniques, using the bright aluminum substrate as a second surface mirror and a solar cell with electrical measurements as a detector, are presented in Table 3-8.

The results comparing the three primers for their UV stability, when applied to solar cells, are shown in Table 3-9. As these data demonstrated there was no substantial difference in the stability of the Z6020, Q1-6082, and Q1-6011 primer systems. It should be noted that this series of exposures was performed with the test cells maintained at an elevated temperature (100 °C) significantly higher and potentially more harsh than the previous test performed at room temperature (20 °C).

Low-Energy Proton Testing Plus UV Testing. Low-energy proton exposure testing was performed on a group of five encapsulated cells at a constant 40-keV energy and a flux of 1.1×10^{14} p+/cm^2-sec. These cells were thermally cycled after exposure from room-temperature to liquid nitrogen temperature (-196 °C). They were next submitted to a UV irradiation exposure of 330 equivalent suns while being maintained at 100 °C. The results presented in Table 3-10 are only indicative and inconclusive. During the proton exposure, a leak developed in the vacuum chamber and some backstreaming of oil from the diffusion pump systems occurred. This resulted in deposition of an oil film on the specimens which became polymerized during proton exposure, resulting in a brown varnish on the cells and sample holder. Evidence of contamination was also obtained from optical measurements on a second surface mirror mounted alongside the samples. Sufficient time was lacking for a more detailed follow-on test.

Table 3-8

COMPARISON OF EFFECTS OF ULTRAVIOLET EXPOSURE ON SPRAYLON COATED SUBSTRATES MAINTAINED AT ROOM TEMPERATURE (~ 18°C)

Substrates	Uncoated	Coated With Spraylon/Z6020 Primer	
		Before Exposure	After Exposure
Bright Etched Aluminum			
1	$\alpha_S = 0.093$	$\alpha_S = 0.107$	$\alpha_S = 0.111$
2	$\alpha_S = 0.093$	$\alpha_S = 0.106$	$\alpha_S = 0.112$
Silicon Solar Cell			
1	$I_{sc} = 150.8$	$I_{sc} = 152.7$	$I_{sc} = 149.0$
2	$I_{sc} = 151.2$	$I_{sc} = 152.3$	$I_{sc} = 149.2$

Fluence: 1200 Equiv. Sun-hr at 5 Suns

Table 3-9

EFFECT OF ULTRAVIOLET EXPOSURE AT ELEVATED TEMPERATURE (100°C) ON ELECTRICAL PERFORMANCE (I_{sc}) OF SILICON SOLAR CELLS ENCAPSULATED WITH SPRAYLON AND THREE SELECT PRIMERS

Primer	Number of Specimens	Change in Short Circuit Current — Bare Unexposed Cells and Exposed Coated Cells (%)	Fluence, (Equivalent Sun Hr, ESH)
Dow Corning Q1-6011	10	Average: 4.4 Range: 2.3 to 6.9	1178 ESH at 5 suns
	1	— 6.8	2356 ESH at 10 suns
Dow Corning Q1-6082	10	Average: 1.7 Range: 1.1 to 3.0	1178 ESH at 5 suns
	1	— 1.5	2356 ESH at 10 suns
Dow Corning Z6020	2	1.8 and 2.1	1178 ESH at 5 suns

Table 3-10

EFFECTS OF ULTRAVIOLET EXPOSURE (330 ESH, 5 SUNS) AT ELEVATED TEMPERATURE (100°C) ON THE ELECTRICAL PERFORMANCE (I_{SC}) OF SILICON SOLAR CELLS ENCAPSULATED WITH SPRAYLON AND THREE PRIMERS, AFTER PRIOR EXPOSURE TO LOW-ENERGY PROTONS (40 keV)

Primer	Specimen	Change in Short Circuit Current After UV Exposure (%)	Proton Exposure Prior to UV (p^+/cm^2)
Q1-6066	(S-44)	8.9*	5×10^{14}
	(S-45)	3.0	5×10^{14}
Q1-6082	(S-20)	1.9	5×10^{14}
	(S-135)	0.9	5×10^{14}
Z6020	(S-56)	9.3	5×10^{14}

*Cells chipped during mounting.

Table 3-11

EFFECT OF HIGH-ENERGY ELECTRON EXPOSURE ON ELECTRICAL PERFORMANCE OF COATED SILICON SOLAR CELLS

Specimen Description	Change in Maximum Power Due to Irradiation (%)	Change in Short Circuit Current (%)	Fluence 1 MeV Electrons (e^-/cm^2)
Spraylon Coated 2 by 2 cm Cell			
1	17.5	12.6	4×10^{14}
2	18.2	14.4	
3	8.1	13.4	
4	15.4	13.3	
Conventionally Covered 2 by 2 cm Cell (15 cells)	Average: 17.4	Average 14.4	4×10^{14}

Spraylon System Stability to High-Energy Electrons. In order to complete the irradiation exposure picture, a test was conducted to determine the susceptibility of the Spraylon encapsulated solar cells to damage by high-energy electrons. Four 2 by 2 cm solar cells, with electrical tabs attached, were encapsulated with 2 mils of Spraylon, using Z6020 as the adhesion promoter. These cells were measured electrically and added to an electron irradiation test being performed on 15 of LMSC's conventionally covered (fused silica) cells. The exposure consisted of 5×10^{14} e^-/cm^2 at 1 MeV. The four Spraylon cells were measured for electrical characteristics before and after the exposure. The results are presented in Table 3-11.

An examination of the data and the Spraylon-coated cells indicates that no apparent damage occurred to the encapsulant or to the interface. The Spraylon cells' electrical characteristics were degraded no worse with 2 mils of Spraylon than were the conventionally covered cells with 12 mils of cover slips plus their adhesives, indicating that the transmittance characteristics of the Spraylon were not altered.

Spraylon Exposure to UV at Elevated Temperatures. As a final verification of the UV stability of the Spraylon system with Z6020 primer, and to determine the temperature dependence of the degradation mechanism, a series of test coupons was prepared and exposed. These bright aluminum coupons, each covered with 2.5 mils of Spraylon, were divided into three sets. The first set, unexposed, served as the control. The remaining two sets were exposed to 1000 ESH of simulated UV in vacuum. One set was maintained at room temperature (20°C) while the other set maintained at 50°C.

After the exposure tests, all three sets had their topcoat (with primer attached) peeled-off for spectral transmittance measurements. The results are shown in Fig. 3-19.

A comparison of these results with those given in the previous data of Table 3-8 shows a good correlation. The observed UV irradiation damage of the Spraylon-primer system increases with increasing sample temperature, as would be expected. Fortunately, as seen in this figure, the major area of transmittance change is in the shorter wavelength region where typical solar cell response is decreasing rapidly.

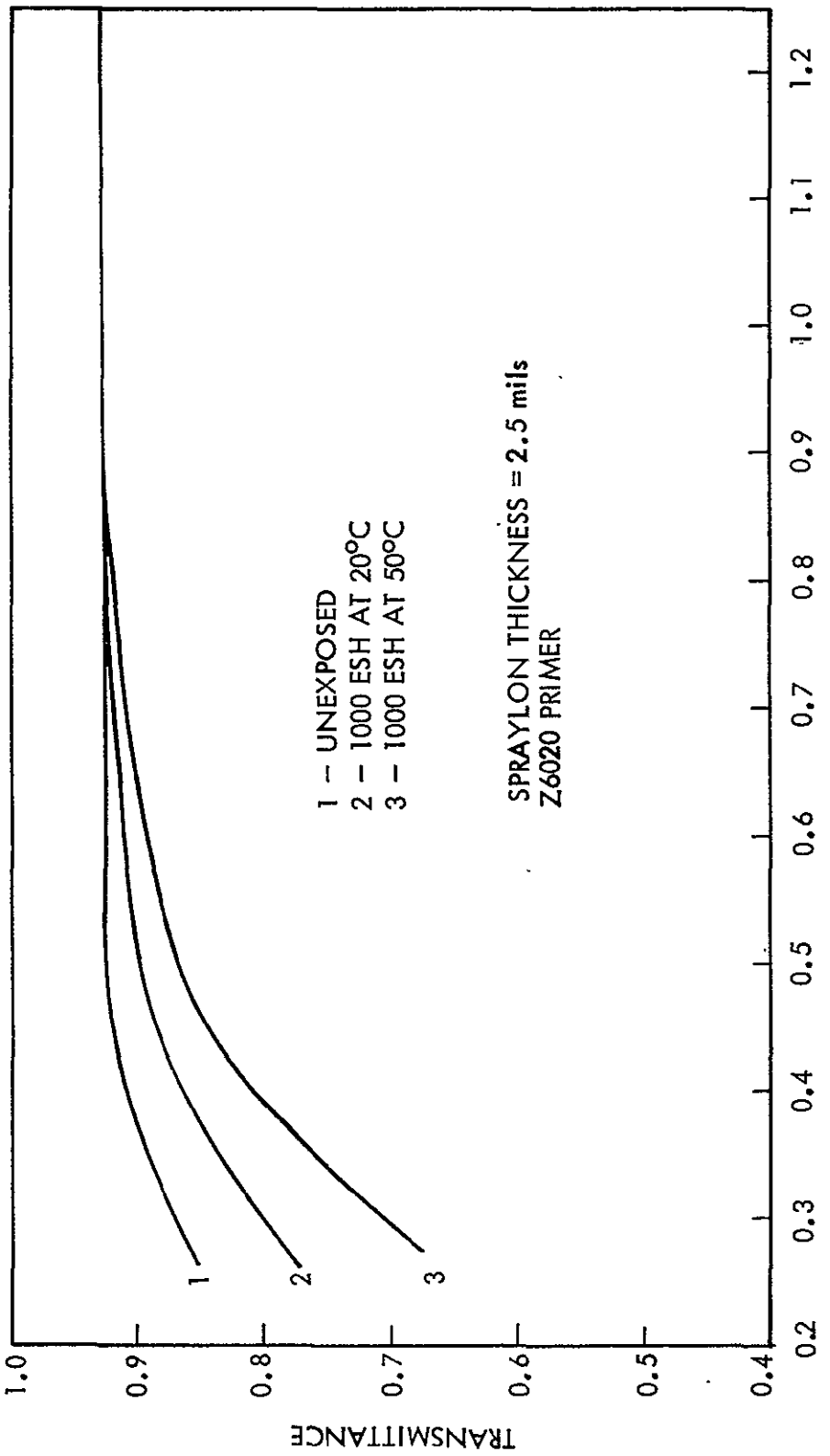

Fig. 3-19 Effect of Temperature on UV Degradation of Spraylon

3.4 PROCESS OPTIMIZATION

The knowledge and experience gained as a result of performing the three prior tasks were used in the selection of optimum processing conditions for Spraylon encapsulation of silicon solar cells and cell coupons. Through these parametric studies, appropriate tradeoffs were evaluated for the definition of optimum processing conditions relative to the selected deposition techniques. The significant factors that contribute materially to optimization and that were addressed are discussed in the following paragraphs.

3.4.1 Solar-Cell Cleaning

The silicon solar cell must be meticulously clean prior to Spraylon processing. The entire surface must be free of foreign polymers and contaminants, so that the primer (adhesion promoter) can actually wet the cell's surface. Although great care generally is taken in processing and handling the solar cells through all the steps from fabrication to the point of encapsulation, there is always a potential for unsuspected contamination. The initial set of cells supplied and used for testing were of a 1968 manufacture and were found to have a surface coating contaminant which would not come off with conventional solvent or detergent scrubbing. Rather harsh abrasive cleaning procedures were needed to physically remove the film. Removal of the coating could be readily seen by a change in deepening of the surface's blue color and by primer wetting. It is believed that this contaminant film on the cells' faces was a polymerized oil-like coating from the cell manufacturer's process vacuum system. The manufacturer verified that their processing at the time used a system with oil diffusion pumping and electron-beam evaporation. This procedure easily accounts for the polymerized contaminant film; however, the procedure has been eliminated in current fabrication techniques, and batches of fresh cells confirm that the surfaces are indeed free of contaminants as shown by the ease and completeness of primer wetting. The only practical test available to the investigators to determine acceptable cleanliness of the cell's surface is wettability by the primer. The use of spectral measurements, such as solar reflectance and room temperature emittance, would not have been sensitive enough to detect and quantify the contaminant.

Good adhesion of Spraylon over the complete cell surface is very important. This is particularly true over the buss-bar region of the soldered-type cells since this area produces a step in the surface and imposes an additional stress potential to the film during thermal cycling. Any areas where electrical connections are made by conventional solering must be absolutely clean of flux. Therefore, good practice dictates that all cells and coupons be thoroughly cleaned by solvent wash and thoroughly dry before encapsulation begins. In most cases, high quality isopropyl alcohol proves a suitable cleaner.

3.4.2 Solar Cell Priming

It is mandatory that a primer be employed prior to the Spraylon encapsulation so that adequate cell and coupon coverage is obtained. As described earlier in the primer section, the material considered in the tradeoffs as the optimum was Union Carbide Z6020. This is an amino functional silane: N, beta (amino ethyl) gamma amino propyl tri-methoxy silane. In the tradeoffs, consideration was given to the superior adhesion imparted by the primer and the potential hazard for both thermal and photodegradation. To achieve an optional compromise, it was decided to use this material at a dilution in methanol of approximately 0.05 percent.

The primary procedure established — to ensure that complete coverage was obtained, that the primer thickness was minimal, and that the priming reaction (hydrolysis of the silane substituents) had proceeded — was as follows. The solvent cleaned cells were immersed for 2 min in the freshly prepared 0.05 percent conentration of Z6020 in absolute methanol. Adsorbed moisture on the cell's surface provided the source to drive the hydrolysis reactions. At the appropriate time, the cells were removed and the excess primer rinsed off with clean methanol. In the case of larger modules, the fresh primer was applied onto the surface by brush techniques and rinsed by spray. After priming and rinsing, the surface was air dried and oven baked at 50° to 60°C for 2 min.

3.4.3 Solar Cell Encapsulation

Spraylon encapsulation has to be applied immediately after the primer has dried (by oven cure) to prevent loss of surface reactivity. It soon became apparent in the optimization process that it was necessary to coat the cell edge as well as the surface, to minimize the high stress concentrations which can develop and initiate coating delamination during rapid cooling to temperature extremes. Once started, the slightest delamination was observed to quickly result in catastrophic failure during liquid nitrogen immersion. Fortunately, edge coverage (and attendant edge protection) is normally acquired by the anticipated process of overcoating the preassembled modules in the automated process.

The selection of the 15 percent solids for use as the encapsulant material was based on ease of handling, acceptability of processing viscosity, and control of ultimate thickness of the film. The concentration and viscosity, as shown elsewhere in this report, have no effect on the optical, mechanical, or stability characteristics of the final product. They were selected solely on the basis of compatibility with the processing, and can be easily altered to fit other systems as needed. For a solar cell nominally 12 mils thick, the Spraylon dry film coating should not exceed 3 mils in thickness, if the system is expected to be thermally shocked to -196 °C. The study of the stresses imposed upon the solar cell by Spraylon at the lower temperatures is described elsewhere in this report. It serves as a controlling guide for the selection of coating thickness to meet the penetrating radiation protection requirements without imposing a potential for thermal cycling failure.

3.4.4 Solar Cell Encapsulant Cure

As soon as possible after the Spraylon is applied, it must be placed in the heated drying zone and processed. The primed substrate, after application of the required amount of Spraylon (approximately 12 mils of wet 15 percent solids film for each 1 mil of desired dry film), is quickly placed in a vented oven and brought up to 180 °C

in 10 minutes to facilitate solvent flash-off. The complete curing is achieved by maintaining the coating at 180 °C for an additional 15 min. This additional processing is vital to ensure that all residual solvents have been driven off from the coating. Without this assurance, a potential source of degradation exists.

3.4.5 Solar Cell Encapsulation Quenching

After the processing to make certain that all residual solvents have been removed, the hot encapsulated solar cell's cured film is then subjected to either one of two post-deposition treatments. The cooling process can be a programmed slow cool-down or a rapid quench (in cold water, for example). The former treatment results in a diffuse film surface finish, while the latter produces a clear, nonscattering specular film. Since the main objective of this program was to develop Spraylon as a solar cell cover material, the cold-water quench treatment was used. A comparison of the specular and the diffuse results of the film processing was described earlier.

A comparison of the results presented in Table 3-12 indicates that the Spectrolab solar cells exhibited a detectable decrease in maximum power (about 1 to 3%) because of heating while soldering measurement tabs onto the bus bar strip. The power-loss effect of next subjecting the cells, with the tabs attached, to the processing temperature used to cure the Spraylon is also shown in the Table to be essentially equivalent (about 1 to 3 percent) to the loss due to the soldering.

The effect on the maximum power of solar cells (with the tabs already attached) by subjecting them to the complete Spraylon encapsulation is also shown in the Table. These results indicate that there is little difference in the decreases in maximum power attributable to the processing temperatures. The conclusion, therefore, is that the Spraylon film processing per se contributes little to the overall loss in maximum power. This result is not surprising in view of the very high transmittance of the Spraylon and low refractive index, which provides an excellent match with the antireflection coating on the cells.

Table 3-12

COMPARISON OF CHANGES IN CELL PERFORMANCE DUE TO PROCESS PARAMETERS

Sample Series	Cell Electrical Characteristic, (Power MW)					
	P_o	P_f	$P_o - P_f$	Change (%)	Change Due to Soldering (%)	Change Due to Encapsulation (%)
Series 1 — Fast Quench in Water	62.56	62.24	-0.32	-0.51	-1.67	Average* value = -2.80
	63.06	61.48	-1.58	-2.50	-2.49	
	65.71	64.77	-0.94	-1.40	-1.53	
	66.08	65.00	-1.08	-1.60	-0.71	
	66.13	65.74	-0.39	-0.60	-1.73	
Series 2 — Slow Cool at Room Temperature	65.89	65.32	-0.57	-0.87	-1.01	Average* value = -3.82
	65.75	64.03	-1.72	-2.6	-1.20	
	66.13	65.04	-1.09	-1.6	-1.42	
	66.69	66.74	+0.05	+0.08	-2.95	
	67.30	66.36	-0.94	-1.4	-1.95	

*These results are the average of three cell measurements.

Section 4
CONCLUSIONS AND RECOMMENDATIONS

The Lockheed proprietary Spraylon system has been shown to offer a promising alternative to conventional adhesive-bonded fused-silica cover glasses for spacecraft solar arrays. The results of this research and development effort have demonstrated that the Spraylon system:

- Has been optimized with respect to processing parameters compatible with a conceptual automated solar-array manufacturing facility
- Can be viscosity controlled by adjusting solids content to conform to conventional application requirements characteristics of spraying, rolling, or dipping techniques
- Is compatible with the substrate and interconnect materials anticipated for use in the fabrication of flexible arrays, as well as selected potting materials
- Has very high solar transmission properties comparable with fused silica
- Provides high emittance ($\epsilon > 0.8$) on silicon solar cells for film thickness 1 mil (0.001 in.) or greater
- Provides excellent adhesion to solar cells, interconnect members, and module substrates when appropriate priming techniques are employed
- Retains high solar transmittance under short-term ultraviolet and electron irradiation at temperatures below 40°C
- Requires the use of a compromise primer system that undergoes some UV and thermal degradation
- Exhibits satisfactory mechanical behavior, including tensile strength, flexibility, abrasion resistance, and tear resistance
- Shows no measurable outgassing in terms of total weight loss (TWL) or volatile condensible material (VCM)
- When appropriately primed and applied in thicknesses 3 mils or less (to 12-mil solar cells), survives repetitive thermal cycling between -196° and +100°C, consistent with the analytical stress analysis

- Provides moisture permeability resistance superior to that of the Kapton substrate
- Survives high humidity exposure for extended periods with no evidence of delamination
- Shows good retention of mechanical properties under ultraviolet and low-energy proton exposure
- Exhibits temperature-dependent optical degradation in the ultraviolet and near-visible spectral region that requires further definition with respect to specific mission design requirements

To increase the utility of the Spraylon system with respect to general acceptance and incorporation into the manufacturing technology of low-cost solar arrays, the following efforts are recommended for additional study:

- Evaluation of the long-term radiation stability of the Spraylon system (ultraviolet, electron, proton) with emphasis on high-temperature performance
- More sophisticated stress analysis to define encapsulant parameters critical to specific array designs incorporating advanced state-of-the-art approaches to light-weight, high-performance solar arrays
- Development and evaluation of application techniques for large modules
- Quantification of the Spraylon system technology with the generation of appropriate documentation suitable for eventual incorporation into manufacturing specifications for automated production of solar arrays

Appendix A

EXPERIMENTAL APPARATUS

A.1 STATIC ULTRAVIOLET EXPOSURE APPARATUS

The static ultraviolet exposure chamber is a water-cooled stainless steel bell Jar 35 cm (14 in.) tall and 35 cm (14 in.) in diameter. The solar cells are mounted on a water-cooled, semicylinder copper sample holder concentric with the ultraviolet source and at a distance of 10 cm (3.9 in.), which results in nominal irradiances of 10 suns of ultraviolet energy. A flux density of 1 sun of ultraviolet energy is defined as the flux density of extraterrestrial radiation at 1 AU from the sun, in the wavelength interval of 0.2 to 0.3 μm (2000 to 3000 Å). It is possible to reduce the intensity at the sample plane by interposing a neutral density screen between the lamp and specimen. Conversly, intensities greater than 10 suns can be achieved by the use of copper blocks on the sample table, which bring the samples closer to the source. A calibration curve of the variation of intensity with sample-to-lamp distance has been obtained.

At the nominal 10-sun intensity, specimens are maintained between 35° and 45°C, depending on the optical characteristics of the material. Thermal contact of the sample with the water-cooled block is provided by dual screws and washers which bear on the sample edges pressing the specimens against the copper holder. Specimens can be maintained at elevated temperatures (up to 150°C) by substituting an ethylene glycol bath with a temperature-controlled circulating system for the tap-water cooling. Vacuum is established prior to initiation of ultraviolet exposure with a cryogenic sorption roughing pump and a high vacuum ion pump to avoid potential oil contamination problems. The chamber pressure is typically 2×10^{-7} torr.

The source of ultraviolet energy is a 1-kW A-H6 (PEK Labs Type C) high-pressure mercury-argon capillary arc lamp. Approximately 35 percent of the lamp's radiant

output is in the interval 0.2 to 0.4 μm (2000 to 4000 Å). The total output of the lamp is in the interval 0.2 to 2.6 μm (2000 to 26,000 Å). The lamp is water cooled and has a quartz water jacket and velocity tube. This assembly is lowered into a quartz envelope extended into the exposure chamber from the top. The assembly can be withdrawn to change lamps without disturbing the established vacuum. Unless a lamp ruptures, it is run for 100 hr and then replaced. Each test begins with a new lamp. This procedure is followed because the A-H6 output decreases with time more in the 0.2 to 0.3 μm (2000 to 3000 Å) interval than in the 0.3 to 0.4 μm (3000 to 4000 Å) interval. Therefore, for materials that are degraded primarily by energy of wavelengths less than 0.3 μm (3000 Å), an old lamp will produce less degradation than a new lamp for the same total ultraviolet exposure, expressed in sun-hours. Some control over this effect is achieved by following this standard replacement procedure.

The ultraviolet intensity is monitored external to the vacuum chamber with a calibrated RCA 935 phototube in conjunction with a Corning 7-54 filter, which transmits only the near-ultraviolet output of the lamp. The output of the phototude is automatically measured and recorded for a few minutes each hour with a recording microammeter. The intervening quartz window and 7-54 filter are periodically checked for degradation in spectral transmittance and cleaned or replaced as necessary. When desired, a Corning 0-54 filter is used to compare the intensity in the 0.2 to 0.3 μm (2000 to 3000 Å) region with that in the 0.3 to 0.4 μm (3000 to 4000 Å) region as a measure of the relative degradation of lamp output in the shorter wavelength regions.

A.2 COMBINED ENVIRONMENT CHAMBER

The chamber, which affords simulation of three separate environments concurrently (proton only, ultraviolet only, and combined proton-plus-ultraviolet), is fabricated from 301 stainless steel with an extensive cryogenically cooled baffling system enclosing the test sample table during exposure. The sample table is so designed as to allow variation of exposure temperature from 77° to 423°K. The pumping is provided by suitably baffled diffusion pumps. The system is capable of maintaining a pressure of 5×10^{-7} torr during exposure conditions.

The proton source is an Ortec rf ion source and mass analyzer unit consisting of an rf source, an Einzel lens, and a crossed field (magnetic x electrostatic) analyzer. The unit operates with accelerating voltages between 1 and 50 keV. Absolute proton intensity at the test sample location is determined using a series of Faraday buttons which are interchangeable with the test table and can traverse the entire proton beam at the sample location. During proton exposure a Faraday button in the sample plane is monitored continuously as a measure of beam stability and reproducibility.

Ultraviolet radiation is provided by an AH-6 water-cooled mercury arc (1 kW), and is introduced as a collimated beam through a fuxed silica window in the chamber. UV intensity is mapped by the use of a calibrated Eppley thermopile mounted in the sample plane.

The Chamber facility is shown schematically in Fig. A-1.

A.3 THERMAL DECOMPOSITION/VOLATILIZATION-SMOKE TEST APPARATUS

A chromium-plated stainless steel chamber, nominally 3 in. in diameter and 2 in. in length provides a container for the test specimen mounted on a flat plate. The stainless steel chamber is fastened to a water-cooled copper block in a vacuum chamber. A front surface aluminum mirror, also mounted to the cooled block, is used to collect products of thermal decomposition/volatilization that emanate from the heated test material.

The spectral reflectance of the mirror is measured prior to and subsequent to specimen heating to evaluate the optical properties of condensed material evolved from the test specimen.

Chromel-alumel thermocouples are mounted on the front surface of the test panel and temperature history is recorded during heating. A bank of quartz envelope tungsten lamps, located outside the quartz bell jar, are used to irradiate the stainless steel chamber and the sample back face.

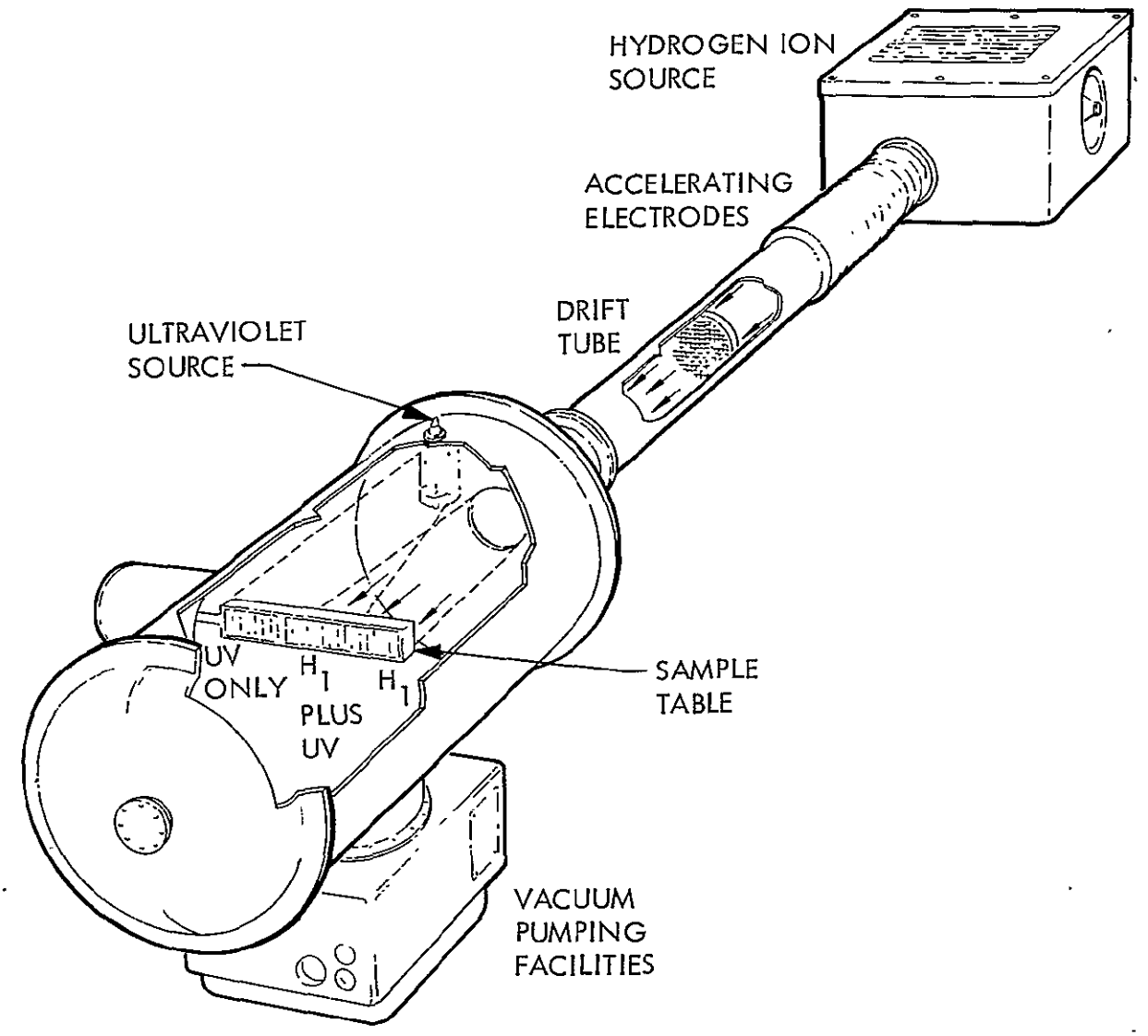

Fig. A-1 Lockheed Combined Environments Chamber

This facility is used to supplement the standard SRI test which measures total weight loss (TWL) and volatile condensible material (VCM). It provides additonal insight into the nature of condensed effluents with respect to effects on the optical properties of adjacent surfaces of operational spacecraft. Figure A-2 shows the facility schematically.

A.4 THERMAL CYCLING EQUIPMENT

Two methods of thermal cycling were used in this program. Initial thermal cycling efforts employed a bell jar vacuum system with a liquid nitrogen plate to which samples were mounted. Cooling was achieved conductively, and heating was provided by quartz envelop tungsten lamps mounted internally. Subsequently, attempts were made to allow radiative cooling by isolating the solar cell specimens from the cold wall. However, the design of this facility did not permit total observation of the coated cells during thermal cycling and it became difficult to correlate specimen failures with thermal history. Consequently, a new approach to the thermal cycling task was taken.

The second approach, which proved to be more practical, involved the use of a finned copper tray instrumented with thermocouples. Solar cell specimens placed in the tray were cooled as the apparatus was lowered gradually into a liquid nitrogen bath. Specimens were cooled readily to -196°C without immersion of the cells in the liquid nitrogen. Additionally, when required cells could be held under in liquid nitrogen medium. The heating regime of the thermal cycling was accomplished by raising the tray and subjecting it to radiant heating. Figure A-3 shows the facility in a schematic fashion.

A.5 OPTICAL MEASUREMENTS

Spectral reflectance measurements on solar cells and coated aluminum coupons were performed using a Cary Model 14 spectrophotometer equipped with an integrating sphere attachment. The wavelength region of measurements covered 0.27 to 1.8 μm.

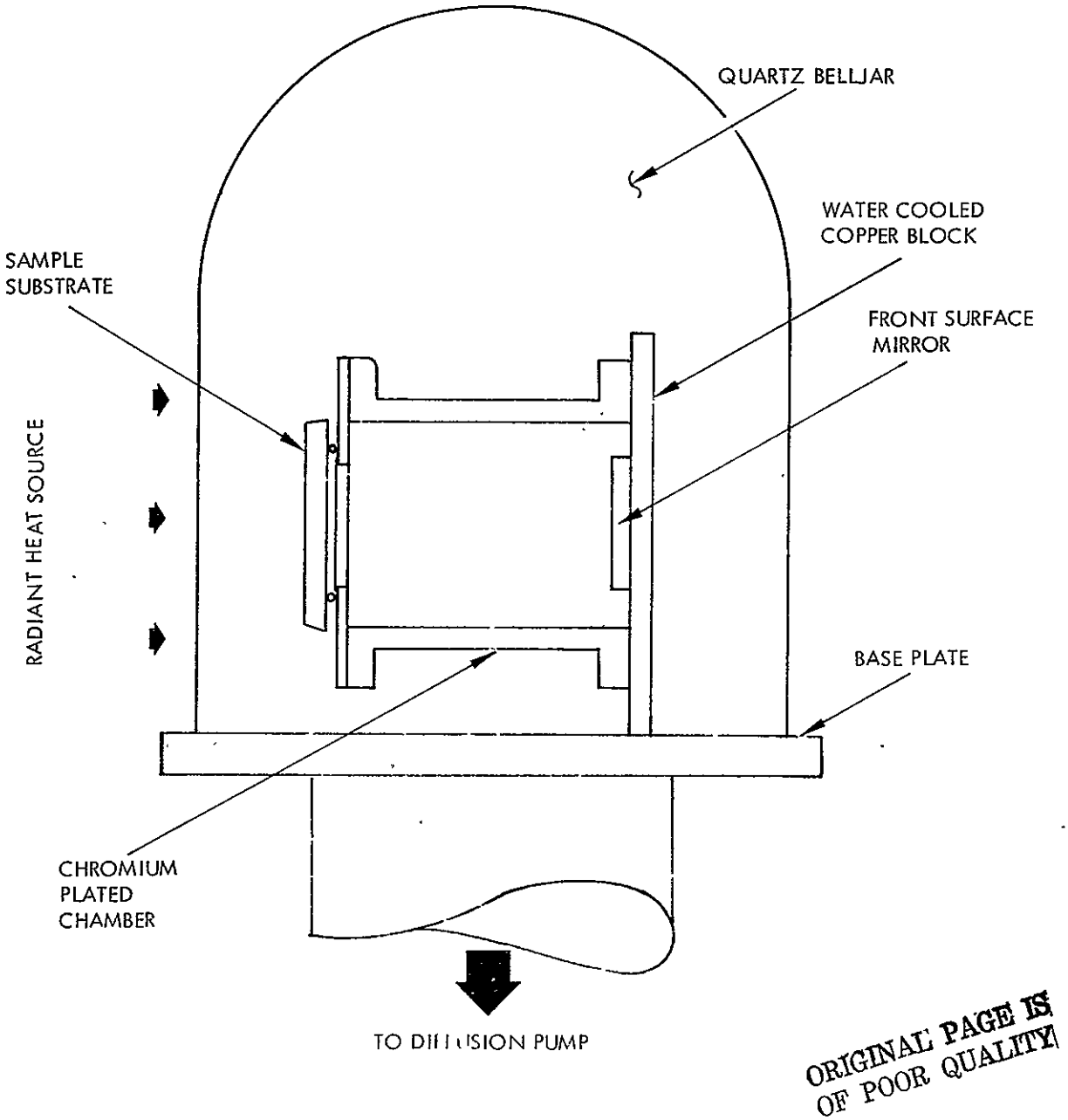

Fig. A-2 Schematic of Smoke Test Apparatus

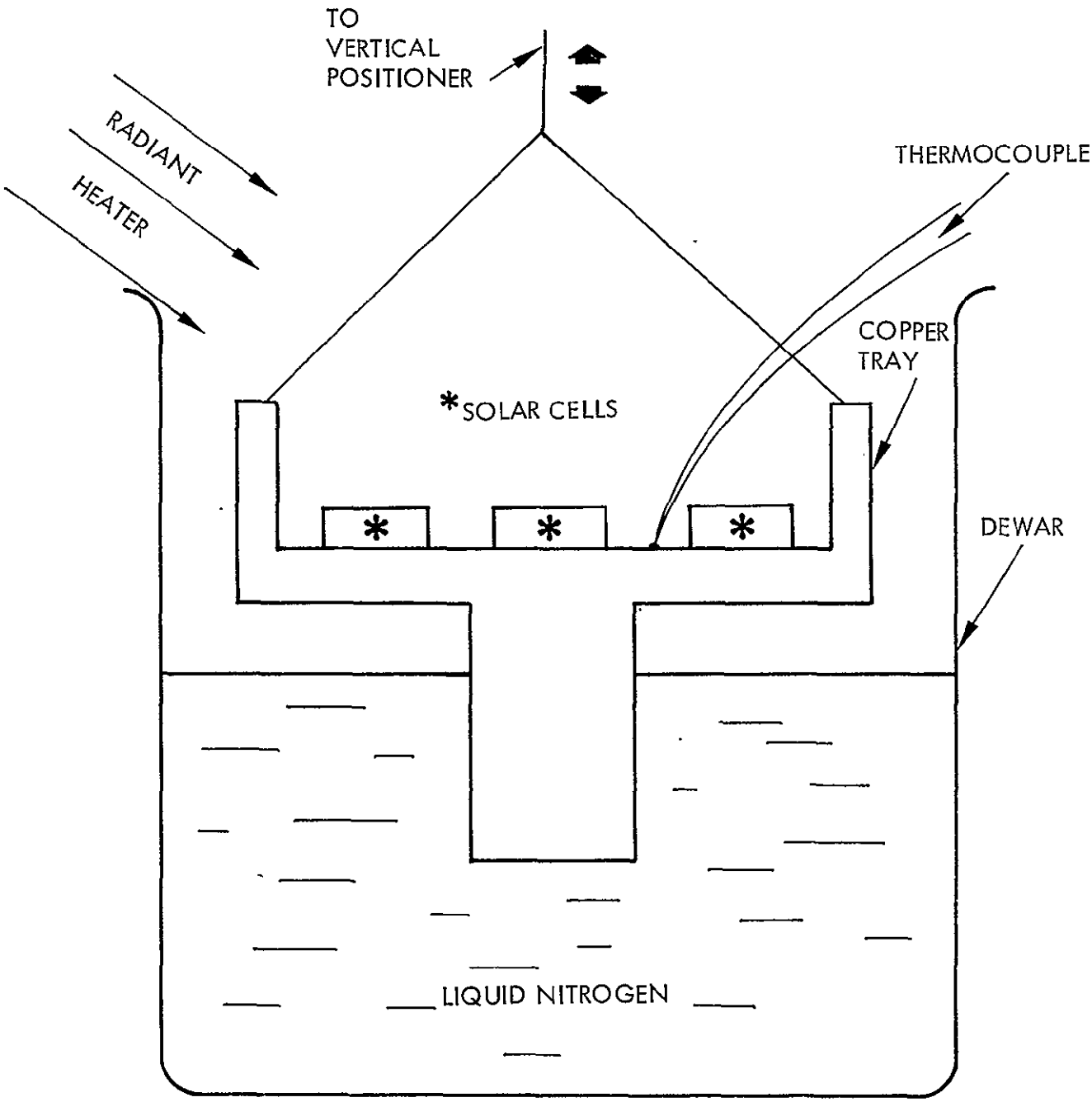

Fig. A-3 Schematic of Thermal Cycling Apparatus

Spectral transmittance measurements of free-standing Spraylon films were determined by placing specimens in the optical train of the Cary spectrophotometer.

Emittance values of Spraylon-coated solar cells were determined with a Gier Dunkle DB-100 infrared reflectometer. This technique provides a good approximation of the total hemispherical emittance at room temperature.

Appendix B

MECHANICAL TEST RESULTS
SPRAYLON FLUOROCARBON ENCAPSULANT
FOR SILICON SPACE SOLAR CELLS AND ARRAYS

F. L. Bouquet

1. Summary

The results of the initial mechanical tests performed by JPL in support of a NASA evaluation of Lockheed-formulated fluorocarbon encapsulation (Spraylon) for space solar cell arrays are presented. Six types of tests were performed, namely adhesion, tensile, flexure, abrasion, tear and VCM (outgassing). Descriptions of the specimen configurations and the test procedures are presented. The test data are shown in detail for both unirradiated and ultraviolet plus proton exposed specimens. A final report on the mechanical tests for the optimized Spraylon material is planned at a later date.

2. Introduction

The mechanical test results presented herein are in support of NASA evaluation of a Lockheed-formulated transparent fluorocarbon protective coating (Spraylon) for space solar cell arrays. The overall effort is specifically oriented towards integration of the concept to fit the needs of an automated solar cell array fabrication process being developed by JPL.

In this report, the initial mechanical testing of Spraylon specimens consisting of widely varying composition is treated. Various thicknesses of the polymer material were tested as (a) free-standing films and (b) on substrates and solar cells. The types of base material and the number of specimens are shown in Table 2-1.

Both unirradiated and exposed Spraylon specimens were characterized using ASTM procedures (Table 2-2). The test results for this intital phase are treated in detail in the following section.

The work described in this report was performed by the Structures and Materials Section, Applied Mechanics Division of the Jet Propulsion Laboratory.

Table 2-1

SPECIMENS FOR INITIAL MECHANICAL TESTING

UNEXPOSED SPECIMENS MECHANICAL TEST	FORM	NUMBER OF SPECIMENS
1. Adhesion Strength	Solar Cells	90
	Substrates	30
2. Tensile Strength	Films	15
3. Flexure Strength	Solar Cells	15
	Substrates	15
4. Abrasion Resistance	Aluminum Panels	15
5. Tear Strength	Films	15
6. VCM	Solar Cells	15
	Films	5
IRRADIATED SPECIMENS		
7. Adhesion Strength	Solar Cells	2
8. Flexure Strength	Solar Cells	2

Table 2-2

LIST OF MECHANICAL TESTS

TYPE OF TEST	ASTM TEST DESCRIPTION
1. Adhesion	"Bell" Peel Test (Modified)
2. Tensile	D 882-73
3. Flexure	D 813-59
4. Abrasion	D 968-51
5. Tear	D 1938-67
6. VCM	Special JPL Test - Micro VCM (Solar cells) - Macro VCM (Films)

3. Mechanical Tests

3.1 Adhesion Strength.

The adhesion tests were performed according to the Bell peel test shown schematically in Figure 3.1-1. Two separate types of adhesive properties were measured (a) adhesion of the Spraylon to the surface of the solar cell and (b) adhesion to the Kapton * substrate. In both cases, the base material was bonded to a 10 inch aluminum base. (See Figure 3.1-2). The two inch Spraylon tabs extending beyond the solar cells are clearly shown. The results of the measurements are tabulated in Table 3.1-1 and summarized in Table 3.1-2. The average adhesion load was 1.1 lbs. An example of delamination for a typical specimen on the basic substrate is shown in Figure 3.1-3.

Four types of failure were observed:

(a) failure at the bond line,

(b) cracking of the silicon solar cell,

(c) lifting-off of the cell from the rigid substrate (epoxy-aluminum-solar cell bond), and

(d) peeled failure.

The tensile strength tests are treated in the following section.

*Du Pont registered trademark for its proprietary polyimide film.

FIGURE 3.1-1

SCHEMATIC OF ADHESION STRENGTH TESTS

OBJECTIVE - To determine the load required to separate Spraylon from substrates and solar cells, simulating array forces.

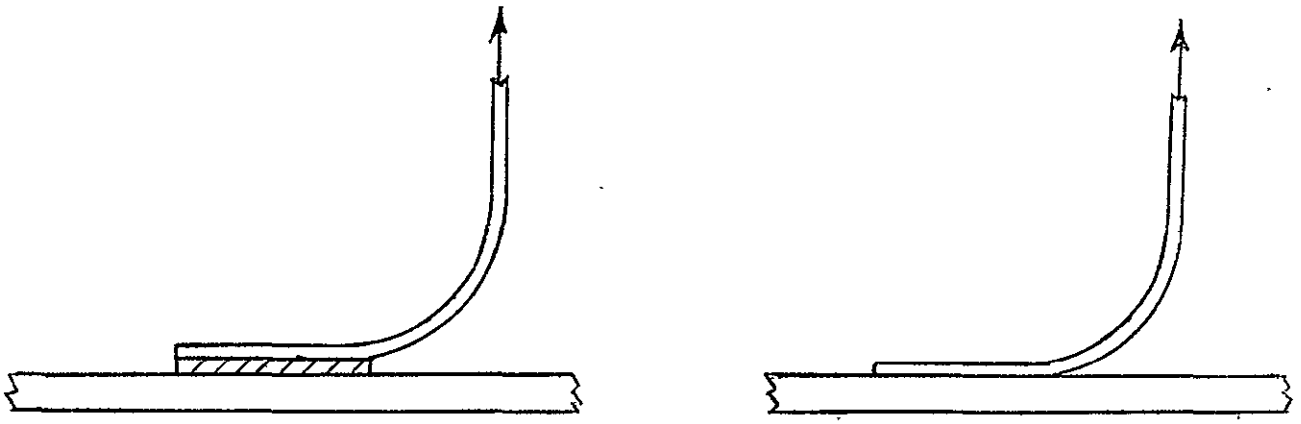

TEST - Spraylon film was pulled off solar cells and substrates in an Instron machine and load measured.

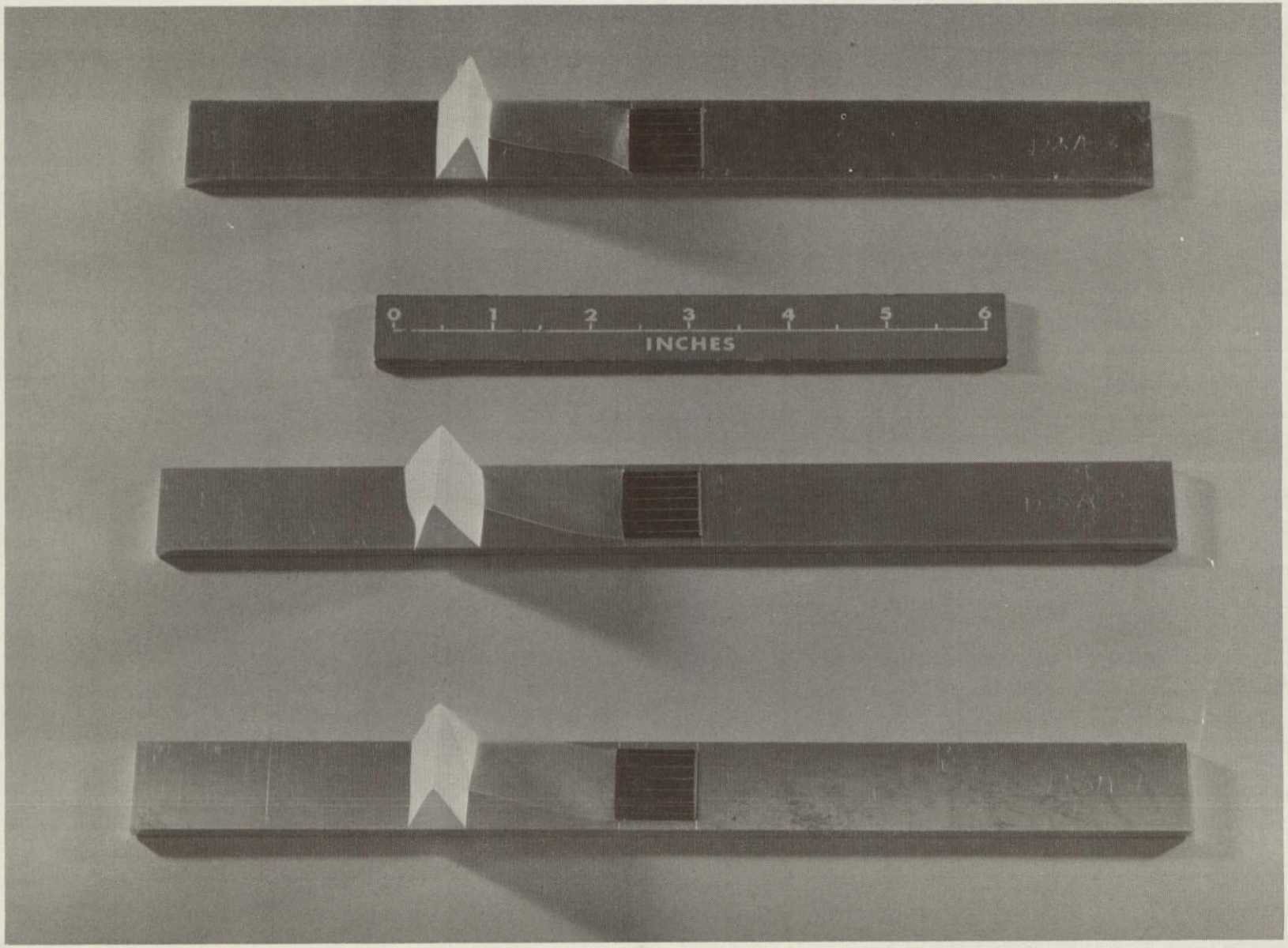

Fig. 3.1-2 Photo of Typical Spraylon Specimens on Solar Cells Before Adhesion Testing

Table 3.1-1

RESULTS OF ADHESION STRENGTH TESTS

Sample	Width (in.)	Thickness (in.)	Max. Tear Load *	Avg. Peel Load *	Max. Peel Load *	Min. Peel Load *	Comments
10A-1	0.788	0.0030	3.50				Failed at bond line
10A-2	0.788	0.0035		0.60	0.98	0.20	Peeled, cracked 0.2" of solar cell
10A-3	0.788	0.0035		1.50	3.12	0.50	Peeled, cracked 0.2" of solar cell
10A-4	0.788	0.0042		2.10	4.00	0.43	Peeled, solar cell poorly bonded
10A-5	0.788	0.0030	3.26				Cracked 0.3" of solar cell, failed at bond line
10A-6	0.788	0.0037		1.00	1.90	0.28	Peeled, cracked 0.1" of solar cell
10A-7	0.788	0.0036		2.10	4.35	0.55	Peeled, cracked 0.1" of solar cell
10A-8	0.788	0.0035	2.35				Lifted cell from Al
10A-9	0.788	0.0035	5.63				Cracked 0.3" of solar cell, failed at bond line
10A-10	0.788	0.0037		2.20	4.68	0.38	Peeled, crack (corner of cell)
12.5A-1	0.788	0.0032					Control Samples
12.5A-2	0.788	0.0028					
12.5A-3	0.788	0.0032		3.00	4.96	0.60	Peeled, cracked 0.2" of solar cell
12.5A-4	0.788	0.0028		0.70	1.28	0.10	Peeled, cracked 0.2" of solar cell
12.5A-5	0.788	0.0025		2.00	2.62	0.20	Peeled, cracked 0.2" of solar cell
12.5A-6	0.788	0.0034		2.00	3.45	0.42	Peeled, cracked corners of solar cell
12.5A-7	0.788	0.0038		0.40	1.80	0.23	Peeled, cracked corners of solar cell
12.5A-8	0.788	0.0033	2.28				Failed at bondline

* (lbs)

Table 3.1-1

RESULTS OF ADHESION STRENGTH TESTS (CONT.)

Sample	Width (in.)	Thickness (in.)	Max. Tear Load*	Avg. Peel Load*	Max. Peel Load*	Min. Peel Load*	Comments
12.5A-9	0.788	0.0028		0.60	0.72	0.26	Failed at bondline some peel
12.5A-10	0.788	0.0043	1.68				Lifted cell from Al
15A-1	0.788	0.0030	0.58				No peel, failed at bond line
15A-2	0.788	0.0050		0.50	1.80	0.27	Peeled, corner of cell cracked
15A-3	0.788	0.0042	0.82				Lifted cell from Al
15A-4	0.788	0.0027	1.15				No peel, failed at bond line
15A-5	0.788	0.0038		1.50	2.82	0.65	Peeled, gummy adhesive
15A-6	0.788	0.0027		1.80	3.00	0.58	Peeled, corner of cell cracked.
15A-7	0.788	0.0028		2.20	2.60	0.18	Peeled gummy adhesive
15A-8	0.788	0.0022	3.12				Cracked 0.2" of solar cell, failed at bond line
15A-9	0.788	0.0025		2.40	2.65	0.28	Cracked 0.2" of solar cell, peeled, gummy adhesive.
15A-10	0.788	0.0028		1.20	1.90	0.30	Peeled, corners of cell cracked.
20A-1	0.788	0.0026		2.00	3.16	0.45	Peeled,cracked corners, failed at bond line.
20A-2	0.788	0.0040		3.00	5.65	0.78	Peeled,cracked 0.2" of cell, failed at peel in bonded area
20A-3	0.788	0.0030	4.62				Cracked 0.2" of cell, failed at bond line
20A-4	0.788	0.0026					Failed at bond line

Table 3.1-1

RESULTS OF ADHESION STRENGTH TESTS (CONT.)

Sample	Width (in.)	Thickness (in.)	Max. Tear Load*	Avg. Peel Load*	Max. Peel Load*	Min. Peel Load*	Comments
20A-5	0.788	0.0020	1.08				Failed at bond line
20A-6	0.788	0.0025	1.18				Failed at bond line
20A-7	0.788	0.0018		1.70	2.15	0.30	Peeled gummy adhesive
20A-8	0.788	0.0020	1.70				Cracked large corner, failed at bond line.
20A-9	0.788	0.0025		3.00	3.12	0.65	Peeled, cracked 0.3" of solar cell
20A-10							
K10A-1	0.812	0.0042		2.00	3.02	0.70	Lifted 0.3" Kapton, peeled Spraylon before tearing
K10A-2	0.820	0.0038		0.70	1.25	0.50	Peeled Kapton from Al
K10A-3	0.822	0.0027		0.80	1.15	0.32	Peeled Kapton from Al
K10A-4	0.822	0.0035		0.40	0.78	0.18	Peeled Kapton from Al
K10A-5	0.841	0.0032		0.80	1.35	0.48	Peeled Kapton from Al
K15A-1	0.810	0.0037		1.25	1.75	0.58	Peeled 1/2 of Spraylon, tore at bond line
K15A-2	0.812	0.0038		0.96	1.60	0.88	Peeled
K15A-3	0.825	0.0025		1.90	2.40	0.86	Peeled
K15A-4	0.834	0.0032		1.20	1.50	0.98	Peeled, tore at bond line
K15A-5	0.828	0.0032		2.00	2.40	1.65	Peeled, tore at bond line

Table 3.1-1

RESULTS OF ADHESION STRENGTH TEST (CONT.)

Sample	Width (in.)	Thickness (in.)	Max. Tear Load*	Avg. Peel Load*	Max. Peel Load*	Min. Peel Load*	Comments
102AF1	0.788	0.0028		2.40	3.08	1.73	Cracked 0.1" of cell; peeled, tore at crack break.
2	0.788	0.0028		3.30	3.40	-	Cracked 0.2" of cell, uniform peel, tore at crack.
3	0.788	0.0020		2.90	2.40	2.45	Cracked 0.1" of cell, peeled.
4	0.788	0.0020		1.40	2.18	0.82	Cracked 0.1" of cell, peeled, no tearing.
5	0.788	0.0017	0.92				Cracked 0.3" corner, tore at bond line,
6	0.788	0.0027		2.00	3.08	0.68	Cracked 0.1" of cell, peeled.
7	0.788	0.0018	1.52				Cracked 0.1" of cell, tore at bond line.
8	0.788	0.0020		2.50	3.18	2.80	Cracked 0.2" of cell, peeled, tore at crack.
9	0.788	0.0028		2.50	3.67	1.05	Cracked 0.2" of cell, peeled, tore at crack.
10	0.788	0.0024		1.60	2.46	1.10	Cracked 0.3" of cell, tore at crack.
15F-1	0.788	0.0030	0.96	0.30			Tore at bond line, peeled 0.2".
-2	0.788	0.0030		0.25	1.02	0.10	Peeled easily.
-3	0.788	0.0035		0.20	1.00	0.15	Peeled easily.
-4	0.788	0.0028		0.18	1.02	0.18	Peeled easily 0.1" corner cracked.
-5	0.788	0.0030		0.10	1.08	0.08	Cracked 0.3" of cell. Peeled easily.

Table 3.1-1

RESULTS OF ADHESION STRENGTH TEST (CONT.)

Sample	Width (in.)	Thickness (in.)	Max. Tear Load*	Avg. Peel Load*	Max. Peel Load*	Min. Peel Load*	Comments
15F-6	0.788	0.0030		0.28	1.50	0.08	Cracked 0.2" of cell. Peeled.
-7	0.788	0.0030		0.25	1.90	0.10	Cracked 0.1" of cell, peeled easily.
-8	0.788	0.0037		0.25	0.94	0.20	Peeled easily.
-9	0.788	0.0028		0.40	0.65	0.25	Peeled easily.
-10	0.788	0.0028		0.08	0.50	0.08	Peeled easily.
-11	0.788	0.0030		0.35	0.63	0.12	Peeled easily.
20FHACI	0.788	0.0038		0.22	0.80	0.05	Cracked 0.1" of cell, peeled easily.
2	0.788	0.0034		0.33	1.18	0.27	Peeled.
3	0.788	0.0040		1.50	1.75	0.40	Cracked 0.1" of corner, peeled, tore at crack
4	0.788	0.0040		0.50	3.15	0.20	Cracked o.1" of cell, peeled, lifted cell
5	0.788	0.0040		0.70	1.28	0.38	Cracked 0.1" of corner
6	0.788	0.0030	0.98				Lifted cell
7	0.788	0.0036		0.78	0.92	0.20	Cracked o.1" of corner
8	0.788	0.0038	0.78				Lifted cell
9	0.788	0.0036		0.30	1.65	0.20	Peeled
10	0.788	0.0038	2.00				Tore at bond line
11	0.788	0.0034		0.36	0.65	0.18	Cracked 0.2" of cell, peeled, lifted cell.
12	0.788	0.0038	4.32				Tore at bond line.

Table 3.1-1

RESULTS OF ADHESION STRENGTH TEST (CONT.)

Sample	Width (in.)	Thickness (in.)	Max. Tear Load*	Avg. Peel Load*	Max. Peel Load*	Min. Peel Load *	Comments
K15AF-1	0.842	0.0055		1.10	1.86	0.90	Peeled
K15AF-2	0.848	0.0035	3.08				Tore at bond line
K15AF-3	0.848	0.0040		0.10	1.88	0.10	Peeled easily after initial pull.
K15AF-4	0.815	0.0040		0.12	0.27	0.11	Peeled easily
K15AF-5	0.836	0.0032		0.15	0.80	0.13	Peeled easily
K152AF1	0.850	0.0034	1.53				Tore at bond line
K152AF2	0.812	0.0018	0.82				Tore at bond line
K152AF3	0.818	0.0028		0.35	0.90	0.30	Lifted Kapton
K152AF4	0.847	0.0037		0.35	1.60	0.24	Peeled easily
K15F1	0.865	0.0040		0.10	0.58	0.09	Peeled easily
K15F2	0.802	0.0042		0.08	0.98	0.06	Peeled easily
K15F3	0.834	0.0044		0.50	0.95	0.26	Peeled
K15F4	0.822	0.0040		0.15	0.30	0.10	Peeled easily
K15F5	0.820	0.0046	3.90				Bonded at start to Al, tore at start.

Table 3.1-1

RESULTS OF ADHESION STRENGTH TEST (CONT.)

Sample	Width (in.)	Thickness (in.)	Max. Tear Load*	Avg. Peel Load*	Max. Peel Load*	Min. Peel Load*	Comments
K15FHAC1	0.811	0.0028	1.12				Tore at bond line
2	0.828	0.0023		0.45	0.65	0.35	Lifted Kapton
3	0.814	0.0020		0.80	1.20	0.60	Peeled
4	0.810	0.0022		0.50	0.90	0.25	Peeled
5	0.836	0.0035		0.60	1.08	0.43	Lifted Kapton
6	0.832	0.0024		0.70	0.92	0.30	Peeled
10A/F1	0.788	0.0017	0.25 lbs				Cracked 0.4" of cell, lifted entire cell.
2	0.788	0.0005		1.20	1.55	0.52	Cracked 0.3" of cell, peeled remainder
3	0.788	0.0020	0.78				Cracked 0.4" of cell, tore at bond line
4	0.788	0.0015	0.92				Tore at bond line
5	0.788	0.0018	0.96				Tore at bond line
6	0.788	0.0018	3.13				Cracked 0.3" of cell, tore at crack break
7	0.788	0.0028		1.50	2.05	0.62	Cracked corner 0.2" deep, peeled, tore at crack break
8	0.788	0.0020		2.00	2.78	1.03	Cracked 0.3" of cell, peeled, tore at crack break
9	0.788	0.0024		1.00	1.58	0.48	Cracked 0.4" of cell, peeled, lifted cell

Table 3.1-1

RESULTS OF ADHESION STRENGTH TEST (CONT.)

Sample	Width (in.)	Thickness (in.)	Max. Tear Load*	Avg. Peel Load*	Max. Peel Load*	Min. Peel Load*	Comments
202AF1	0.788	0.0030		0.40	0.90	0.35	Peeled uniformly, load increased after 0.3".
202AF2	0.788	0.0034		1.42	1.83	0.88	Peeled, began to tear.
202AF3	0.788	0.0035		0.10	0.30	0.05	Peeled easily.
202AF4	0.788	0.0027		0.86	1.52	0.38	Peeled jaggedly.
202AF5	0.788	0.0034		0.25	0.44	0.22	Peeled easily.
202AF6	0.788	0.0037		0.30	0.94	0.22	Peeled easily.
202AF7	0.788	0.0022		0.30	0.90	0.30	Peeled easily.
202AF8	0.788	0.0043		0.17	0.28	0.10	Peeled easily.
202AF9	0.788	0.0040		0.10	0.28	0.06	Peeled easily.

Table 3.1-2

RESULTS OF ADHESION STRENGTH TESTS

SPECIMEN CODE	NO. OF SPECIMENS	AVG. ADHESION LOAD (LBS.)
10A	6	1.58
10A/F	4	1.42
102AF	8	2.32
12.5A	6	1.45
15A	6	1.6
15F	11	0.24
20A	4	2.42
20FAC	8	0.60
202AF	9	0.43
K10A	5	1.46
K15F	4	0.21
K15AF	4	0.37
K152AF	2	0.35
KFHAC	5	0.61

Average Adhesion Load = 1.1 lbs. for 2 cm width.

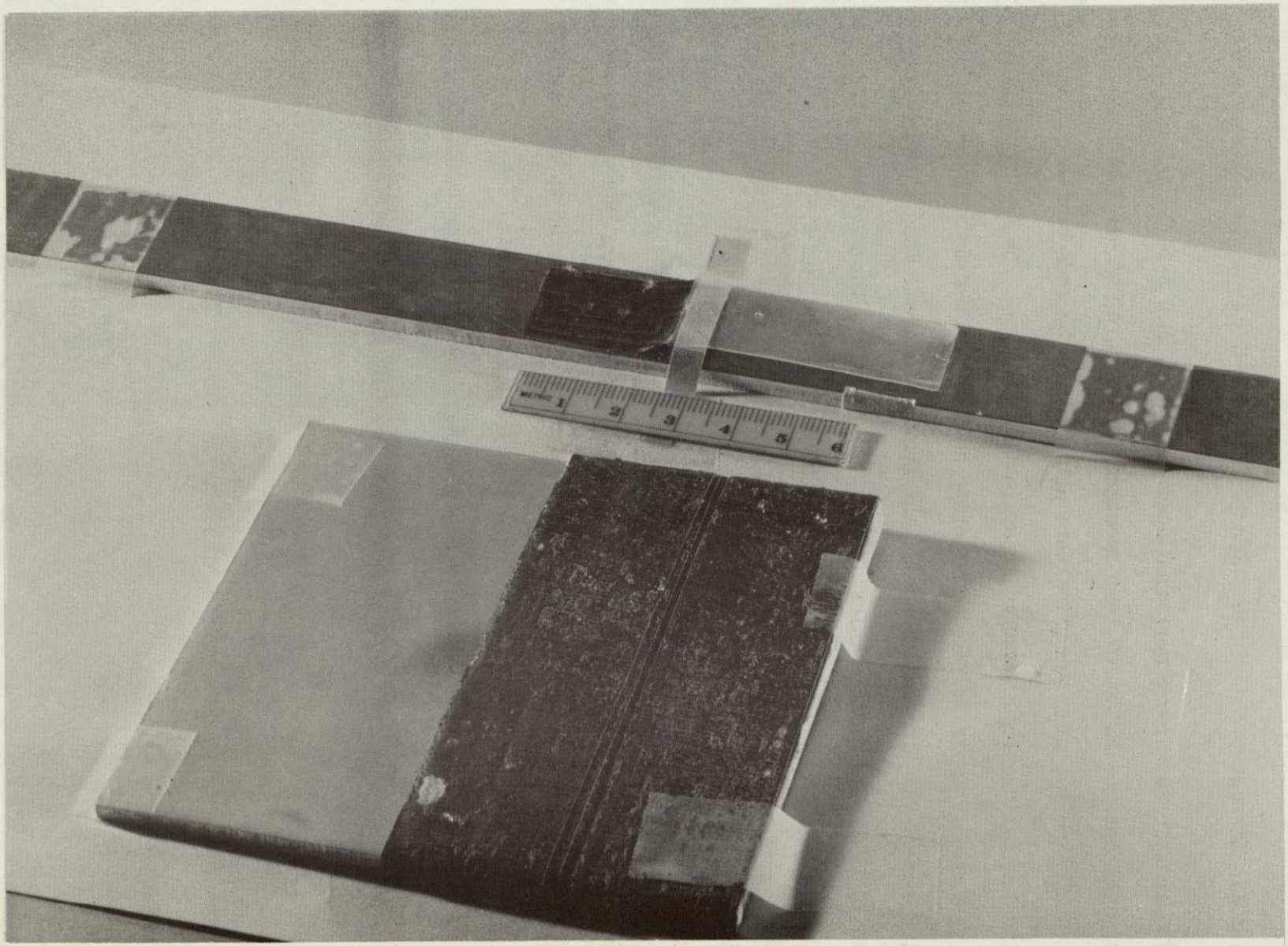

Fig. 3.1-3 Photo of a Typical Adhesion Specimen After Testing.
In the Foreground, a Typical Abrasion Specimen is shown.

3.2 Tensile Strength

The tensile tests were performed according to ASTM D 882-73, and a typical Spraylon 1" x 10" test specimen is shown in Figures 3.2-1 and 3.2-2. Special aluminum grips were attached to the ends of the specimen and the failure load measured in an Instron machine. The test results are shown in Table 3.2-1. Considering only those specimens tested at 1.0 inches per minute head speed, the average ultimate load strength was 18.46 lbs. The average thickness was 4.07 mils and the average width was 0.989 inches. The average strength for this set was 4586 lbs/in^2.

In general, the specimens did not fail at the aluminum grips. A typical specimen after tensile testing is shown in Figure 3.2-3.

The results of these tests on the Spraylon film are given in the following tables; Table 3.2-2 gives the results of tests to determine the ultimate tensile strength, Table 3.2-3, film elongation, and Table 3.2-4, the elastic modulus. The average elongation was 7.8% while the average elastic modulus was 176,000.

FIGURE 3.2-1

SCHEMATIC OF THE TENSILE TESTS

OBJECTIVE - To determine load in Spraylon at failure, simulating array tension.

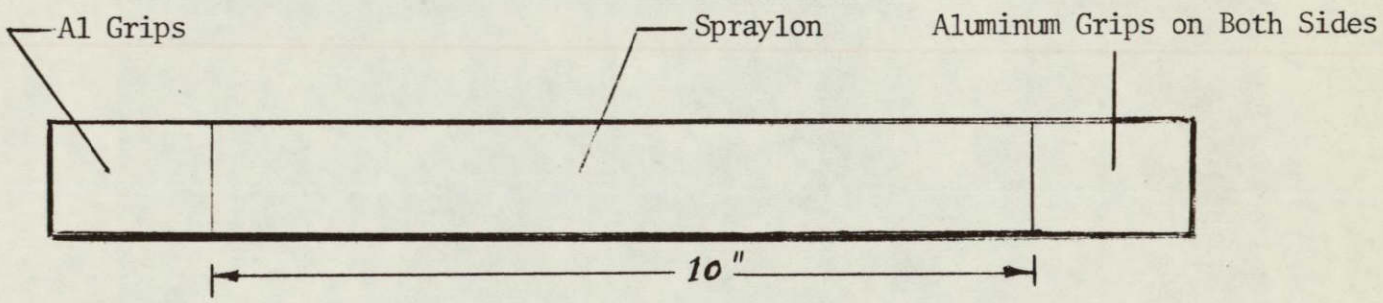

TEST - Tension was applied to both ends of a free-film specimen until failure in an Instron machine and the load measured.

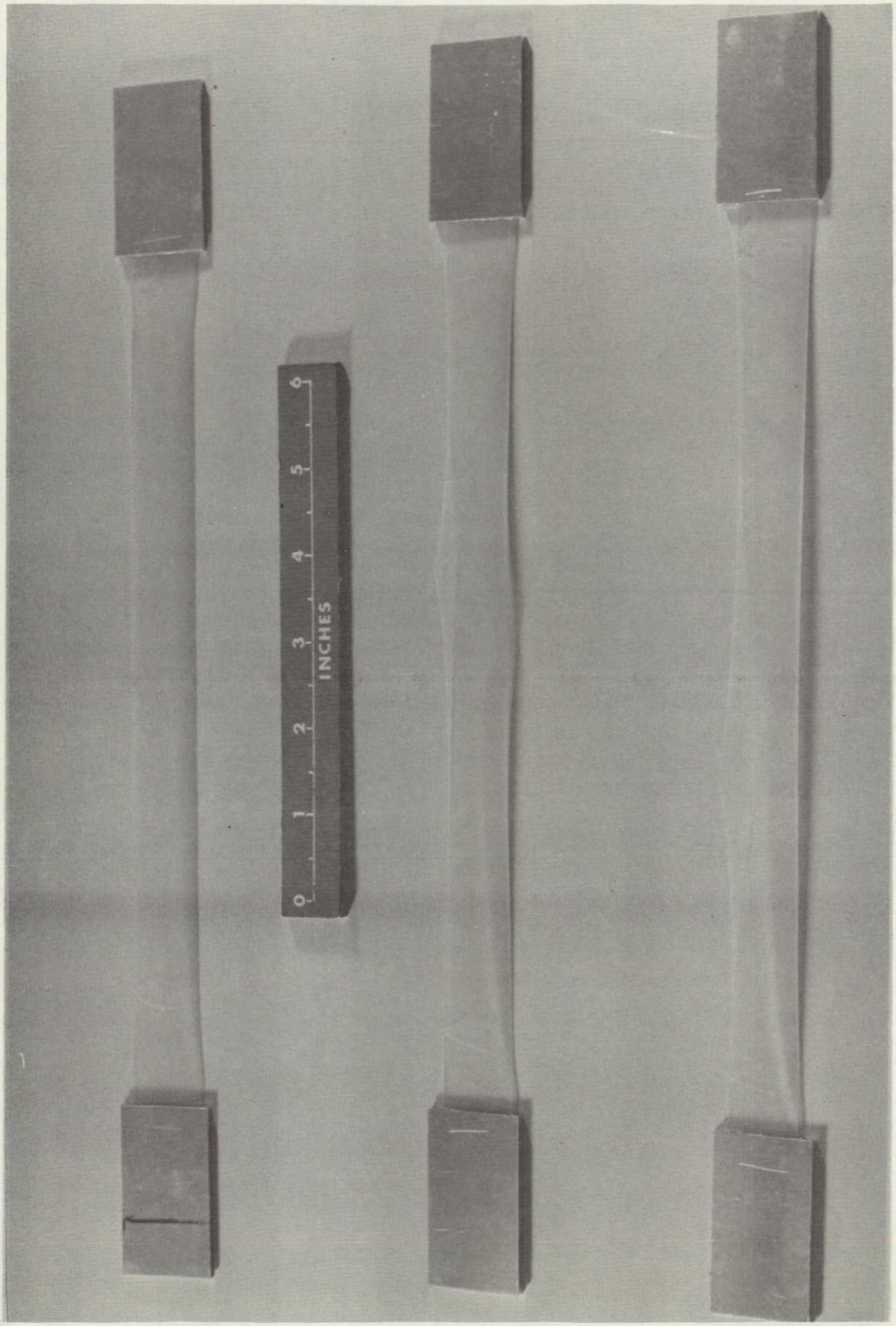

Fig. 3.2-2 Photo of Typical Spraylon Specimen Before Tensile Testing

Table 3.2-1

RESULTS OF TENSILE STRENGTH TESTS OF

SPRAYLON FILMS 1" x 10"

Specimen Designation	Length (in)	Width (in)	Thickness (x 10^3 in)	Ultimate Load (lbs)	Test Head Speed
T-1	X	X	X	X	Control
T-2	X	X	X	X	"
T-3	10.00	0.997	3.1	16.0	10 inches per min.
T-4	10.06	0.998	3.0	13.0	0.1 " " "
T-5	10.02	0.945	3.4	15.0	1.0 " " "
T-6	9.99	0.992	3.5	16.3	1.0 " " "
T-7	10.03	1.001	3.7	17.1	1.0 " " "
T-8	10.03	1.022	3.8	18.3	1.0 " " "
T-9	10.00	1.018	4.4	21.0	1.0 " " "
T-10	10.07	0.920	4.2	17.7	1.0 " " "
T-11	10.00	1.010	3.9	17.3	1.0 " " "
T-12	10.06	0.962	4.4	19.1	1.0 " " "
T-13	10.00	1.014	4.6	20.0	1.0 " " "
T-14	10.07	0.992	4.5	20.7	1.0 " " "
T-15	10.05	1.004	4.4	20.6	1.0 " " "

RESULTS OF TENSILE STRENGTH TESTS

OF SPRAYLON FILMS 1" x 10" (Cont.)

Specimen Sample No.	Dimension to Nearest Failure Point (cm)	Dimension to Farthest Failure Point (cm)	Total Length of Failed Specimen (cm)	Comments
T-1	—	—	—	Control
T-2	—	—	—	Control
T-3	8.8	17.3	26.1	Heavy Fraying and Strain on One End.
T-4	10.1	15.9	26.0	Both Ends Frayed, Strained Length at 1.8 cm.
T-5	6.5	19.2	25.7	Half Serrated - Half Frayed Fracture, Little Strain.
T-6	5.0	20.9	25.9	Light Fraying - One End. Heavy Strain, 1.5 cm.
T-7	4.5	21.2	25.7	Double Angle Failure Both Ends Frayed.
T-8	0	25.6	25.6	Serrated Break at Tab, Heavy Strain, 0.6 cm.
T-9	0	25.5	25.5	Break at Tab End, Heavy Strain, 0.4 cm.
T-10	3.6	22.3	25.9	Both Ends Frayed, Little Strain.
T-11	1.7	24.4	26.1	One End Frayed, Strained Length,at 2 cm.
T-12	0.5	25.2	25.7	One End Heavily Frayed, With Double Failure.
T-13	1.5	24.8	26.3	Both Ends Frayed, Heavy Strain at 1.0 cm.
T-14	1.3	25.3	26.3	Both Ends Serrated, Strain 1.8 cm.
T-15	1.3	25.1	26.4	Both Ends Serrated, Strain 2.0 cm.

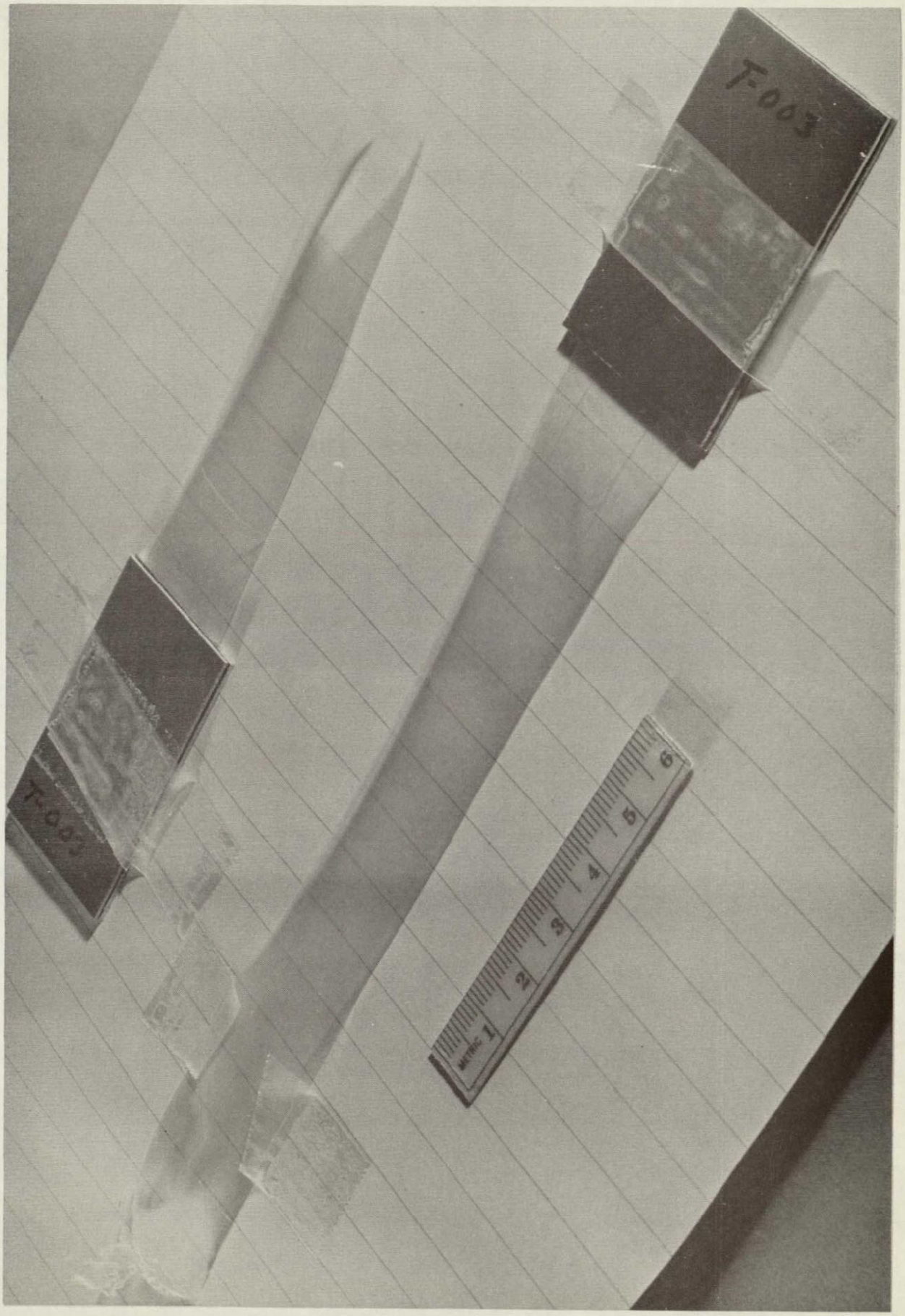

Fig. 3.2-3 Photo of Typical Spraylon Film After Tensile Test

Table 3.2-2

RESULTS OF ULTIMATE STRENGTH MEASUREMENTS

Specimen Code	Test Head Speed	Ultimate Tensile Strength (lbs/in^2)
T-1	Control	——
T-2	Control	——
T-3	10 inches/minute	5,160
T-4	0.1 inch/minute	4,330
T-5	1.0 inch/minute	4,690
T-6	"	4,790
T-7	"	4,620
T-8	"	4,690
T-9	"	4,670
T-10	"	4,540
T-11	"	4,440
T-12	"	4,550
T-13	"	4,260
T-14	"	4,600
T-15	"	4,680

Average = 4,594 psi; standard deviation $\sigma = \sqrt{\frac{\sum(x_i-\bar{x})^2}{n}} = 138.5$ psi

Table 3.2-3

RESULTS OF ELONGATION MEASUREMENTS

Specimen Code	Test Head Speed	Elongation (Percent)
T-1	Control	-
T-2	Control	-
T-3	10 inches/minute	6.4
T-4	0.1 inch/minute	12.9
T-5	1.0 inch/minute	8.2
T-6	"	9.5
T-7	"	9.6
T-8	"	7.3
T-9	"	4.8
T-10	"	9.4
T-11	"	8.0
T-12	"	7.8
T-13	"	7.2
T-14	"	6.6
T-15	"	7.8

Average Elongation = 7.8%

Standard Deviation, $\sigma = \sqrt{1.8124} = 1.35\%$

Table 3.2-4

RESULTS OF ELASTIC MODULUS MEASUREMENTS

Specimen Code	Test Head Speed	Elastic Modulus ($\times 10^3$)
T-1	Control	-
T-2	Control	-
T-3	10 inches/minute	193
T-4	0.1 inch/minute	190
T-5	1.0 inch/minute	194
T-6	"	188
T-7	"	168
T-8	"	174
T-9	"	164
T-10	"	179
T-11	"	174
T-12	"	172
T-13	"	170
T-14	"	178
T-15	"	170

Average = 176,000

Standard Deviation $\sigma = \sqrt{\frac{\sum(x_j - \bar{x})^2}{n}} = 5{,}290$

C-2

3.3 Flexure Strength

The flexure strength tests were performed according to ASTM D 813-59. Two types of Spraylon specimens were tested;(a) Spraylon on solar cells and, (b) Spraylon on the printed circuit substrate (see Figure 3.3-1). Both types of specimen were bent through an angle of 90° as shown in Figure 3.3-2. The terminology used is for two cases:

(a) The bend on the same side as the solar cells, abbreviated S-side, as shown in the above figure.

or (b) The bend in the opposite direction to the solar cell location (θ equal to -90°).

The results of the tests are tabulated in Table 3.3-1, and a typical specimen is shown in Figure 3.5-2. A summary of the entire results is shown in Table 3.3-2.

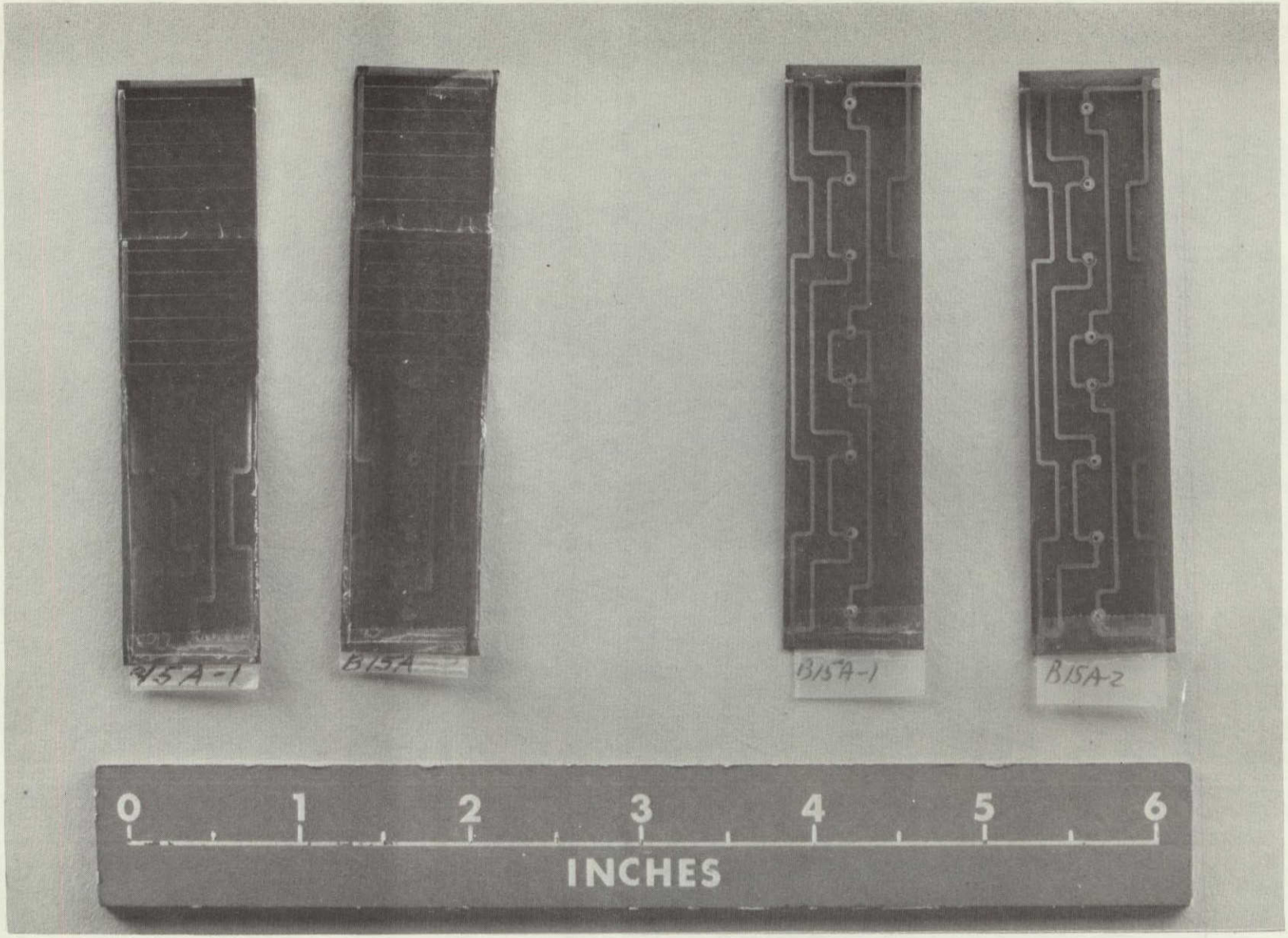

Fig. 3.3-1 Photo of Spraylon on Kapton Substrate (Top) and Solar Cells (Bottom) Before Flexure Testing

FIGURE 3.3-2

SCHEMATIC OF FLEXURE STRENGTH TESTING

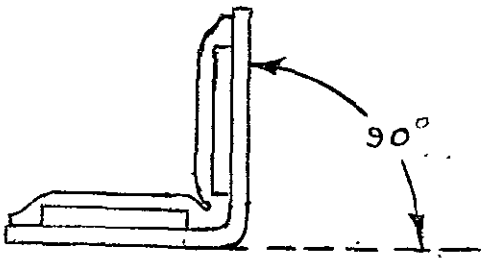

(a) Same Side (or S-Side) Flexure

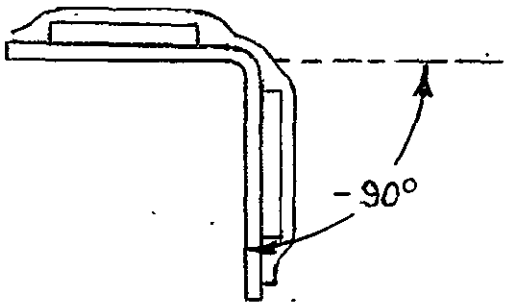

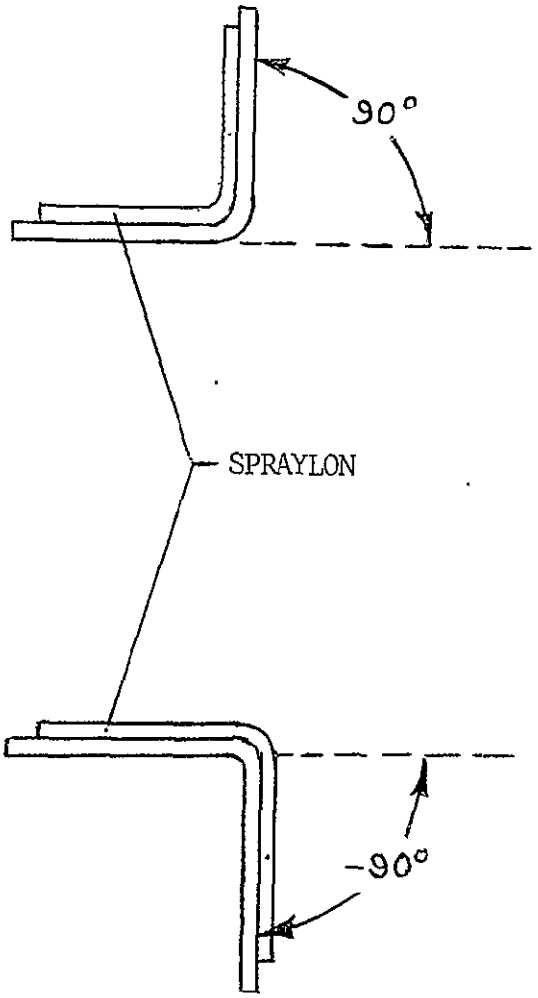

(b) Opposite Flexure

Table 3.3-1

RESULTS OF FLEXURAL STRENGTH TESTS

Specimen Code	Total Number Bends (Cycles)	Comments
Without Cells		
B15A-3 S-Side	10	Slight crease at bend, no abrasion
	50	No change
	100	No change, no cracks, no peeling
B15A-4 Opposite	10	Slight crease at bend, no abrasion
	50	No change
	100	No change, no cracks, no peeling
B15A-5 S-Side	10	
	50	
	100	Creased at bend, no cracks, no peeling
B15A-6 Opposite	10	
	50	
	100	Creased at bend, no cracks, no peeling
With Cells		
B15A-3 S-Side	10	60% of area large bubbles before test, lifted at cells next to bubble
	50	80% of bend area lifted
	100	85% of bend area lifted between cells
B15A-4 Opposite	10	15% of area bubbles, lifted edges of bubbles
	50	No change
	100	20% lifted
B15A-5 S-Side	10	10% of area bubbles, slight crease
	50	Lifted edges of bubbles
	100	Lifted edges of bubbles approx. 10% area between cells, no cracks

Table 3.3-1 (Continued)

Specimen Code	Total Number Bends (Cycles)	Comments
Without Cells		
B15AF-1 S-Side	10	Creased at bend, no abrasion
	50	No change
	100	No change, no cracks, no peeling
B15AF-2 Opposite	10	Creased at bend, no abrasion
	50	No Change
	100	No change, no cracks, no peeling
B15AF-3 S-Side	10	
	50	
	100	Creased at bend, no cracks, no peeling
B15AF-4 Opposite	10	
	50	
	100	Creased at bend, no cracks, no peeling
B15AF-5 S-Side	10	
	50	
	100	Creased at bend, no cracks, no peeling
With Cells		
B15AF-1 Opposite	10	Slight crease at bend, 5% debonded
	50	No change
	100	35% of bend area debonded, no cracks
B15AF-2 S-Side	10	Slight crease
	50	15% of bend area debonded
	100	60% of bend debonded
B15AF-3 S-Side	10	40% of area between cells debonded
	50	90% of area between cells debonded
	100	95% of area between cells debonded

Table 3.3-1 (Continued)

Specimen Code	Total Number Bends (Cycles)	Comments
With Cells (Cont.)		
B15AF-4 Opposite	10	20% of area between cells debonded
	50	40% of area debonded
	100	60% of area debonded
B15AF-5 S-Side	10	5% of area between cells debonded
	50	10% of area debonded
	100	15% of area debonded
Without Cells		
B15F-1 S-Side	10	Creased at bend, abrasion due to fixture
	50	Double abrasion due to fixture
	100	Abrasion increased slightly, no cracks, no peeling
B15F-2 Opposite	10	Slight abrasion due to fixture (modified fixture)
	50	No change
	100	Creased at bend, no cracks, no peeling
B15F-3 S-Side	10	
	50	
	100	Creased at bend, no cracks, no peeling
B15F-4 Opposite	10	
	50	
	100	Creased at bend, no cracks, no peeling
B15F-5 S-Side	10	
	50	
	100	Creased at bend, no cracks,no peeling

Table 3.3-1 (Continued)

Specimen Code	Total Number Bends (Cycles)	Comments
With Cells		
B15F-1 S-Side	10	10% of bend area debonded between cells
	50	80% of bend area debonded
	100	90% of bend area debonded, no cracks
B15F-2 Opposite	10	15% of bend area debonded between cells
	50	40% of bend area debonded
	100	50% of bend area debonded
B15F-3 S-Side	10	Debonded 20% of area between cells
	50	Debonded 60% of area
	100	Debonded 70% of area
B15F-4 Opposite	10	Debonded 10% area between cells
	50	Debonded 15%
	100	Debonded 20% area between cells, no cracks
B15F-5 S-Side	10	Debonded 5% of area
	50	Debonded 20% of area
	100	Debonded 30% of area between cells

Table 3.2-2

RESULTS OF FLEXURE STRENGTH TESTS

Specimens	No.	Cells	Percent Area Damaged 10 Cycles	50 Cycles	100 Cycles
B15A	4	No	Creases	Creases	Creases
B15A	3	Yes	28.3	35	38.3
B15AF	5	No	Creases	Creases	Creases
B15AF	5	Yes	13.0	31.0	53.0
B15F	5	No	Creases	Creases	Creases
B15F	5	Yes	16.0	43.0	52.0

Area debonded varies 13 - 53 percent

Average area debonded = 19% per 10 cycles

= 36% per 50 cycles

= 48% per 100 cycles

3.4 Abrasion Resistance

The abrasion tests were included to determine the toughness of the Spraylon to environmental influences. The response to falling sand impact was measured commensurate with ASTM Test D 968-51. The results would indicate the relative resistance of the polymer to sand impact due to terrestrial and/or planetary environments.

The test set-up is shown schematically in Figure 3.4-1, and the pre-test and post-test specimens are shown in Figures 3.4-2 and 3.4-3 respectively. Half of each 4 x 4 inch square sample was protected from the sand for optical comparison measurements, to be performed at a later time. A maximum of 200 lbs. of sand was dropped on each specimen.

The test results are shown in Table 3.4-1. The average thickness loss measured at the center of the target area was 0.26 mil/200 lbs. of sand.

FIGURE 3.4-1

SCHEMATIC OF ABRASION RESISTANCE TESTS

OBJECTIVE - To determine the effect of rubbing on Spraylon, simulating array deployments.

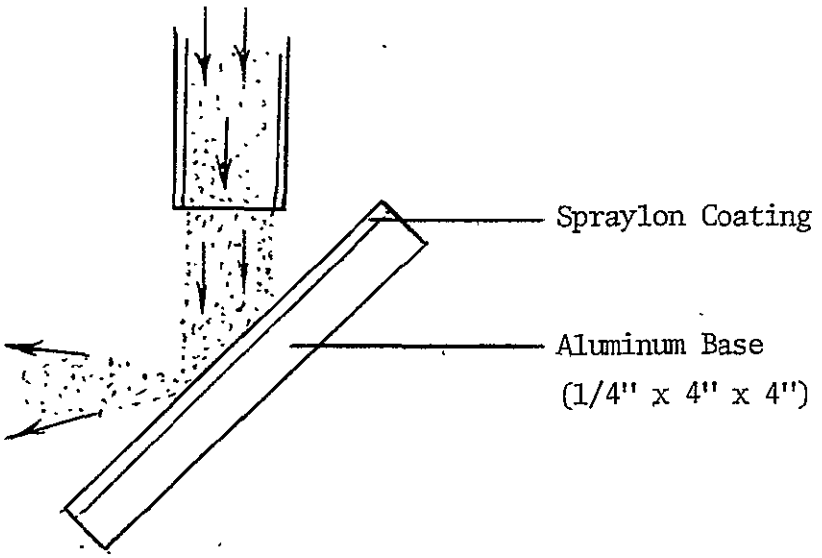

TEST - 200 lbs of sand were dropped on each Spraylon coating and thickness decrease was measured.

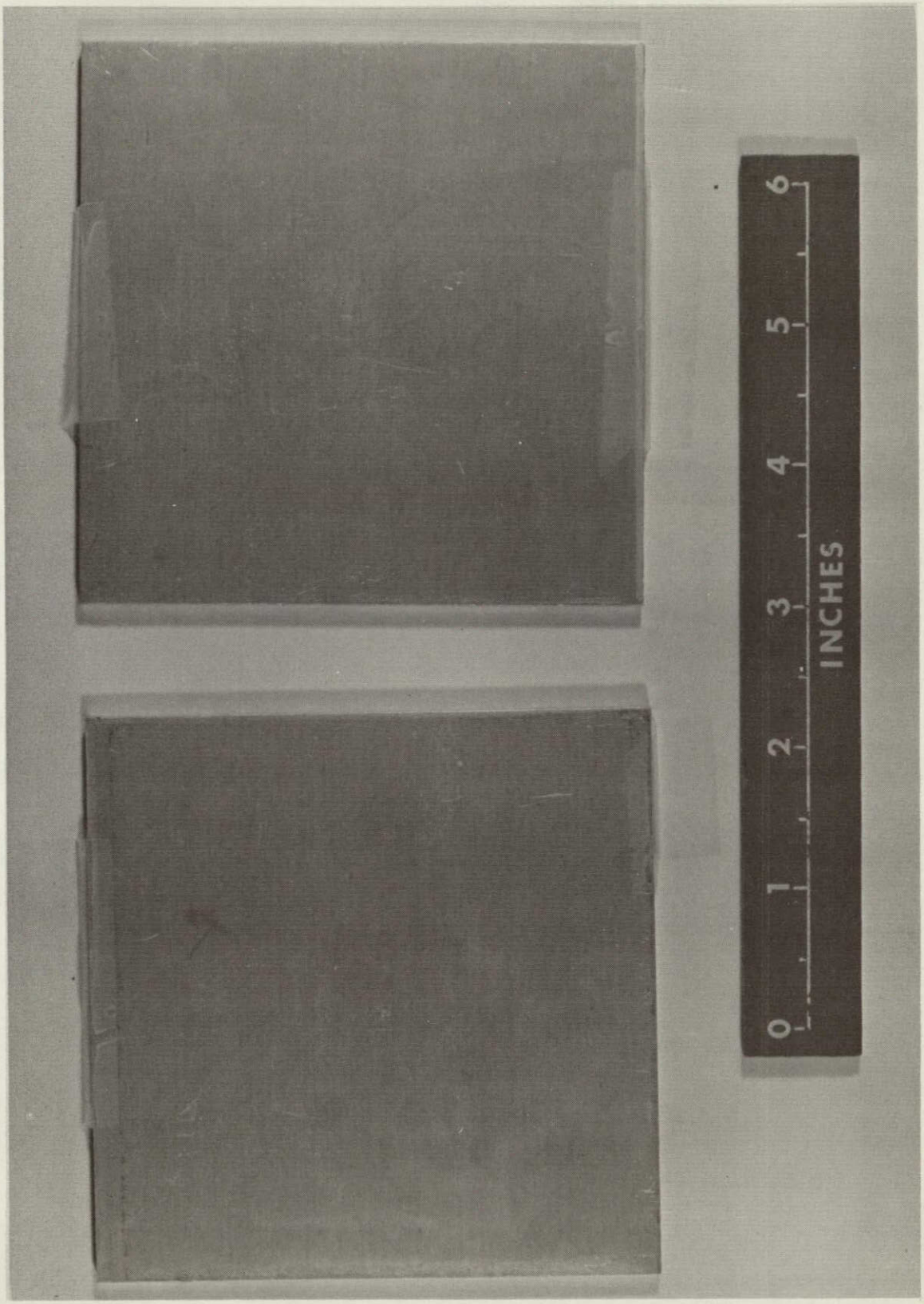

Fig. 3.4-2 Photo of Typical Spraylon Specimens Before Abrasion Testing

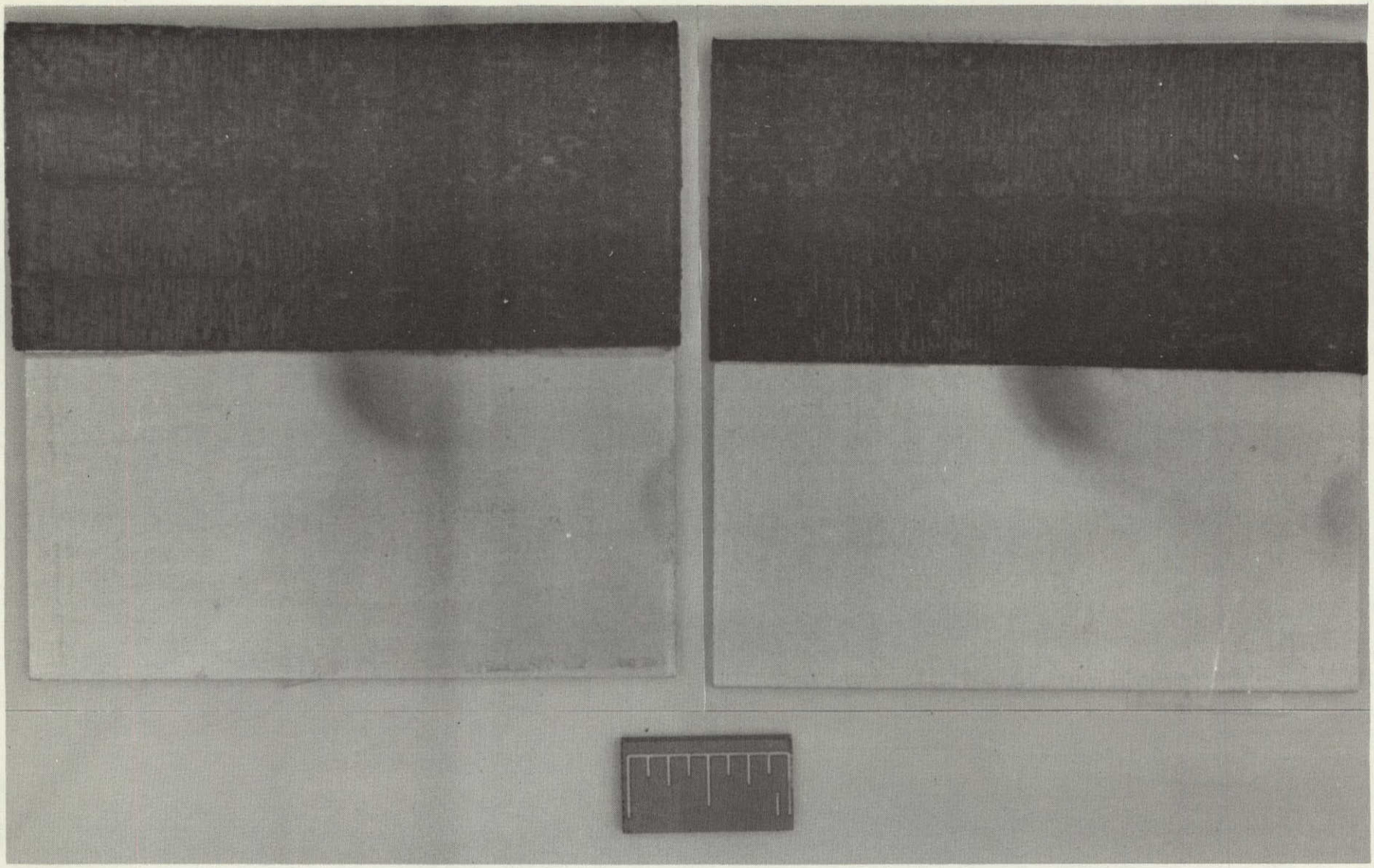

Fig. 3.4-3 Photo of Typical Spraylon Specimens After Abrasion Testing

Table 3.4-1

RESULTS OF ABRASION RESISTANCE TESTS

Specimen Code	Thickness - Inches		
	Initial	Final	Thickness Loss
ABR-1	0.1270	0.1268	0.0002
ABR-2	0.2180	0.1279	0.0001
ABR-3	0.1290	0.1285	0.0005
ABR-4	0.1285	0.1282	0.0003
ABR-5	0.1280	0.1279	0.0001
ABR-6	0.1285	0.1282	0.0003
ABR-7	0.1285	0.1281	0.0004
ABR-8	0.1280	0.1279	0.0001
ABR-9	0.1274	0.1270	0.0004
ABR-10	0.1275	0.1272	0.0003
ABR-11 (Control)	------	------	------
ABR-12	0.1280	0.1278	0.0002
ABR-13	0.1278	0.1275	0.0003
ABR-14 (Control)	------	------	------
ABR-15	0.1281	0.1279	0.0002

Average Thickness Loss for 200 Lbs. Sand = 0.26 Mil.

3.5 Tear Strength

For the tear strength measurements, 17 Spraylon specimens were prepared by Lockheed. Fifteen were tested while two were controls. Two untested specimens (T-3 and T-4) are shown in Figure 3.5-1 along with a centimeter scale. Each specimen strip was approximately one inch wide and three inches long, with an additional two inch length for gripping at one end. Two pairs of one-half inch wide aluminum gripping plates were bonded in parallel.

The results of the tear strength measurements are summarized in Table 3.5-1 and a typical specimen after test is shown in Figure 3.5-2 (top). A sketch showing the specimen dimensions and angular relationship identified in the data is shown (Figure 3.5-3.) The median of the average tear load was determined to be 180 grams while the tear dimensions, angles and extent of serrations were random.

3.6 VCM (Outgassing)

Outgassing tests were performed on the Spraylon samples using the Volatile Condensable Material (VCM) test. Both macro - and micro - VCM tests were undertaken and the results are shown in Tables 3.6-1 through 3.6-3.

In the macro-VCM tests, the results show that the outgassing VCM is less than 0.01%, the lower limit of detectability of the test apparatus.

In the two micro-VCM, the average VCM losses in percent were 0.004 and 0.01. The overall average weight loss for the specimens was 0.099 while the average VCM result was 0.006.

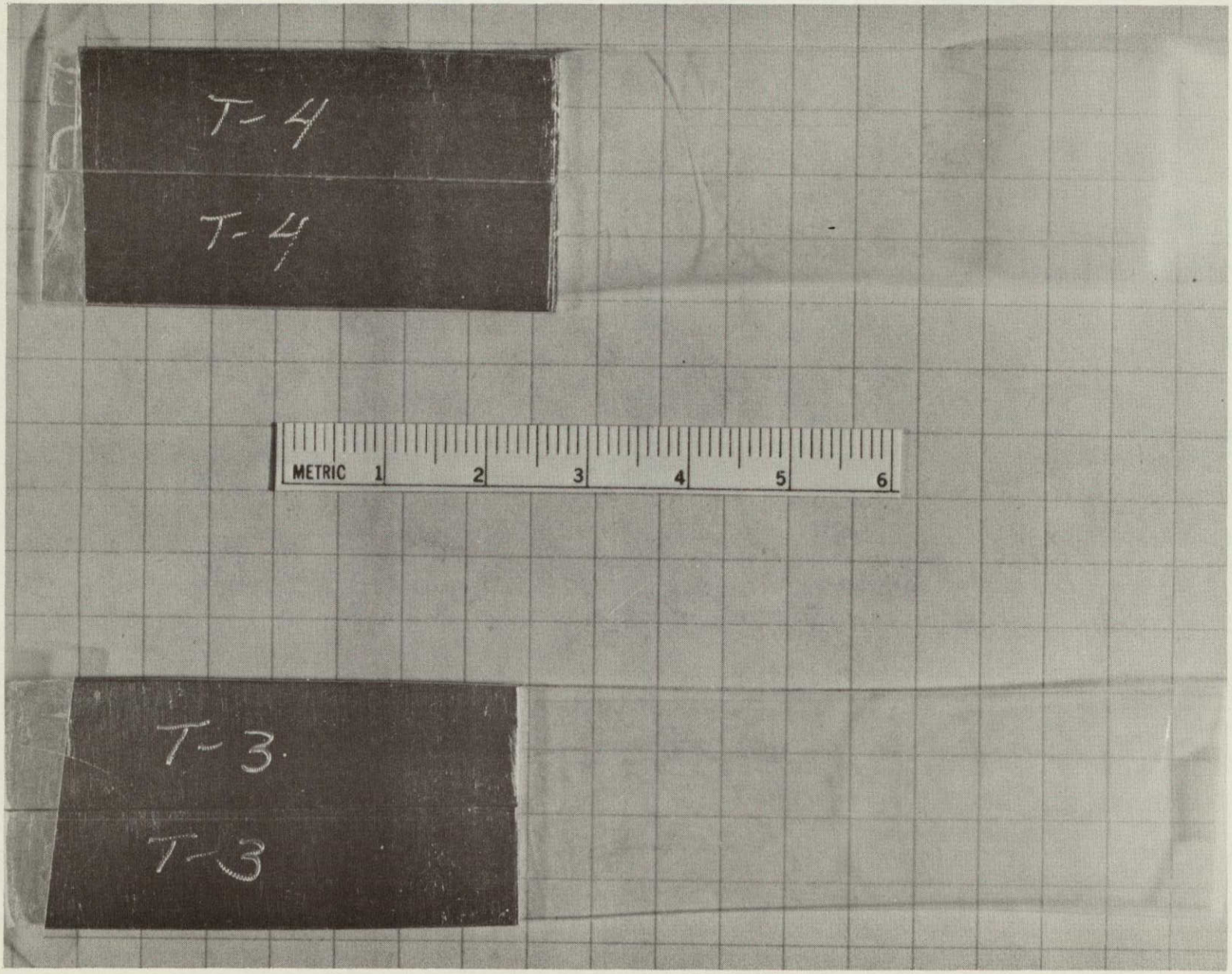

Fig. 3.5-1 Photo of Two Typical Tear Specimens Prior to Testing

Table 3.5-1

RESULTS OF TEAR STRENGTH MEASUREMENTS

Specimen Code	t (mils)	Initial tear point (g)	Avg. tear load* (g)	Final tear point (g)	Pull speed
T-1	5.3	——— Control ———			
T-2	4.9	——— Control ———			
T-3	2.5	107	163	150	1.0"/min
T-4	3.1	130	175	197	
T-5	2.0	127	137	85	
T-6	3.6	217	245	334	
T-7	1.8	120	160	97	
T-8	1.4	159	180	172	
T-9	6.0	415	445	435	
T-10	3.5	195	224	296	
T-11	2.0	125	160	200	
T-12	4.5	210	232	210	
T-13	2.1	75	161	145	
T-14	4.7	276	334	298	
T-15	2.4	128	230	230	
T-16	4.4	175	215	200	
T-17	3.4	153	170	200	

*Avg. tear load here refers to the straight line load value on the load-time curve.

Median of the avg. tear load = 180 grams

Table 3.5-1

RESULTS OF TEAR STRENGTH MEASUREMENTS (CONT.)

Specimen Code	Length of Tear, X_1 (cm)	Length Remaining to Edge, X_2 (cm)	Angle of Tear, (degrees)	Comments
T-1	----	----	----	Control
T-2	----	----	----	Control
T-3	2.9	2.3	2	Medium Tear Serrations
T-4	2.2	2.9	2	Light Tear Serrations
T-5	4.0	1.1	12	Medium Serrations
T-6	4.6	0.5	5	Light Serrations
T-7	2.4	1.4	22	Medium Serrations
T-8	5.0	0	3	Large Serrations - Completely Torn
T-9	2.9	1.9	0	Medium Serrations
T-10	3.8	1.0	0	Light Serrations
T-11	2.7	2.2	5	" "
T-12	2.5	2.5	0	" "
T-13	2.4	2.4	6	Medium Serrations
T-14	3.4	2.5	0	" "
T-15	2.0	2.8	1	Light Serrations
T-16	2.1	2.8	0	" "
T-17	3.3	1.5	0	" "

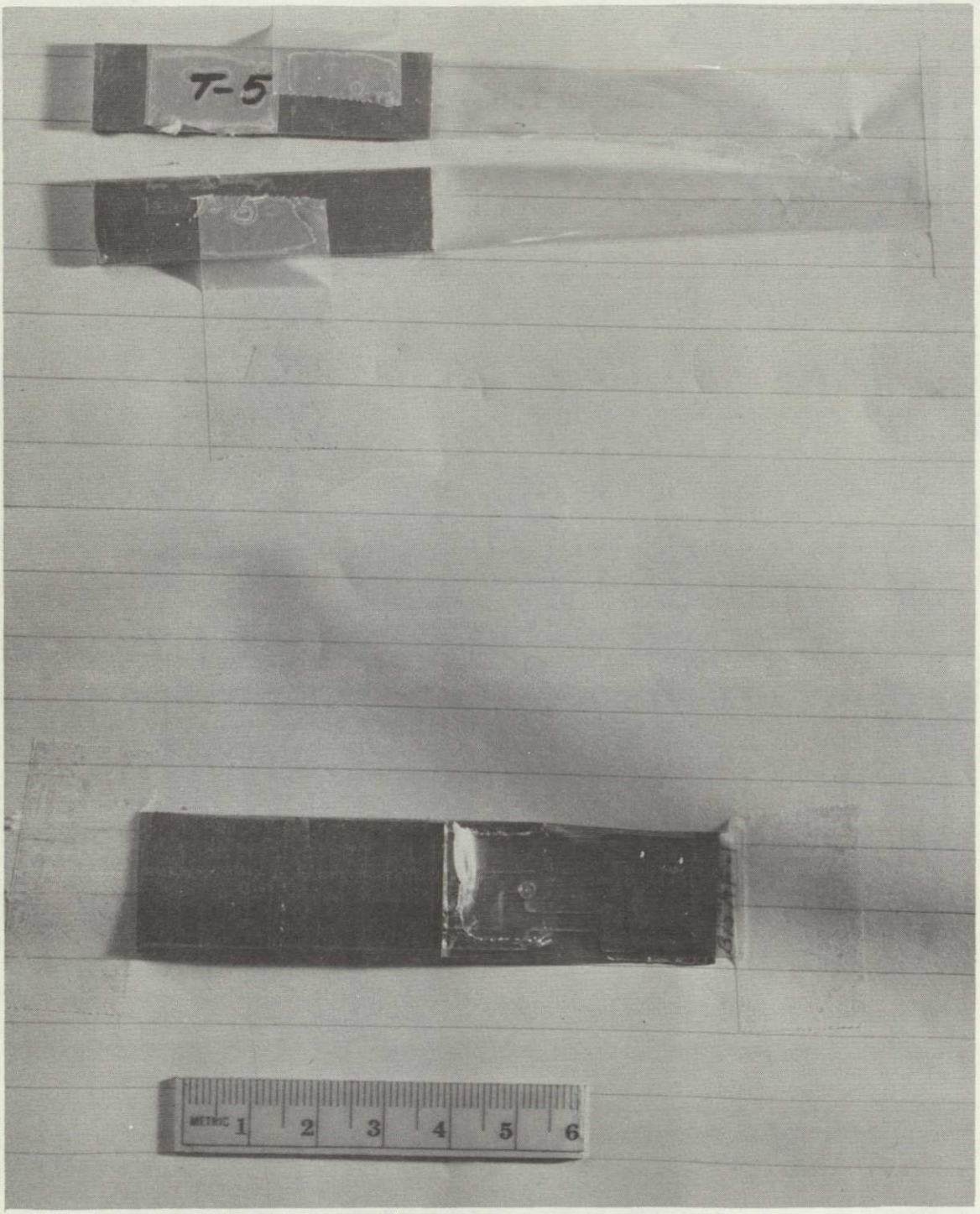

Fig. 3.5-2 Photo of Tear (Top) and Flexure (Bottom) Specimens After Testing

Figure 3.5-3

SKETCH OF A TYPICAL TEAR
SPECIMEN AFTER TEST

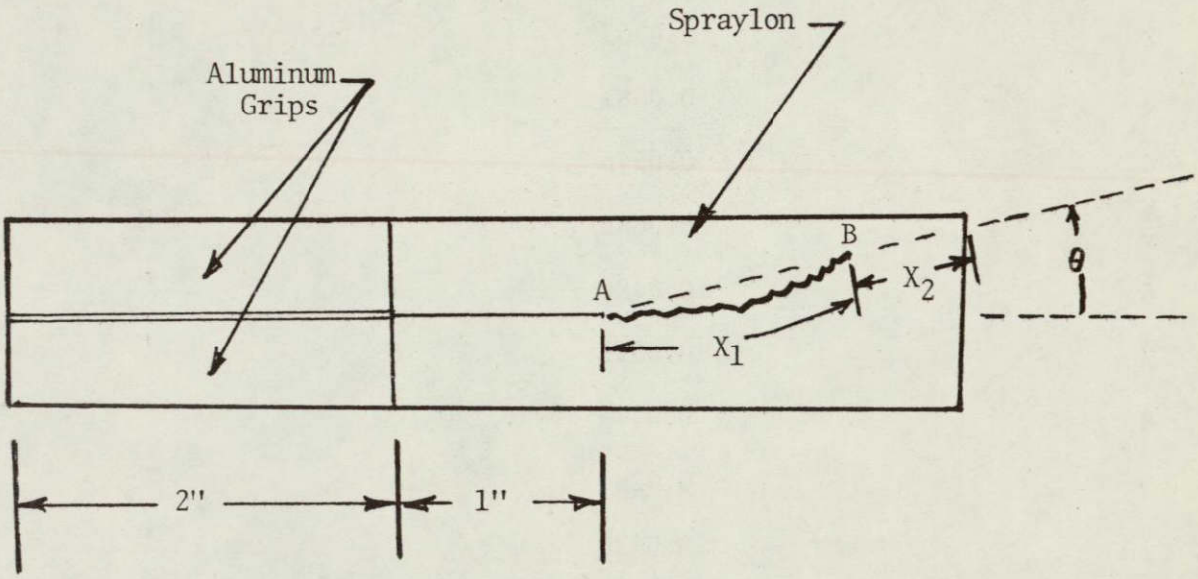

A = Start tear point

B = Final tear point

Table 3.6-1

RESULTS OF MACRO-VCM (OUTGASSING) MEASUREMENTS

FROM FREE STANDING FILMS

Specimen Number	Coating Weight (Grams)	VCM (%), Tested at 125°C for 24 Hours at 10^{-6} Torr
1	0.0550	Less than 0.01%, Limit of Detection
2	0.0763	"
3	0.0681	"
4	0.0546	"
5	0.0682	"
6	0.0486	"
7	0.0511	"
8	0.0449	"
9	0.0280	"
10	0.0420	"
11	0.0538	"
12	0.0393	"
13	0.0464	"
14	0.0500	"
15	0.0438	"

Table 3.6-2

RESULTS OF MICRO-VCM MEASUREMENTS OF SPRAYLON FREE STANDING FILMS

- SPECIMEN SIZE = 2 cm x 2 cm

Specimen Number	Weight Loss %	VCM %
1	0.10	0.01
2	0.10	0.00
3	0.10	0.01
4	0.09	0.00
5	0.08	0.00

AV. Weight Loss (%) = 0.094

AV. VCM (%) = 0.004

Table 3.6-3

RESULTS OF MICRO-VCM MEASUREMENTS ON FREE STANDING FILMS

- SPECIMEN: 4 inches x 5 inches

1A	0.11	0.01
1B	0.11	0.01

AV. Weight Loss (%) = 0.11

AV. VCM (%) = 0.01

4. Mechanical Tests After Combined Ultraviolet/Proton Exposure

4.1 Adhesion Strength

Two Spraylon specimens (Figure 4.1-1) were tested for adhesion strength after exposure to simulated space radiation. The exposure levels were 3250 equivalent solar ultraviolet and 1.04×10^{16} protons (50 kev) per square centimeter at 80°C.

The radiation exposures were carried out at Lockheed and delivered to JPL for testing. The exposes specimens (Posit 1 and 6) are shown in Figure 4.1-1 and the test results are given in Table 4.1-1.

4.2 Flexure Strength

Two Spraylon specimens exposed to simulated space radiation identical to that above were tested for flexure strength. Both specimens were bent in the "opposite" direction with the Spraylon in tension (See Figure 3.2-2).

One of the two specimens (Posit 7, 8) survived to 100 bending cycles although peeling did occur. Both, however, survived 50 cycles with no debonding. Coloration due to the radiation was negligible.

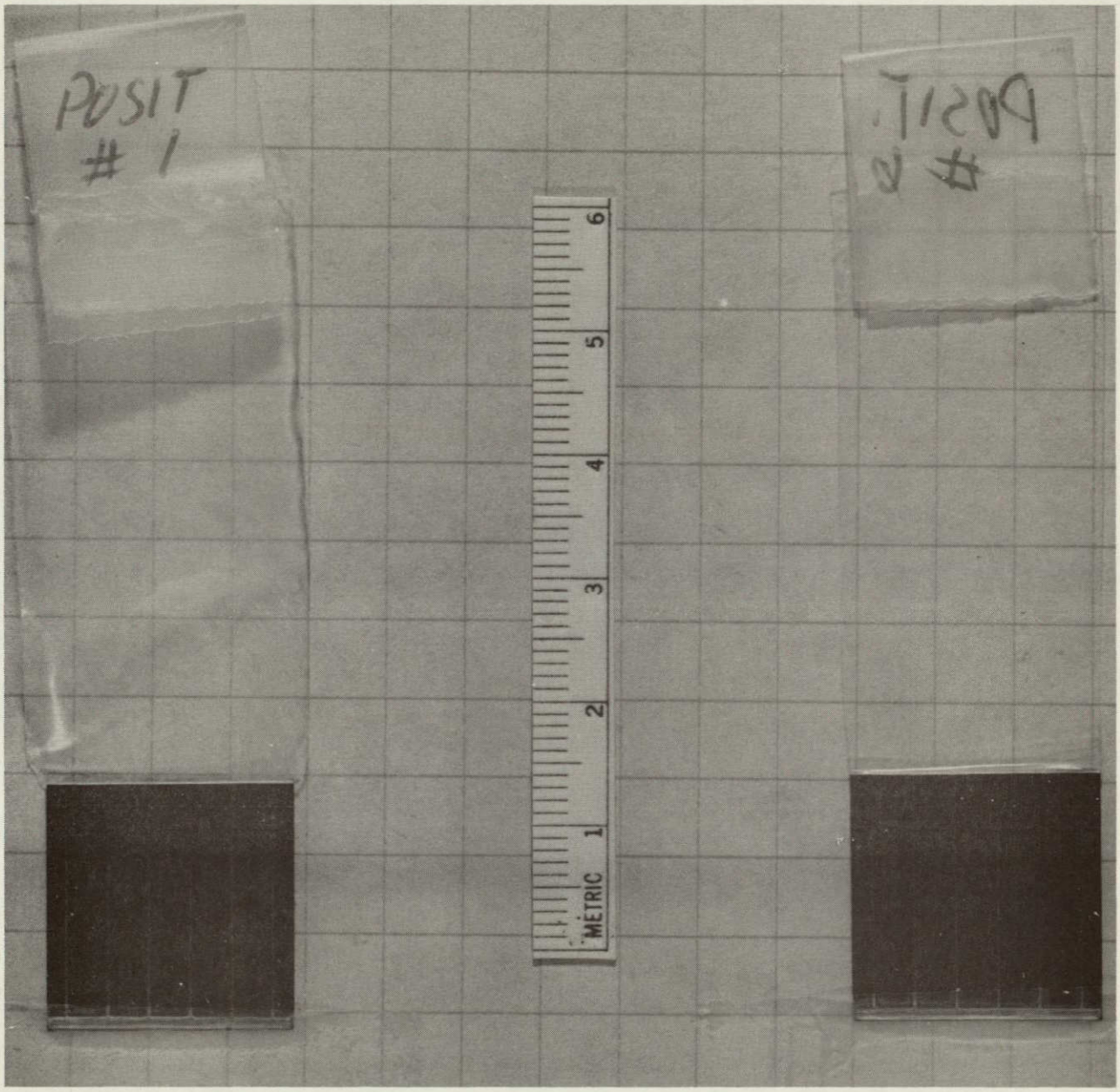

Fig. 4.1-1 Photo of Spraylon Specimens Prior to Adhesion Testing

ORIGINAL PAGE IS
OF POOR QUALITY

Table 4.1-1

RESULTS OF ADHESION MEASUREMENTS ON IRRADIATED SPECIMENS

Specimen Code	Width (in.)	Thickness (in.)	Max. Tear Load (Lbs.)	Avg. Peel Load (Lbs.)	Max. Peel Load Lbs.)	Min. Peel Load (Lbs.)
Posit 1	0.790	0.0031	2.52	----	----	----*
Posit 6	0.790	0.0027	----	0.34	0.61+	0.20**

* No peel data obtained. Specimen failed at the edge of the solar cell.

** This specimen did not tear. A uniform peel across the solar cell was obtained.

\+ Within the range of the unirradiated specimens.

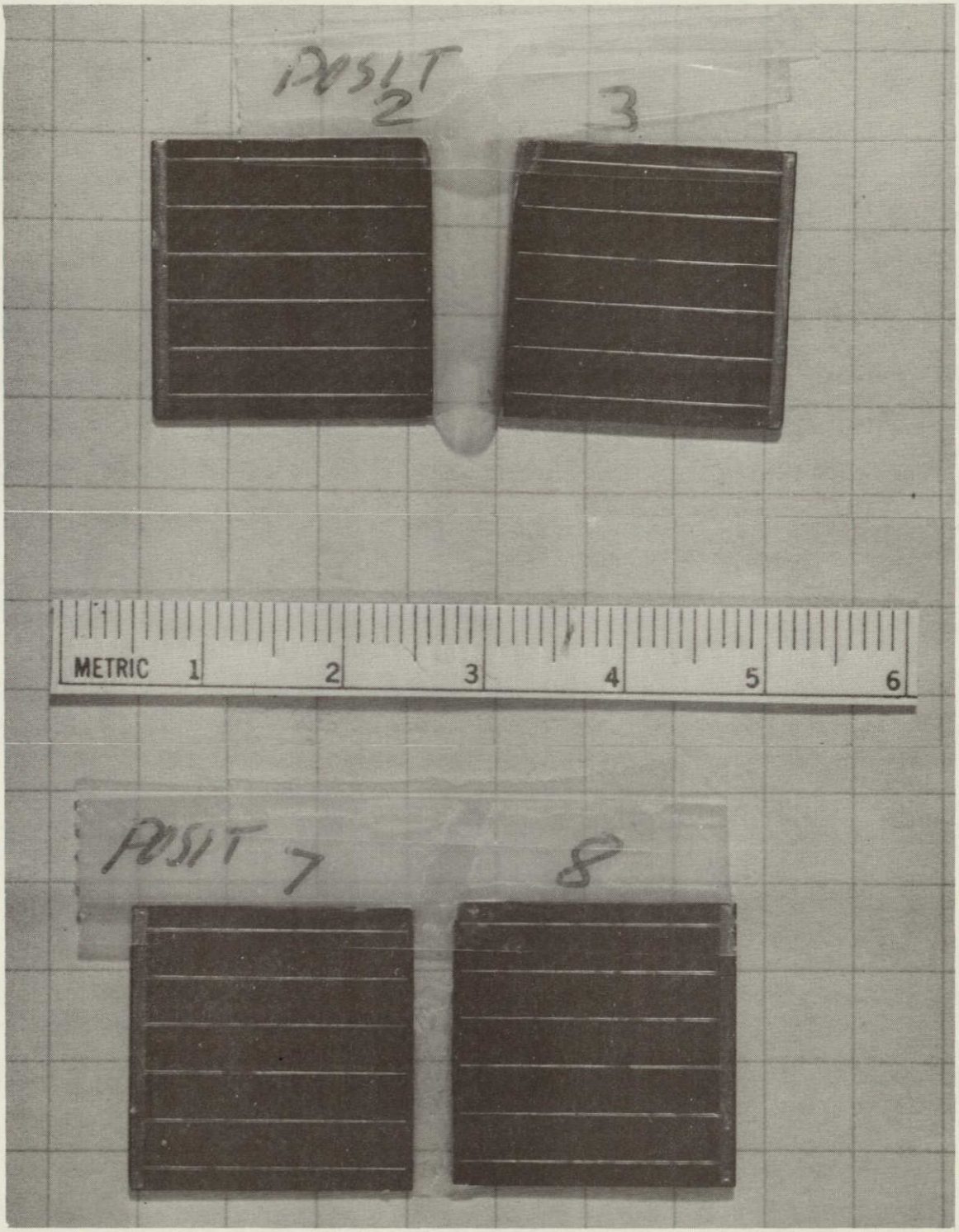

Fig. 4.2-1 Photo of Spraylon Specimens Prior to Flexure Testing

Table 4.2-1

RESULTS OF FLEXURE MEASUREMENTS ON IRRADIATED SPECIMENS

Specimen Code	Width (in.)	Thickness (in.)	Debonded Area No. of Cycles		
			10	50	100
Posit 2, 3	0.79	0.0036	None	None	*
Posit 7, 8	0.79	0.0032	None	None	**

* After 70 cycles, the Spraylon failed at the edge of solar cell posit 2.

** After 80 cycles, the Spraylon began to peel away from the solar cells. Test was completed to 100 cycles.

5. Conclusions and Recommendations

The mechanical testing data for the Spraylon encapsulation are summarized in Table 5 -1. The range of the tests results as well as the average values are shown. The data from the irradiated specimens are summarized in Table 5 -2. The Spraylon specimens appeared resistant to both the ultraviolet and proton exposures. Only faint color changes were noted. One adhesion specimen retained a high maximum peel load (0.61 lbs./2 cm) and the flexure specimens both exhibited no debonding before 50 cycles.

These data were obtained from unoptimized configurations of Spraylon fluorocarbon encapsulation in the initial phase of the Lockheed effort. It is recommended that the work continue to develop the optimized encapsulation configurations and their mechanical tests performed. These tests are planned, at present, for later this year and the mechanical tests will be performed by JPL. The results of those tests will be reported at that time.

Table 5 -1

SUMMARY OF MECHANICAL TESTING

OF SPRAYLON FLUOROENCAPSULATION

UNEXPOSED SPECIMENS

Test	Range	Average
Tensile Strength	13-21 lbs *	18,5 lbs *
Adhesion Strength	0.3-5.6 lbs **	1.1 lbs **
Flexure Strength	13-53%	19% per 10 Cycles 36% per 50 Cycles 48% per 100 Cycles
Abrasion Resistance	0.1-.5 mil	0.26 mil
Tear Strength	97-435 grams	180 grams
VCM	0-0.01%	0.006%

* Per inch width

** Per 2 cm width

Table 5 -2

SUMMARY OF MECHANICAL TESTING

OF SPRAYLON FLUOROENCAPSULATION

IRRADIATED SPECIMENS

Specimen Code	Type of Test	Test Results -Survival Level	Comments
Posit 1	Adhesion	Failure	Negligible Coloration
Posit 6	Adhesion	0.61 lbs/2 cm	Negligible Coloration
Posit 2, 3	Flexure	70 Cycles	Failure at Solar Cell Edge, Negligible Colorati
Posit 7, 8	Flexure	80 Cycles	Peeling, Negligible Coloration

Appendix C
NASA/LEWIS TEST PROGRAM

The early results of the ATS-6 solar cell flight experiment (Ref. 5), which compared the performance characteristics of a variety of solar cell configurations in a synchronous orbit environment, indicated that FEP Teflon-covered solar cells suffered substantial degradation. Since those cells showed a dramatic drop in electrical output during the eclipse season, it was surmised that delamination of the heat sealed FEP (with possible subsequent junction damage), resulted from mechanical stresses related to the deep thermal cycling.

In order to test this hypothesis, a series of thermal-vacuum tests were performed at NASA-Lewis Research Center in which FEP covered solar cells were subjected to accelerated ultraviolet radiation (11 suns) followed by thermal cycling simulating the ATS-6 eclipse temperature profile. By arrangement with JPL, Spraylon covered cells were included in the tests.

At the time of the initial test, the Spraylon system was still in an optimization phase, necessitating a calculated risk in the definition of processing parameters of cells submitted for evaluation. Specifically, optimization studies had concentrated on environmental performance at temperatures at or below 40 °C, rather than the target 80 °C temperature scheduled for the NASA-Lewis evaluation. Because adhesion of the Spraylon coating to the silicon solar cells during thermal cycling was a major consideration, it was felt to be necessary to use relatively thick primer layers of the best primer previously investigated (Dow-Corning Z6020), despite the fact that no data on thermal or ultraviolet stability were available at the proposed test temperature. (Subsequent investigation indeed revealed that for the thicknesses used in this test, the Z6020 primer tended to discolor at temperatures above 60° C.)

The results of the first NASA-Lewis test indicated that, whereas all the Spraylon-coated cells (3 to 4 mils of coating) survived the thermal cycling without mechanical damage,

they did exhibit a drop in maximum power output of approximately 10 percent. The degradation of cell performance was due to a marked brown discoloration induced by the nominal 2000 equivalent sun-hour ultraviolet exposure at 11 equivalent suns. Detailed examination of the cells after exposure indicated that the exposure temperature was far in excess of 80 °C since definite signs of melting of both the Spraylon and solder bus strip were observed. Unfortunately, all the thermocouples attached to the cells failed to function so that actual temperatures could not be determined. However, it was estimated that the cell temperatures may have exceeded 180 °C.

A second series of tests was performed at the NASA-Lewis test facility. In an attempt to ameliorate the effects of primer discoloration at elevated temperatures, an alternate system GE SS-4120 was employed. Although this primer exhibits somewhat better optical stability than Z6020 at elevated temperatures, it provided poorer adhesion properties for the Spraylon, necessitating the use of excessively thick primer coats on the cells. Although the risks associated with heavy primer coats were recognized, time constraints precluded more complete optimization of the system. The compromise system, however, did not provide better performance than the Z6020. Although the measured cell temperatures remained in the 80° to 100 °C range, the Spraylon coating system discolored under extended ultraviolet radiation, with maximum power degradation of 10 to 12 percent.

As a result of the NASA-Lewis test sequences it became apparent that the Spraylon system under development, while adequate at exposure temperatures below 40 °C, exhibits optical degradation at temperatures in excess of 80 °C. Part of the problem has been identified as related to thermal and UV degradation of the primer. Subsequent to the NASA-Lewis tests, significant progress has been made in reducing this problem through alternate priming techniques. In addition to the primer degradation, it appears that the Spraylon material, as presently constituted, shows a temperature dependent loss in transmittance under extended ultraviolet exposure.

A quantitative evaluation of the performance of the optimized Spraylon system at temperatures up to 120 °C will be performed under Phase II of this effort.

Appendix D
REFERENCES

1. Research Brief LMSC to NASA/Lewis Research Center, Mar 1968

2. TRW Defense and Space Systems, "Flexible, FEP-Teflon Covered Solar Cell Module Development," Final Report, NASA CR-135109, Oct 1976

3. E. I. DuPont de Nemours and Co. (Inc.), Technical Products Bulletin FEP 532-5001, Wilmington, Del.

4. Lockheed Missiles & Space Company, Inc., Investigation of FEP-Teflon as a Cover for Silicon Solar Cells, LMSC-D243070, Aug 1976

5. Goldhammer, L. J. and Corrigan, J. P., "Early Results of the ATS-6 Solar Cell Experiment," paper presented at 11th Photovoltaic Specialists Conference, 1975